MASTER IN CHEMISTRY RESEARCH FOCUS

Chemical synthesis of clickables GDP-mannose analogues for antibody functionalisation

YAHIA BOUDHAR, Rym

Award date:
2023

Awarding institution:
University of Namur

Université de Namur

Faculté des Sciences

CHEMICAL SYNTHESIS OF CLICKABLES GDP-MANNOSE ANALOGUES FOR ANTIBODY FUNCTIONALISATION

Mémoire présenté pour l'obtention

du grade académique de Master Chimie «Chimie du Vivant et des Nanomatériaux» : Finalité Approfondie

Rym YAHIA BOUDHAR

Janvier 2023

“Carbohydrates are fun and challenging molecules”

Carolyn R. Bertozzi

UNIVERSITE DE NAMUR
Faculté des Sciences
Secrétariat du Département de Chimie
Rue de Bruxelles 61 – 5000 NAMUR
Téléphone : +32(0)81 72.54.44 – Téléfax : +32(0)81 72.54.40
E-mail : enseignement.chimie@unamur.be - www.unamur.be/sciences

Synthèse chimique d'analogues clickables de GDP-mannose pour la fonctionnalisation régio-sélective d'anticorps.

Rym YAHIA BOUDHAR

Résumé

Les immuno conjugués cytotoxiques (ADC) sont une classe d'agents thérapeutiques qui attire de plus en plus d'intérêt, notamment dans le traitement des cancers. Ils sont constitués d'un anticorps auquel est liée de façon covalente une molécule cytotoxique, dont le relargage est dirigé préférentiellement vers les cellules tumorales, et ce, grâce à la spécificité de l'anticorps utilisé. Cependant, la conception d'ADCs stables et efficaces demeure complexe, car il est difficile de contrôler le nombre et la régiosélectivité des conjugaisons. Pour pallier à cette contrainte, la fonctionnalisation via les deux chaines glycanes de l'anticorps constitue une bonne option. Cette méthode exploiterait - dans notre cas - deux réactions clés : une mannosylation enzymatique pour insérer un analogue de mannose portant une fonction clickable, suivie d'une réaction click qui permettrait de lier une charge active régiosélectivement à l'anticorps. Avant de pouvoir tester cette fonctionnalisation via les chaines glycanes, il est nécessaire de synthétiser des analogues clickables de GDP-mannose : des molécules potentiellement donneuses du mannose clickable qui serait alors transféré aux chaines glycanes de l'anticorps lors de la mannosylation. Parmi les analogues possibles, la synthèse de la molécule **1a** a été accomplie, et celle de la molécule **1b** est en cours.

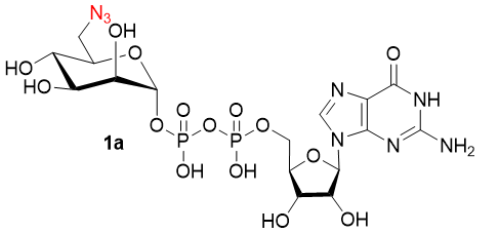

1a

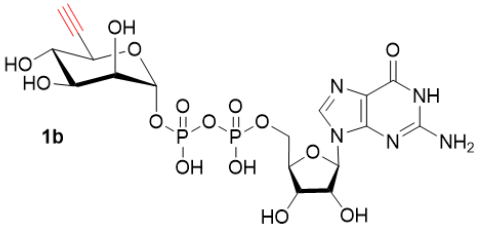

1b

Mémoire de master en Sciences Chimiques à Finalité approfondie

Janvier 2023

Promoteur : Prof. Stéphane Vincent

Remerciements

Je tiens tout d'abord à remercier le professeur Stéphane Vincent pour m'avoir acceptée dans son laboratoire. Durant toute la période de mon mémoire, j'ai pu compter sur ses conseils avisés et toujours pertinents dans l'avancement de mon projet de recherche. Le suivi qu'il a accordé ainsi que la générosité avec laquelle il a transmis son savoir m'ont grandement motivé à mener à bien ce travail. Merci monsieur !

Mes sincères remerciements vont également à mon encadrante : Marine. Tu as été d'un fort soutien depuis le début du projet. Tu as su te montrer toujours disponible pour moi, ce qui a énormément facilité mon adaptation au laboratoire. Ta bienveillance, ta générosité et ta patience ont été centrales dans l'encadrement de mon travail, en plus de tes connaissances et de ta bonne humeur, je t'en suis très reconnaissante pour cela.

Au labo, j'ai aussi pu compter souvent sur l'aide de Loïc et Arnaud que je remercie vivement. Au-delà de votre assistance scientifique et technique, vous avez apporté bonne humeur et convivialité au CBO et, grâce à vous, je comprends le second degré (enfin presque).

Je remercie bien évidemment Jenny et Kévin pour les agréables moments passés, particulièrement durant la pause déjeuner, Ignacio et Giuseppe pour leur gentillesse, et le dernier arrivant Dmytro, à qui je souhaite des jours agréables au labo. Je remercie aussi tout particulièrement Xavier pour les analyses HRMS qu'il a faites pour mon projet. Une pensée va également aux anciens membres que j'ai connu : Léa, dont la thèse m'a bien orientée en rédaction ainsi que Maha, Jun et Timothée.

Cette magnifique aventure au CBO, j'ai eu la chance de la partager avec deux autres camarades : François et Florence, avec qui j'ai pu échanger des joies mais aussi des contraintes de la recherche scientifique. On s'est soutenu mutuellement, je vous remercie pour ça.

Enfin et pas des moindres, je remercie mes parents et ma sœur pour leur soutien infaillible et sans qui je n'aurai jamais pu réaliser ce merveilleux rêve qu'est : la synthèse organique.

Abbreviations and symbols

Å	Angström.
Ab	Antibody.
ADC	Antibody Drug Conjugate.
ADCC	Antibody Dependent Cellular Cytotoxicity.
ADCP	Antibody Dependent Cellular Phagocytosis.
ADP	Adenosine diphosphate.
Ag	Antigen.
AMP	Adenosine monophosphate.
Asn	Asparagine.
BCN	Bicyclononyne.
CDC	Complement Dependent Cytotoxicity
CDI	Carbonyl diimidazole
CuAAC	Copper(I)-Catalysed Alkyne-Azide Cycloaddition.
DAMP	Dimethyldiazomethyl-phosphonate.
DAR	Drug to Antibody Ratio.
DCM	Dichloromethane.
DIBO	Dibenzoannulated-cycloctyne
DMAP	4-Dimethylaminopyridine.
DMF	*N*,*N*-Dimethylformamide.
DMSO	Dimethylsulfoxide.
EGFR	Epidermal Growth Factor Receptors.
Eq	Equivalents.
ESI	Electrospray ionisation.
Fab	Fragment antigen binding
Fc	Crystallisable Fragment.
FcRs	Fc receptors.
FDA	Food and Drug Administration.
GalNAc	*N*-acetylgalactosamine.
GDP	Guanosine diphosphate.
GMP	Guanosine monophosphate.
GMP-Im	Guanosine phosphorimidazolide.
GlcNAc	*N*-acetylglucosamine.
HC	Heavy Chains.
Hex	Hexane.
HPLC	High Performance Liquid Chromatography.
HRMS	High Resolution Mass spectrometry.
Ig	Immunoglobulin.
J	Coupling constant.
LCh	Light Chains.
LDA	Lithium diisopropylamide.
LG	Leaving Group.
Mϕ	Macrophages.
Man	Mannose.
ManT	Mannosyltransferase.
m-CPBA	mata-Chloroperoxybenzoic acid.
MeCN	Acetonitrile.
MeOH	Methanol.
MMAD	Monomethyl dolastatin 10.
mTG	Microbial Transglutaminase
NDP	Nucleoside diphosphate.
NHS	*N*-Hydroxysuccinimide.
NK	Natural Killers.
NMR	Nucleus Magnetic Resonance.
NOE	Nuclear Overhauser effect.
pAF	p-acetylphenylalanine.
ppm	parts per million.
PTM	Post-translational modification.
Rf	Retention factor.
r.t	Room Temperature.
SA	Sialic Acid.
SPAAC	Strain-Promoted Alkyne-Azide Cycloaddition.
TEA	Triethylamine.
THF	Tetrahydrofuran.
TLC	Thin Layer Chromatography
TMS	Trimethylsilane.
tRNA	Transfer Ribonucleic Acid.

Table of contents

I. Introduction

I.1 Antibodies - Generalities

I.1.1. Structure

Antibodies (Ab), also called Immunoglobulin (Ig), are glycoprotein molecules composed of 82 - 96% of protein and 4 - 18% of carbohydrates.[1] They are constituted of four polypeptide chains. Two identical Light Chains (LCh) and two identical Heavy ones (HC), often represented altogether schematically as a Y shape. The two LCh are linked to the HC by cysteine disulfide bridges and by many non-covalent interactions. The two HC are also connected together by cysteines, which form the hinge region: a flexible area between the two Fragments antigen binding (Fab) (the arms of the schematic Y) and the Crystallisable fragment (Fc) (the core of the schematic Y).

Each Fab fragment contains variable domains which contribute to the specific recognition and binding between the antibody and the antigen (Ag). Meanwhile, the Fc fragment which is composed of constant domains, mediates interactions with effector cells and molecules, once the Ab-Ag recognition occurred. Both variable and constant domains display an immunoglobulin fold,[2] which consists of a three dimensional shape made of two antiparallel β sheets, where adjacent β strands are linked together through short loops (Figure 1).[3]

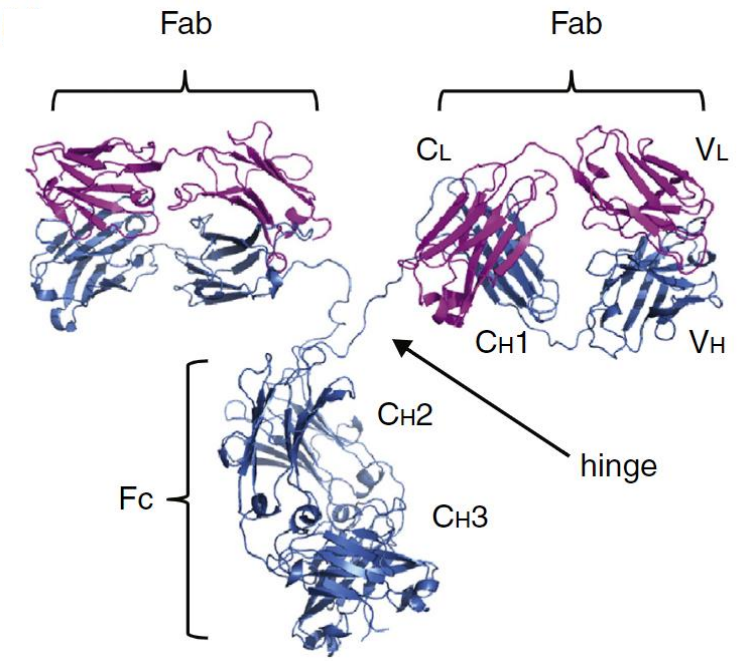

Figure 1. structure of an antibody. Heavy chains in blue, and light chains in magenta.[3]

I.1.2. Isotypes and Subclasses

In humans, there are five distinct antibody isotypes, namely: IgA, IgD, IgE, IgG and IgM, which are defined by five different types of heavy chains known as: α, δ, γ, ε, μ respectively. The apparent difference between them is structural : IgG, IgE and IgD are monomeric, while IgA is dimeric and IgM pentameric or hexameric (Figure 2). Besides, Isotypes can also be divided into subclasses.

This intrinsic difference between isotypes and subclasses is controlled genetically via heavy-chain class switching and plays a role in the biological activity mediated by the Fc region. In fact, each isotype/subclass tends to have a unique Fc binding profile for effector cells and/or molecules.[4]

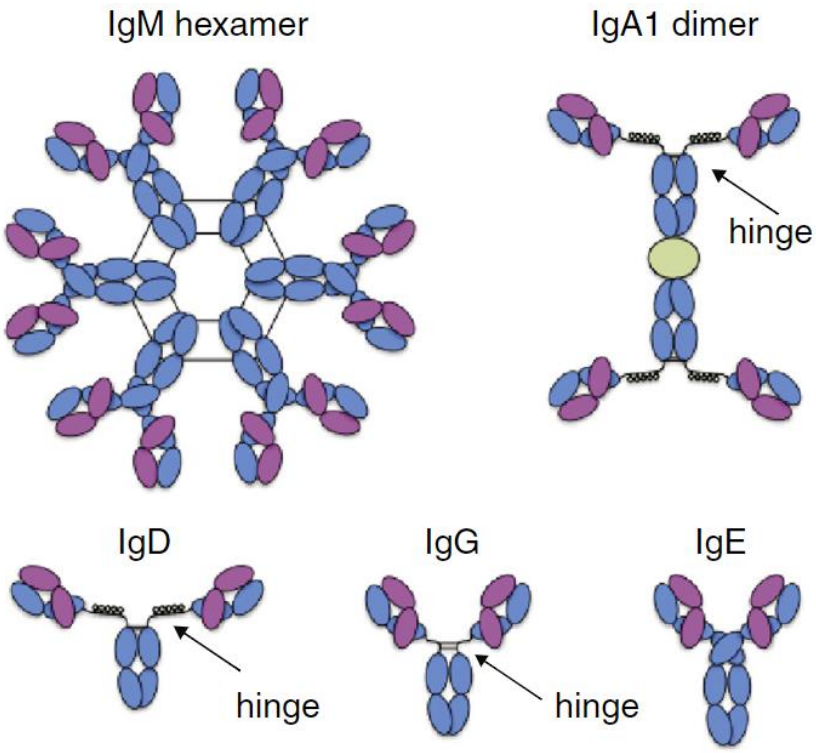

Figure 2. structures of Ig isotypes.[3]

I.1.3. Glycoforms

Immunoglobulin G - the most abundant isotype in human serum- bears two N-linked glycans (one on each HC) attached precisely at asparagine (Asn)- 297 in the Fc region. These chains are added during N-glycosylation which is a well-known post-translational modification (PTM) of proteins. The IgG glycan, which is always biantennary, is composed of the following sequence: two *N*-acetylglucosamine (GlcNAc) - mannose (Man) - mannose antennae - *N*-acetylglucosamine (GlcNAc), (Figure 3). This forms the common core glycan that can be enriched by additional carbohydrates leading to various Fc glycoforms.[4]

The composition of the N-297 glycan chains is important for the Ab stability. Moreover, glycoforms (just like isotypes) impact also the Fc binding affinity for effector cells and molecules. They contribute to modulate the type of effector function triggered during an immune response.[1] The latter will be further discussed in the next section.

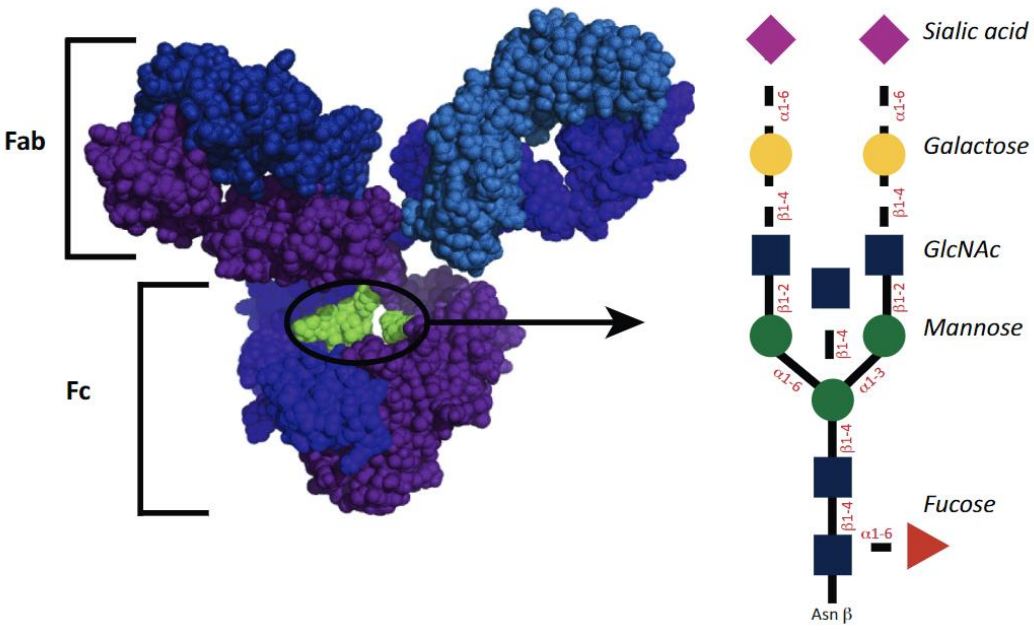

Figure 3. antibody glycans usual structure.[4]

I.2 Antibodies in cancer therapy

Nearly half of the marketed Ab therapeutics are used in oncology.[2] They were first used as antagonists of oncogenic receptor tyrosine kinases, by taking advantage of the high affinity and specificity of Ab towards its antigen. Then, based on the same property, other Ab therapeutics have emerged.[5] They are roughly divided in two categories, depending on the mechanisms of action they induce.

I.2.1. Immunotherapy

The Ab therapeutics of this category tend to engage effector cells and molecules of the immune system. One possibility is through the activation of innate Fc-mediated effector functions, which include (scheme 1) :

- Complement dependent cytotoxicity (CDC): In the classical pathway, the C1q protein of the complement system binds the Ab-labelled tumor cell through specific docking sites present in IgG and IgM isotypes. This leads to the activation of an enzymatic cascade allowing the lysis of the cell.
- Antibody dependent cellular cytotoxicity (ADCC): Effector cells such as Natural Killers (NK) or macrophages (Mϕ) bind the Fc of Ab-labelled tumor cell, depending on the affinity between their respective Fc receptors (FcRs) and the selected Ig isotype/glycoform . Each recruited cell will deploy distinct immune response leading also to the antigen cell lysis. It is noteworthy that macrophages are also able to trigger antibody dependent cellular phagocytosis (ADCP) in order to kill the antigen cell.

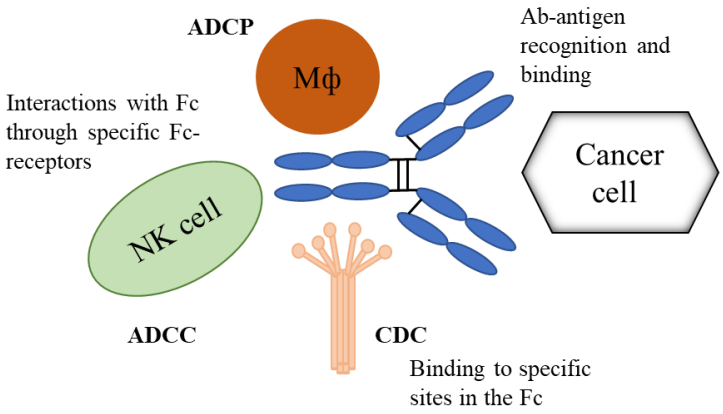

Scheme 1. innate effector functions.

Besides, research in cancer immunotherapy is also interested in the development of Fc engineered antibodies, either with enhanced innate effector functions, or, ones capable of engaging components of the adaptive immune system, particularly cytotoxic T cells. [6]

I.2.2. Antibody Drug Conjugates (ADCs)

ADCs attract a growing interest in cancer therapy because they may be highly potent pharmaceutical drugs. Indeed, they permit to direct the release of the cytotoxic payload selectively toward tumor cells while sparing normal ones during treatment. Consequently, they enable the use of chemotherapeutics, which are too toxic to be applied alone through a systemic route, and hence, allow to increase the overall therapeutic index of cancer drugs.[7,8]

ADCs are composed of an antibody covalently connected to a payload by a chemical linker. Their mechanism of action consists in: firstly, recognizing and binding a specific antigen whose epitope is adapted to the Ab paratope. It is noteworthy that besides the high affinity for Ab, the targeted antigen should be overexpressed only on tumor cells while possessing good internalization properties. Indeed, the second step of the mechanism involves the cellular uptake of ADC-antigen complex. Then thirdly, the release of the payload, which finally, diffuses in the cytosol and damages the tumor cells, (Figure 4).[9,10]

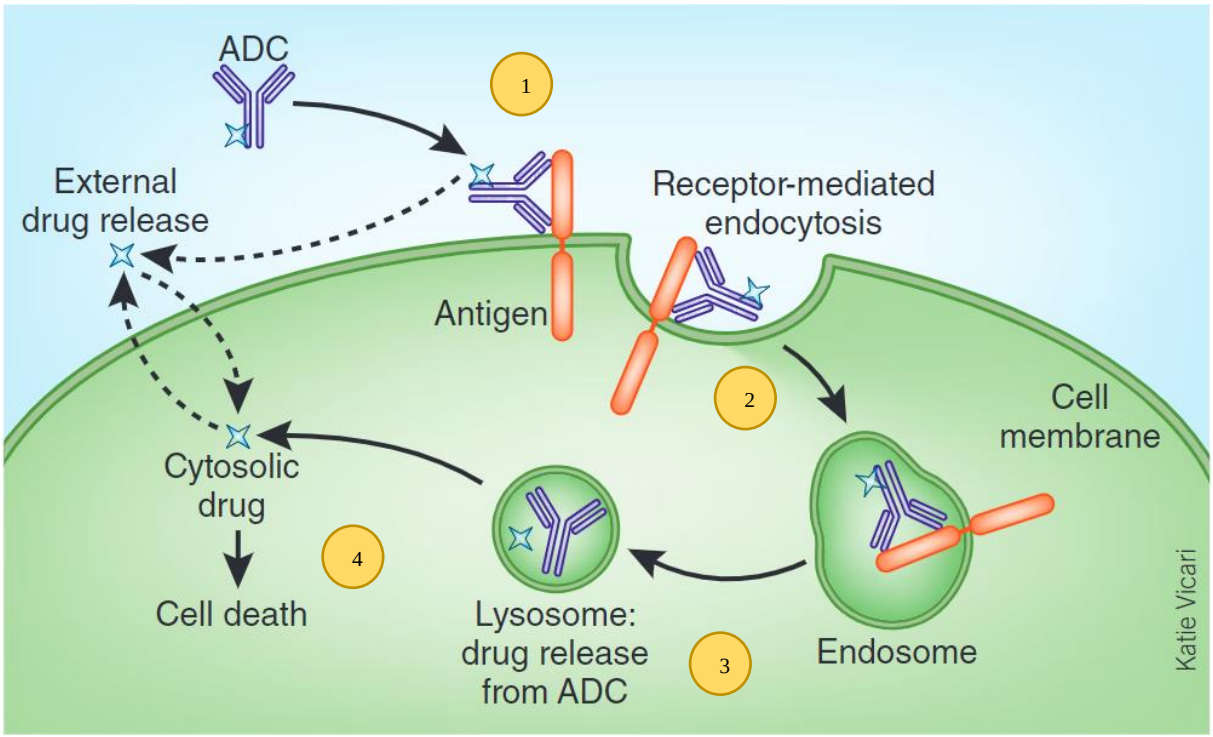

Figure 4. mechanism of ADC-mediated drug delivery.[10]

ADCs might have a promising future, either to expand the druggable targets or to be used in combination with other therapies,. Nevertheless, many challenges are still encountered for the design of stable, non-immunogenic and efficient ADCs. One particular issue lies behind the conjugation chemistry because it is difficult to control the number and the regioselectivity of Ab functionalisations. It is precisely this point that will be further discussed in the following paragraph.

I.3 Protein-mediated Ab functionalisation

Since the first Food and Drug Administration (FDA) approved gemtuzumab ozogamicin in 2000, several other ADCs have been developed using different functionalisation methods. We first present herein those which uses amino acids as conjugation sites.

I.3.1. Conjugation to endogenous amino acids

Targets of such conjugation methods are amino acids already present in the native Ab. Some of these are introduced in the following.

- Lysine acylation

It is one of the most known and conventional way to functionalise an Ab. It involves the nucleophilicity of lysine residues. In fact, the coupling reaction takes place between the primary amine of the lysine and an activated ester carried on the payload linker, mainly *N*-Hydroxysuccinimide (NHS) ester, leading to amide formation (scheme 2). This type of bioconjugation has the advantage of being simple, thanks to the easily accessible lysine residues present on a native IgG for instance. However, lysine modification is random and can hardly be controlled due to the large number of lysine in an Ab. This results in the formation of highly heterogenous ADCs, characterised by a variable drug to antibody ratio (DAR) which makes the process poorly reproducible and negatively impacts both kinetics and dynamics of ADCs. Moreover, such conjugation lacks regioselectivity, allowing the coupling reaction to occur on the variable domains of the Ab, which could decrease the binding affinity toward the antigen resulting in a less specific drug design.[9]

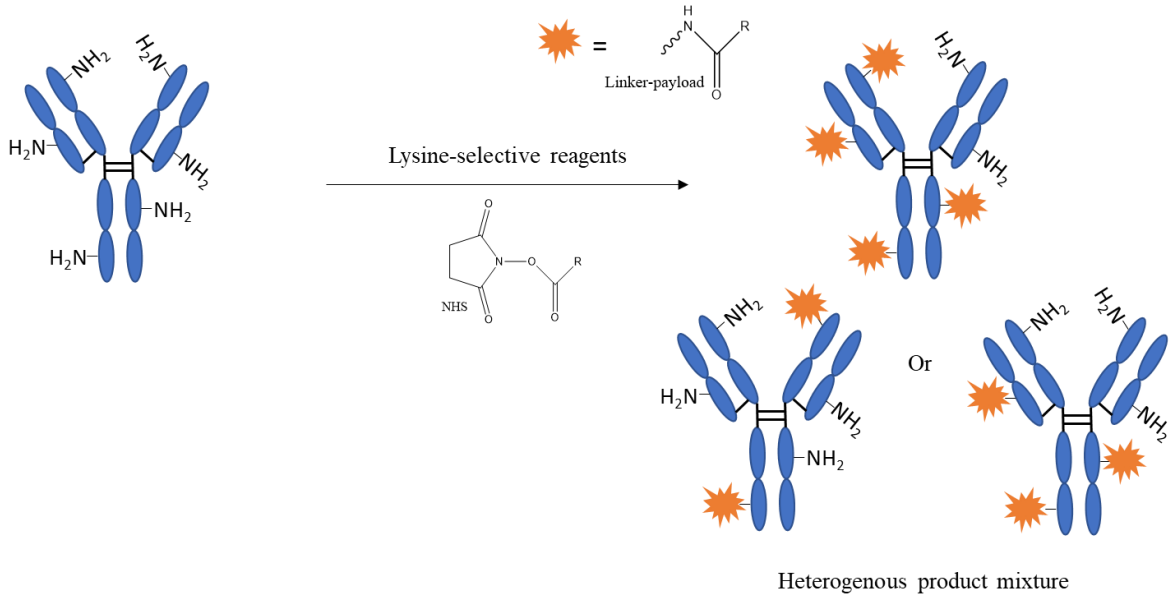

Scheme 2. lysine acylation reaction using NHS ester.

- Cysteine alkylation

Alternatively to lysine acylation, this method exploits the nucleophilicity of cysteine residues to induce the coupling reaction. It has the advantage of being less random, while targeting the four interchains disulfide bridges which are present in less extent than lysine residues and, in well-defined positions. Cysteine modification takes place by: firstly, reducing these disulfide bridges, leading to the formation of up to eight thiol functions. Then, the alkylation of these thiols can be realised for instance, using maleimide present on the payload linker (scheme 3). This type of bioconjugation, which generates ADCs with a maximum DAR of eight, remains somehow stochastic and influences the structure stability of the Ab, especially when all interchains disulfide bridges are reduced.[11]

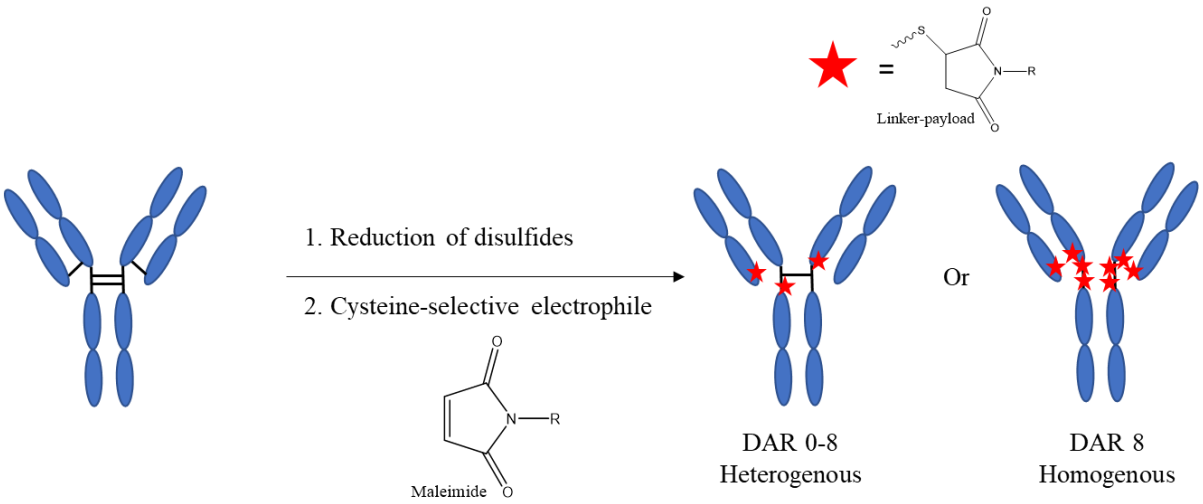

Scheme 3. alkylation of cysteines with a maleimide.

- ThioBridge®

ThioBridge® is the name given to a technology that uses bis-alkylating reagents such as bisulfones to selectively link pair of thiols present in close proximity. As above, they are generated by the reduction of the four interchains disulfide bridges. This re-bridging strategy which proceeds through Michael addition and elimination, permits to conjugate the payload to both thiols of the original reduced disulfide bond, while leaving the Ab structure less impacted than with single cysteine alkylation method (Figure 6).[12] As a consequence, the resulting DAR of this bioconjugation drops to four, which decreases risks of aggregation, toxicity or fast clearance possibly encountered with a DAR of eight.[13]

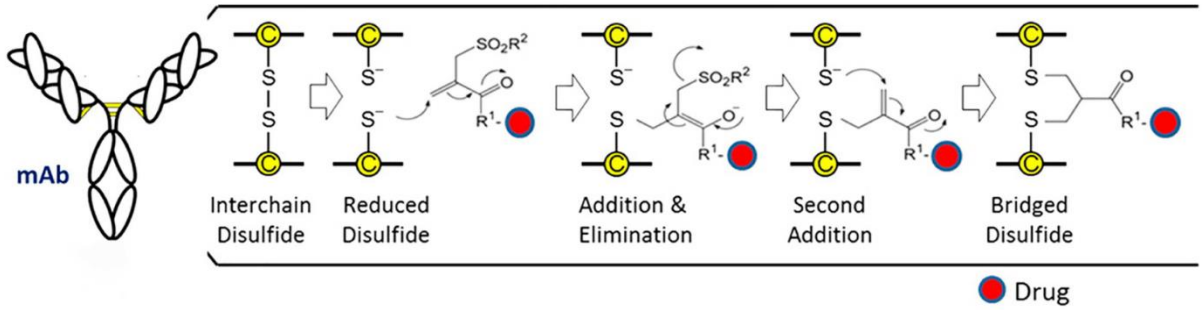

Figure 5. ThioBridge linkage for antibody-drug conjugation.[12]

I.3.2. Conjugation to engineered amino acids

Methods of such category tend to ensure site selective functionalisation by targeting amino acids introduced into the Ab backbone through recombinant technology. They include the following strategies.

- Coupling to unnatural amino acids

This technique requires first the incorporation of a non-canonical amino acid such as p-acetylphenylalanine (pAF) into the Ab backbone through reassignment of a stop codon by tRNA-synthetase.[14] Consequently, the conjugation of the linker-payload occurs in a chemoselective manner by exploiting the unique reactivity of the orthogonal function (ketone, azide…etc) grafted on the unnatural amino acid.[15] One example from the literature consists in introducing site-specifically the unnatural amino acid pAF, in the Fab of an anti-Her2 antibody.[16] The mutant protein is then conjugated to an auristatin derivative (cytotoxic payload) by a stable oxime linkage (scheme 4).

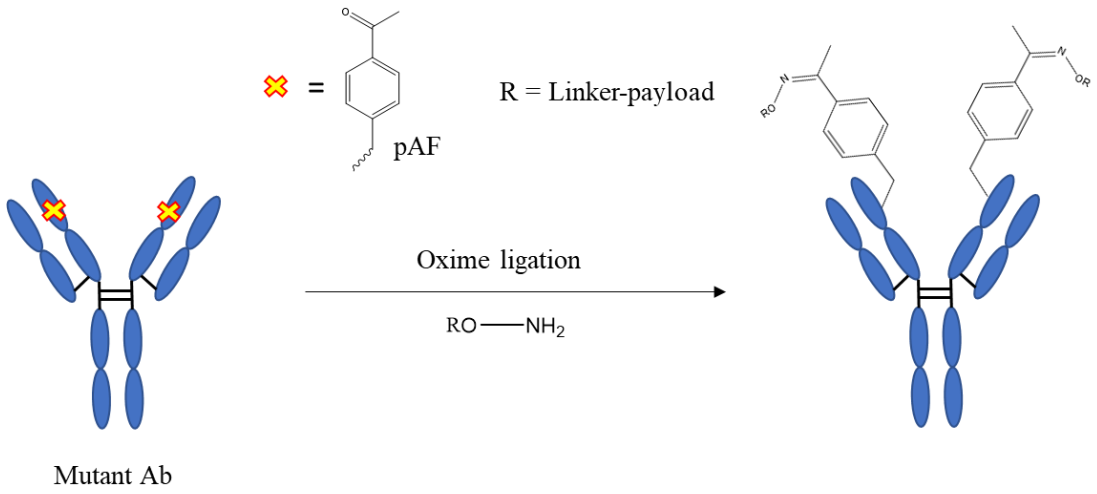

Scheme 4. pAF-mediated antibody conjugation.

- Coupling to short peptide tags

In this conjugation method, a specific short peptide tag (four to six amino acids) is fused with the Ab in a well-chosen location . The purpose is to introduce a suitable environment (motifs), which favours a specific amino acid present in the peptide tag to be conjugated selectively to the linker-payload.[8] Such method was used by Strop *et al* to incorporate a glutamine tag (LLQG) into an anti-EGFR antibody.[17] A microbial transglutaminase (mTG) was also used. The latter recognises selectively the glutamine of the tag and catalyses the formation of the conjugate through reaction between the amine previously grafted on the linker-payload MMAD (monomethyl dolastatin 10) and the amide of the glutamine (scheme 5).

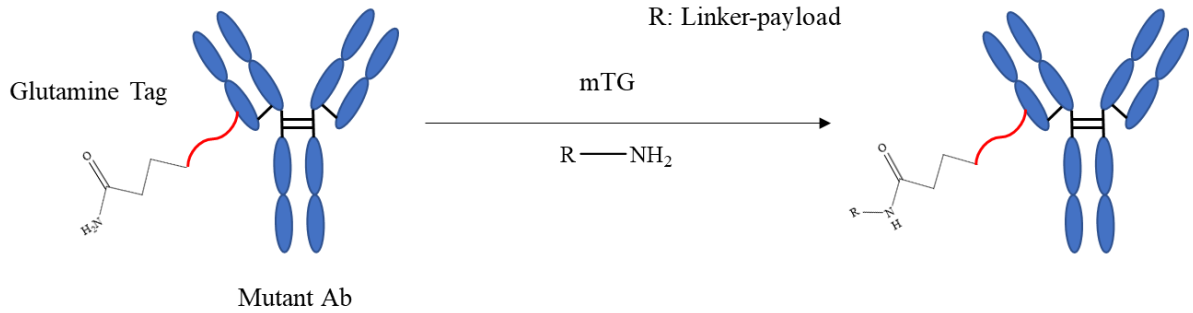

Scheme 5. transglutaminase catalysed antibody conjugation.

ADCs which are developed using recombinant technology are known to be more homogeneous and effective than those made with the traditional lysine conjugates described above.[8] Nevertheless, such conjugation methods involve cell and Ab engineering, laborious optimization while leading sometimes to immunogenic ADCs. This is why, rather than targeting the Ab polypeptide backbone while preserving site selectivity, an interesting alternative would be the use of a glycan-mediated Ab functionalisation. The latter will be the subject of the following section.

I.4 Glycan-mediated Ab functionalisation

The Ab functionalisation method presented herein targets the only two N-297 glycans carried on the Fc region of all IgGs. It is hence, site selective and allows for homogeneity and the control of the DAR. Besides, it avoids modifications of the Fab region, thus preserving the binding affinity toward the antigen. The method relies on a glycoengineering approach which requires special reagents and enzymes along two major steps described below.

I.4.1. Ab glycan remodeling

During this step, the native N-297 glycan chains are modified, either by adding or removing saccharides. While achieving this process metabolically remains hardly attractive due to genetic modification requirements, chemoenzymatic approaches were developed in order to perform the glycan remodeling *ex-vivo*.[18] Such remodeling requires two consecutive steps.

First, a trimming of Ab native glycans is realised with glycosidases which catalyse the hydrolysis of glycosidic bonds. This step permits to homogenise Ab glycans before functionalisation. Otherwise, the starting intrinsic heterogeneity of Ab glycans, characterised by a mixture of glycoforms,[19] may lead to a complex mixture of bioconjugated Abs. Some trimming examples from the literature consist in using a sialidase and a β galactosidase to cleave terminal sialic acid and galactose moieties respectively or, using endoglycosidases which allow the lysis between the two first GlcNAc residues of the Ab core glycan.[20]

Second, a glycan remodeling entails glycosylation using specific glycosyltransferases which catalyse the transfer of suitable saccharides into a glycan chain. The interest of doing such reaction is the installation of an unnatural saccharide bearing a distinct function useful for the following bioconjugation (scheme 6).

For instance, Qasba *et al* discovered and used a mutant galactosyltransferase GalT(Y289L) to insert a C-2 keto galactose into a fully degalactosylated IgG1, which was further conjugated using aminooxy containing auristatin F (scheme 6).[21] Another interesting labelling strategy was the use of the same enzyme to add an azido-GalNac to the core GlcNac previously obtained through trimming.[22] This transglycosylation presents the advantage of introducing a clickable function into the Ab glycans which permits to bioconjugate the payload linker while exploiting chemoselective click reaction. The latter is described below.

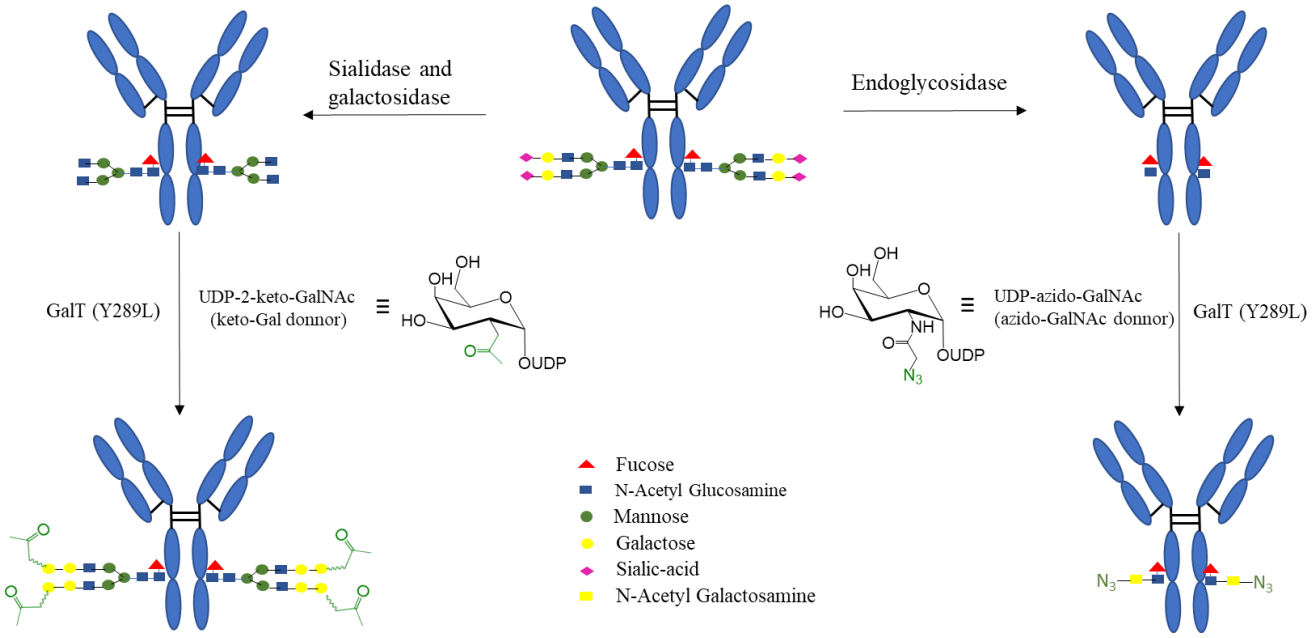

Scheme 6. Examples of glycan remodeling

I.4.2. Bioconjugation: Click chemistry

The desire of a more rapid discovery and production of molecules with new properties, led K.B. Sharpless to first introduce click chemistry which, he defined as a reaction approach capable of linking two molecules of interest in a fast, selective and high yielding manner. Click chemistry emerged hence as a simple but powerful synthetic strategy.[23] Besides, in order to study living organisms, click chemistry reactions could also be applied *in vivo*, where they have to be biorthogonal. Biorthogonality was first described by C.R. Bertozzi and qualifies chemical reactions whose components react selectively with each other, without interfering with the surrounding biomolecules in living systems.[24]

Cycloadditions displayed a particular attention in click chemistry development, especially the Huisgen 1,3-dipolar one between an azide and an alkyne. This reaction as introduced by Rolf Huisgen, requires high temperature or pressure while affording a mixture of regioisomeres. Nevertheless, it was further improved by copper (I) catalysis and led to the Copper Catalysed Azide-Alkyne Cycloaddition (CuAAC), described as the most typical click chemistry reaction. The latter permits to form a triazole ring as depicted in scheme 7, while respecting the criteria of click reactions.

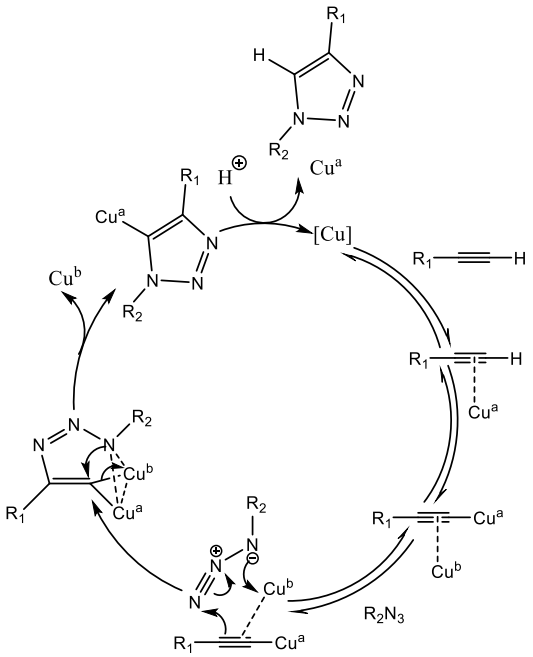

Scheme 7. CuAAC mechanism.

Another cycloaddition-based click reaction is the Strain-Promoted Alkyne Azide Cycloaddition (SPAAC). Instead of using metal catalysis, this reaction relies on activating the alkyne function thanks to the ring strain of cyclooctyne, and hence, presents the advantage of being biocompatible, as it permits to avoid the cytotoxic effect of copper (I) for living organisms.

SPAAC has already been used in glycan-mediated Ab functionalisation. For instance, drug linkers such as bicyclononyne (BCN) and dibenzoannulated cyclooctyne (DIBO) containing cytotoxic payloads, were successfully bio-conjugated to an azido-GalNAc and an azido-SA respectively, previously inserted into Ab glycans through glycan remodeling and leading to homogenous ADCs (scheme 8).[22,25]

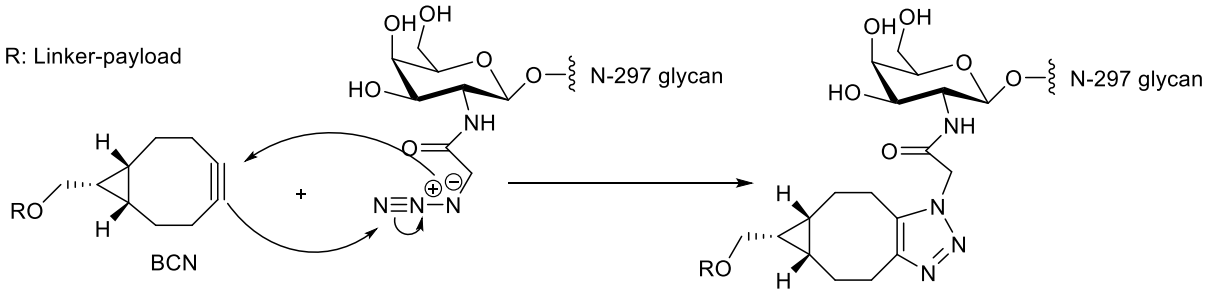

Scheme 8. SPAAC reaction applied for Ab conjugation.

II. Objective

The glycan-mediated Ab functionalisation previously described is attractive, especially when it uses click chemistry to bioconjugate the payload. Indeed, such method allows to take advantage from the regioselectivity of both the glycan remodeling and the follow-up click reaction to afford an Ab conjugate while preserving the integrity of the Fab and hence, the specificity toward the antigen. Moreover, targeting selectively the two N-297 glycans results in an homogenous functionalisation, particularly relevant in ADCs design for the obtention of a constant DAR.

It is therefore evident why such method has already been used to construct new ADCs. In fact, as mentioned at the end of the introduction, clickable sialic acid and N-acetyl galactosamine analogues were successfully exploited and led respectively to anti-CD22 and anti-HER2 ADCs.[22,25] However, such glycan-mediated Ab functionalisation has never been tested using a clickable mannose. It is precisely with the latter saccharide that we have decided to try this Ab functionalisation. It would follow the steps below:

1. Trimming: Ab glycan chains need to be homogenised into a suitable glycoform using a cocktail of glycosidases.
2. Mannosylation: by the action of a mannosyltransferase (ManT), a clickable mannose would be inserted from its possible donor (a clickable GDP-mannose analogue) to the specific acceptor (the trimmed glycans of the antibody).
3. Click reaction: once the glycan remodeling achieved, the payload could be finally joined regioselectively to the antibody through a click reaction (scheme 9).

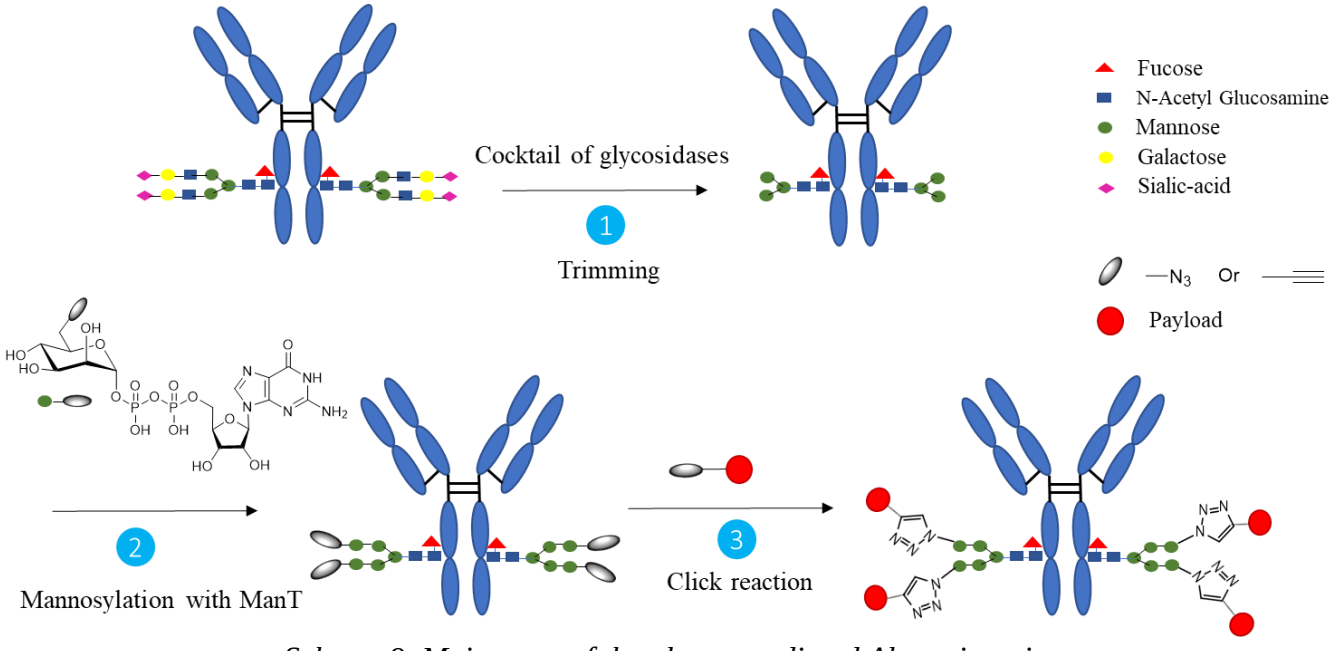

Scheme 9. Main steps of the glycan mediated Ab conjugation

Besides our wish to explore and develop a novel glycoengineering method, using a clickable mannose analogue to functionalise an Ab would expand the possibilities of Ab glycan modifications. It is interesting because any variation in the N-297 glycans could influence the stability, the immunogenicity and the pharmacokinetic of the Ab. Such features, among others, govern the development of better ADC therapy.

In a more fundamental aspect, the pursue of this method permits also to test the tolerance of ManT regarding the clickable modifications. In fact, ManTs use GDP-α-mannose to transfer regio – and stereo selectively a mannose into the suitable acceptor. Such an outcome has to be verified when using clickable GDP- α-mannose analogues, bearing either an azide or an alkyne. Initially, such analogues need to be prepared. Hence, the work established during my Master thesis focused on the chemical synthesis of two GDP-α-mannose analogues, each one carrying a clickable function at position 6 of the mannose:

- The GDP-6-Azido-α-D-mannose **1a**.
- The GDP-α-D-manno-hep-6-ynopyranoside **1b** (scheme 10).

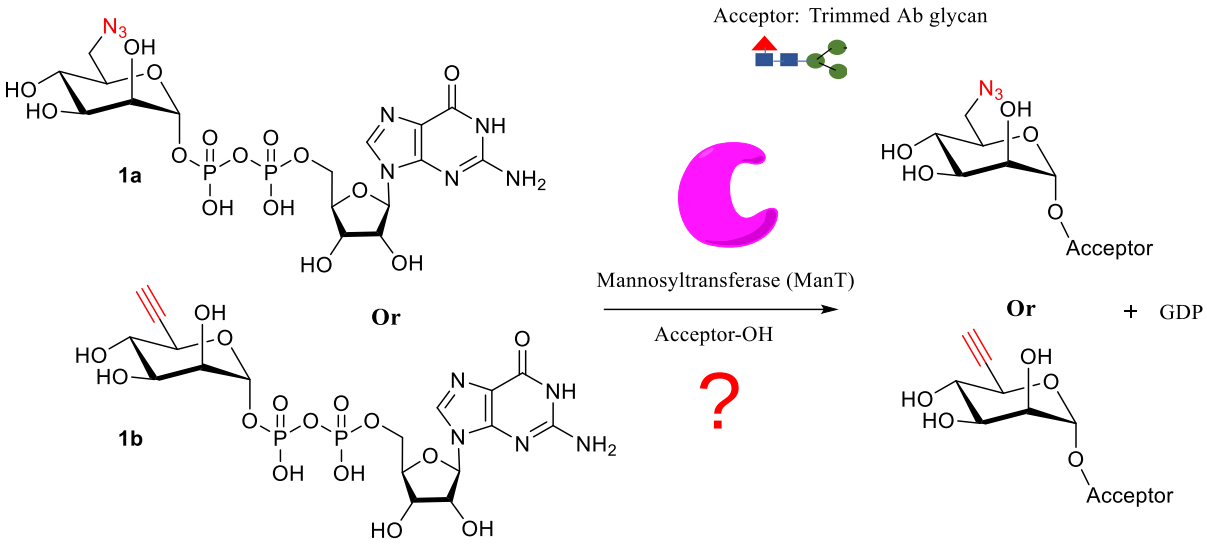

Scheme 10. ManT catalysed mannosylation of an acceptor.

The following section mainly emphasizes the synthetic approach which was pursued to afford GDP-6 azido-α-mannose **1a** while discussing the results obtained. The progress made for the chemical synthesis of the second analogue: GDP-α-manno-hept-6-ynopyranoside **1b**, are presented as well. A conclusion and some perspectives are given at the end of this manuscript.

III. Results and Discussion

III.1 GDP-6 azido-α-D-mannose

The GDP-6 azido-α-D-mannose **1a** belongs to the unnatural nucleoside diphosphate (NDP)-sugars family. It is composed of an azido mannose and a guanosine connected to each other by a pyrophosphate bond. A chemo-enzymatic synthesis of this molecule has already been described by Marchesan *et al.*[26] It uses a pyrophosphorylase enzyme during the last step, to afford the target sugar nucleotide. In order to achieve an enzyme-independent synthesis, we followed a chemical approach, whose key steps are highlighted in the retrosynthetic analysis depicted in scheme 11.

It is noteworthy that the pyrophosphate bond construction through chemical coupling (molecule **1a**) is the limiting step for this sequence, as it is almost always the case with all NDP-sugars chemical syntheses. Besides, the timing of the deacetylation step constitutes a strategic choice. Indeed, the step can be performed at the end of this synthesis,[27] but also, before the coupling reaction, once the stereoselective phosphorylation achieved.[28,29] The latter, is the other important step of the sequence, it aims to stereoselectively obtain isomer **2** with a α configuration necessary for mannosyltransferase's recognition. All this multistep sequence, begins with the regioselective azidation (molecule **3**), starting from the commercially available α-methyl-D-mannopyrannoside **4**.

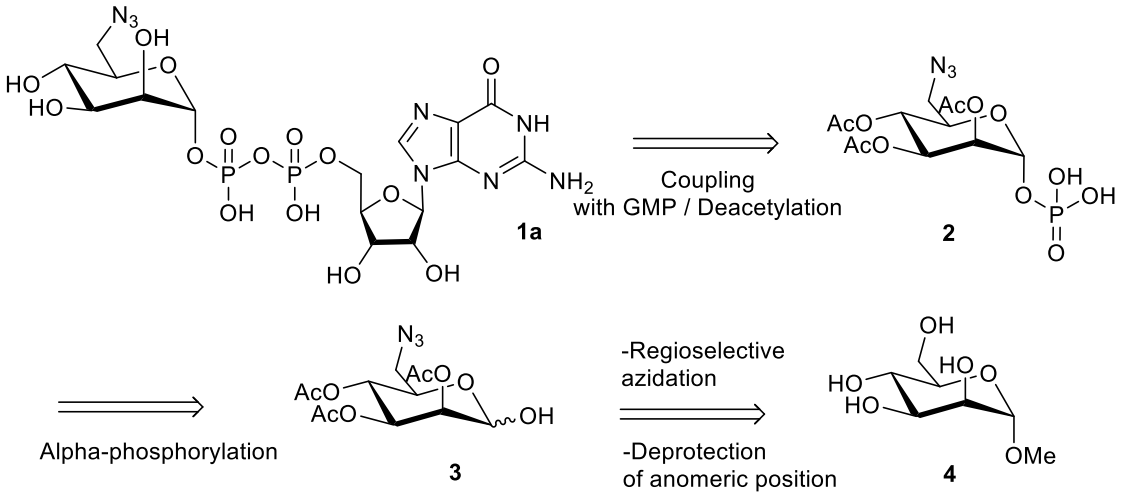

*Scheme 11. Retrosynthetic pathway of GDP-6 azido-α-D-mannose **1a**.*

III.1.1. Synthesis of the triacetylated 6-azido-mannose

In order to obtain the intermediate lactol **3**, we performed the sequence depicted in scheme 12, starting from the commercial precursor α-methyl-D-mannopyrannoside **4**. Besides being cost effective, the latter presents the advantage of bearing a methoxy group which prevents the anomeric position to competitively react with alcohols during the first step of the sequence.

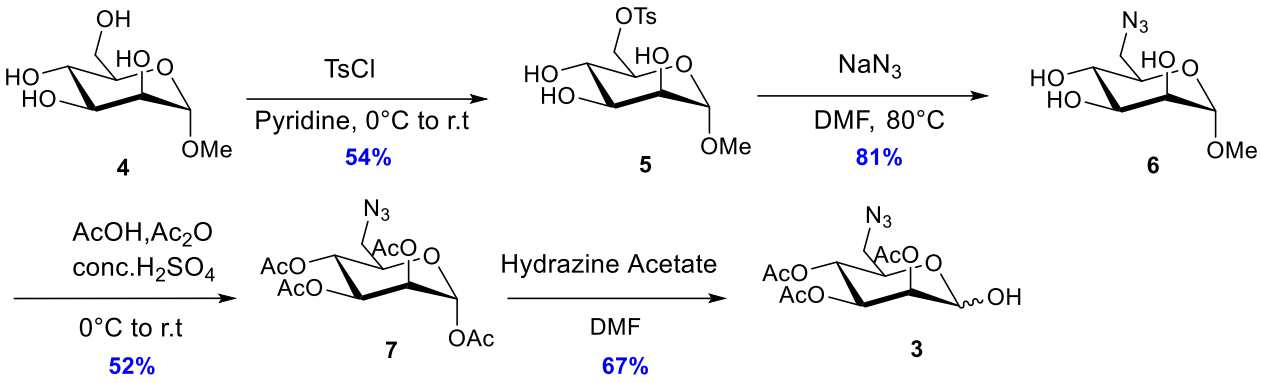

Scheme 12. triacetylated 6-azido-mannose synthesis.

First of all, the primary alcohol of α-methyl-D-mannopyrannoside **4** was regioselectively tosylated to generate a good leaving group. Tosylate **5** was obtained in an average isolated yield of 54%. The use of DMAP as a nucleophilic catalyst increased slightly the conversion (68%). The multigram scale-up of this step decreased the yield, but, afforded enough material to pursue the sequence without further optimisations. The second step was the nucleophilic substitution which, by displacing the tosylate group, gave the desired azide **6** isolated in 81% yield. This good yield was obtained after testing several elution conditions to manage to separate the azido mannose **6** from the tosylate, and it turned out that the best one was 1-10% MeOH in DCM. It is worthy to justify the timing of the latter step. Indeed, the fact that we performed the azidation before the acetylation is based on a previous synthesis of azido-heptosides,[27] which resulted in a better yield following the chosen sequence rather than the reverse one.

The following one pot acetylation/acetolysis which was conducted in acidic conditions, allowed the concomitant acetylation of all secondary alcohols and the acetolysis of the anomeric position through the formation of an oxycarbenium intermediate, which led to the peracetylated 6-azido mannose **7** in 52% yield, without further column chromatography purification.

Finally, the anomeric position was selectively deprotected. This step was actually facilitated by the prior acetolysis. In fact, while the deprotection of the anomeric O-methyl group would require long reaction time, high temperature and strong acids,[30] deprotection of the anomeric acetate was achieved in mild conditions using hydrazine acetate to obtain lactol **3** in 67% isolated yield after silica gel chromatography. The regioselectivity of the deprotection is explained by the fact that the nucleophilic attack of the anomeric ester generates a lactolate, which constitutes a better leaving group than an alcoholate. The reason is that the negative charge resulted in such function is stabilised by the anomeric equilibrium.

According to the ^{1}H NMR of the reaction mixtures, both anomeric acetolysis and deprotection reactions afforded a single anomer, despite going through a cationic sp^2 intermediate. Unambiguously, it is the formation of the α-anomer that has been favoured. In fact, this stereo-purity is due to the anomeric effect in one hand, and, to the steric hindrance displayed by the axial acetyl group carried at C2, which makes difficult the obtention of the β-anomer under the same conditions.

III.1.2. Synthesis of 6-azido mannosyl-1-phosphate

Alpha-phoshorylation

Several synthetic approaches for sugar anomeric phosphorylation have emerged since the first traditional, low yielding MacDonald's reaction, which consists in the α-phosphorylation of peracetylated sugars using phosphoric acid.[31] This growing interest is explained by the fact that glycosyl-1-phosphates are key intermediates in both enzymatic and chemical preparation of sugar nucleotides, and by their high cost and/or lack of commercial availability on the other hand.

Hence, two main chemical strategies can be used in order to achieve the synthesis of glycosyl-1-phosphates:[32]

- Glycosylation reaction using a nucleophilic phosphate and an electrophilic glycoside (scheme 13.A)
- Condensation reaction between an anomeric lactol and an electrophilic phosphorylating agent (Scheme 13.B). The latter, can be either a phosphate (P^V approach) or a phosphite/phosphoramidite (P^{III} approach).

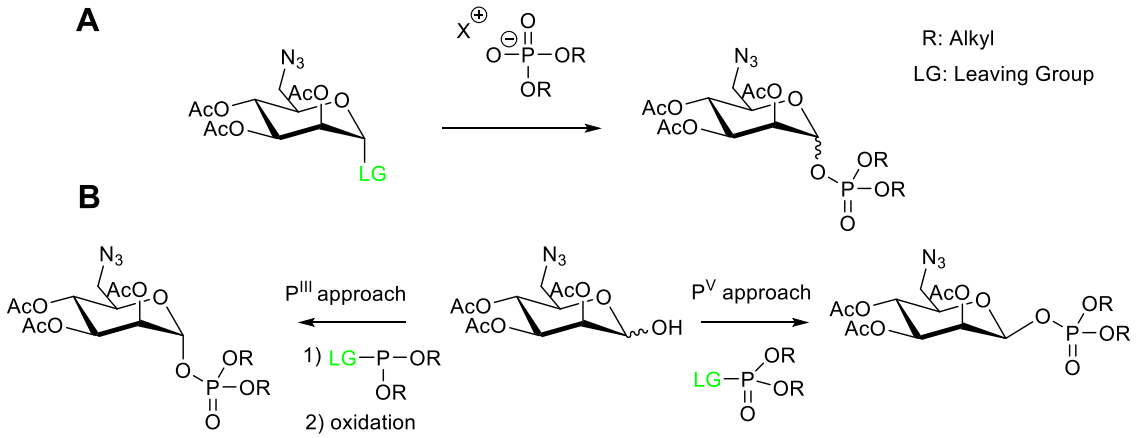

Scheme 13. Main strategies for carbohydrates anomeric phosphorylation.

Based on preliminary studies realised in the CBO laboratory,[27,32] we opted for the second strategy. To do so, the phosphorylating agent had to be well chosen.

Indeed, according to the previously published work, it turns out that, starting from mannopyranosides analogues, chlorophosphate derivatives preferentially afford the β-phosphate anomer, while phosphoramidite derivatives mainly gave the α stereoisomer.[32] It is hence the latter approach, described also as the P^{III} approach, that has been selected to afford the desired α-phosphate **9**.

Actually, phosphoramidites chemistry was initially known and most used in oligonucleotides chemical synthesis.[33] It expanded later on, to the synthesis of glycosyl-1-phosphate[34] and also NDP-sugars.[35] Such reaction most often relies on tetrazole catalysis. Tetrazole is both a catalytic weak acid which permits the protonation of the leaving group nitrogen of the phosphoramidite, and also, a catalytic nucleophile through the formation of a highly reactive tetrazolophosphane intermediate. This dual role was further highlighted by Wittmann et al,[36] who exploited tetrazole catalysis to increase the kinetic of phosphomorpholidate coupling reactions. Herein, both acidic and nucleophilic tetrazole contributions aim to facilitate the condensation of the electrophilic phosphitylating agent and the hydroxy group of lactol **3**, as depicted in the scheme 14.

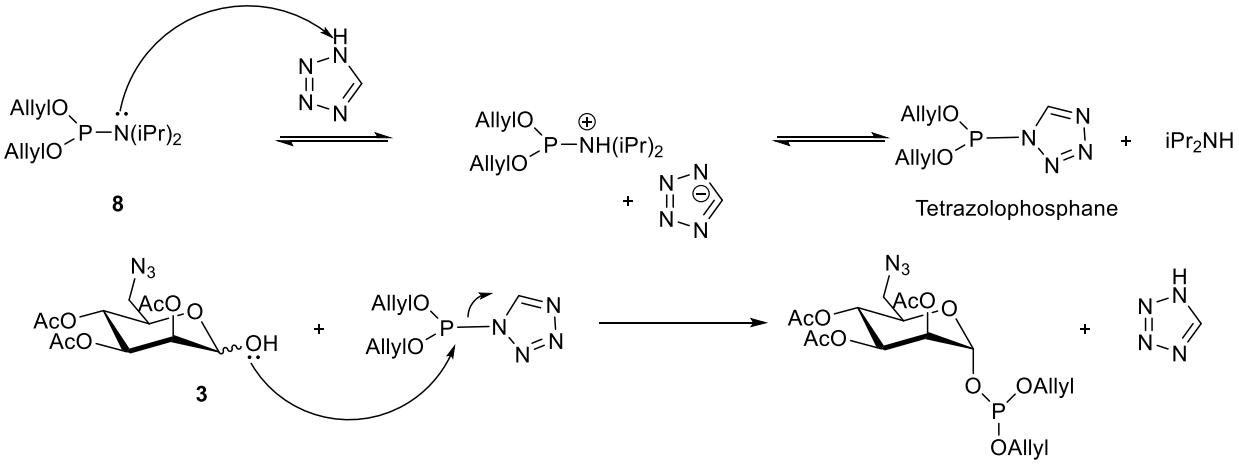

Scheme 14. dual role of tetrazole in the activation of phosphoramidites.

Thus, starting from hemiacetal **3**, the α-phosphorylation was realised in a two steps sequence: Initially, a phosphitylation was performed using tetrazole and diallyl-*N*,*N*-diisopropylphosphoramidite **8** to afford an intermediate diallylphosphite. The latter was then oxidized using mCPBA, to obtain the expected α-phosphate **9** as the major product (8:1 α/β selectivity) in 62% isolated yield (scheme 15).

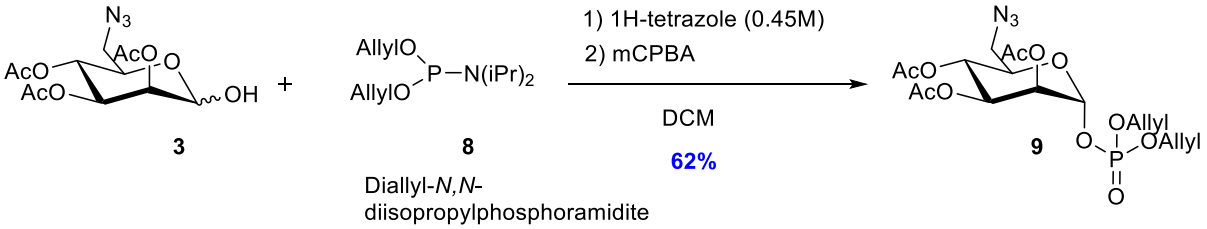

Scheme 15. alpha phosphorylation of 6-azido mannose.

With 1,2-*trans*-pyranosides, α or β absolute configurations might be directly assigned based on ^{1}H-^{1}H coupling constants. When the substituent at C-2 is equatorial, the 1,2-*trans*-diaxial relationship found in the β anomer of such carbohydrates, is detected by a characteristic high vicinal $^{3}J_{1,2}$ coupling constant, while an axial-equatorial coupling which is close enough to the equatorial-equatorial one displays $^{3}J_{1,2}$ constants whose values do not exceed 4Hz. However, in the case of mannosyl-1-phosphates, α and β anomers display equatorial-equatorial and axial-equatorial couplings respectively, as the H2 proton is equatorial. Hence, the anomeric absolute configuration has to be ascertained by another technique than just the scalar coupling. The typical characterization technique for this purpose is the Nuclear Overhauser Effect (NOE) observed in NMR. Rather than focusing on proton interactions through chemical bonds as for coupling constants, this technique allows to detect interactions between protons through space. Indeed, it consists in irradiating a specific nucleus (the anomeric H1 proton herein), and detect the possible resonances of the protons in close proximity with the irradiated one.

The α anomeric configuration of phosphate **9** was thus checked with 1D NOE NMR experiments. The NOE spectrum of **9** shown in figure 6 is different from NOE spectra previously obtained in our laboratory for β-mannopyranosides.[32] Based on these data, a β-anomer would have exhibited characteristic interactions between H1, H3 and H5. Those interactions are not detected herein. The interactions detected around 5.30 ppm may originate from H2 or allylic protons.

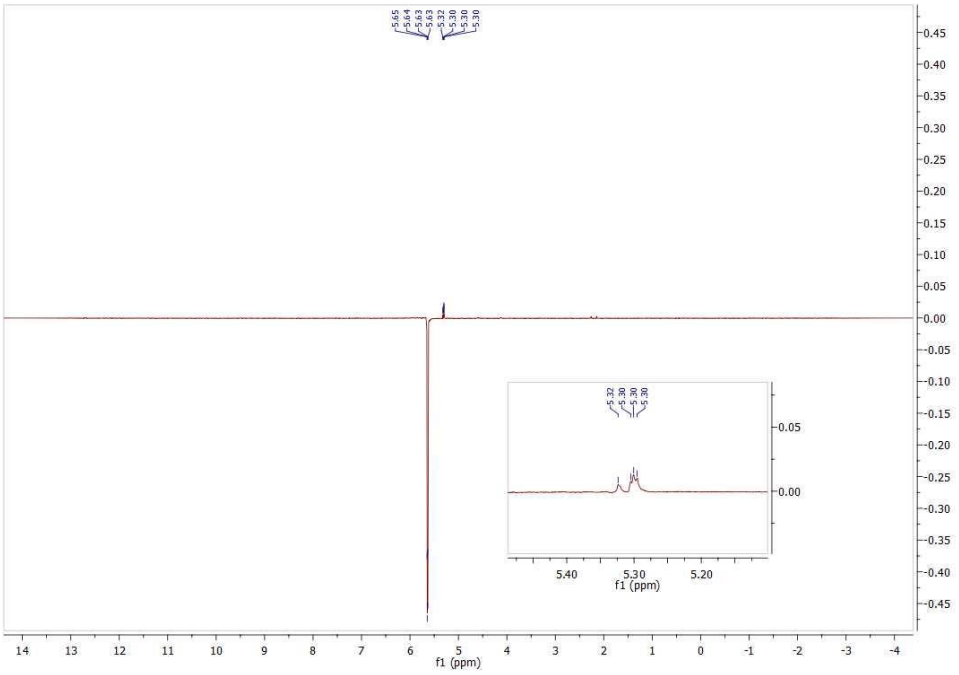

Figure 6. 1D NOE NMR spectrum of phosphate 9

Deprotection strategy

With the aim of engaging the synthesized α-phosphate **9** into the pyrophosphate bond construction, allyl esters had to be chemoselectively deprotected. It is worth noting that the choice of the protecting groups and hence the deprotection strategy are important for this sequence. In fact, they all have to be compatible with the azide group and the anomeric phosphate. Herein, the deprotection of allyl groups which are commonly used in carbohydrate chemistry, may be achieved using several methods. One possibility requires a two-step procedure, which involves firstly the rearrangement of the allyl into a propenyl, either by the action of potassium tert-butoxide (KOtBu) in DMSO, or through transition metal catalysis such as Rh(I), Ir(I), Pd-C, followed secondly by the cleavage of the resulting enol mainly through hydrolysis.[37] Another deallylation possibility, which occurs interestingly in one step, exploits Pd catalysis that induces the cleavage through a π-allyl palladium complex intermediate.[38] In our case, it is the latter strategy that has been adopted to achieve the deallylation of phosphate **9** .

Noteworthy, Pd catalysts active for such reaction are Pd(0) species such as tetrakis triphenylphosphine palladium. Nevertheless, Pd(II) species such as $PdCl_2$ or $Pd(OAc)_2$ can also be used as Pd(0) precursors.[39] They are reduced *in situ* for instance by alcohols before entering into the catalytic cycle. The latter is depicted in the scheme 16 below.

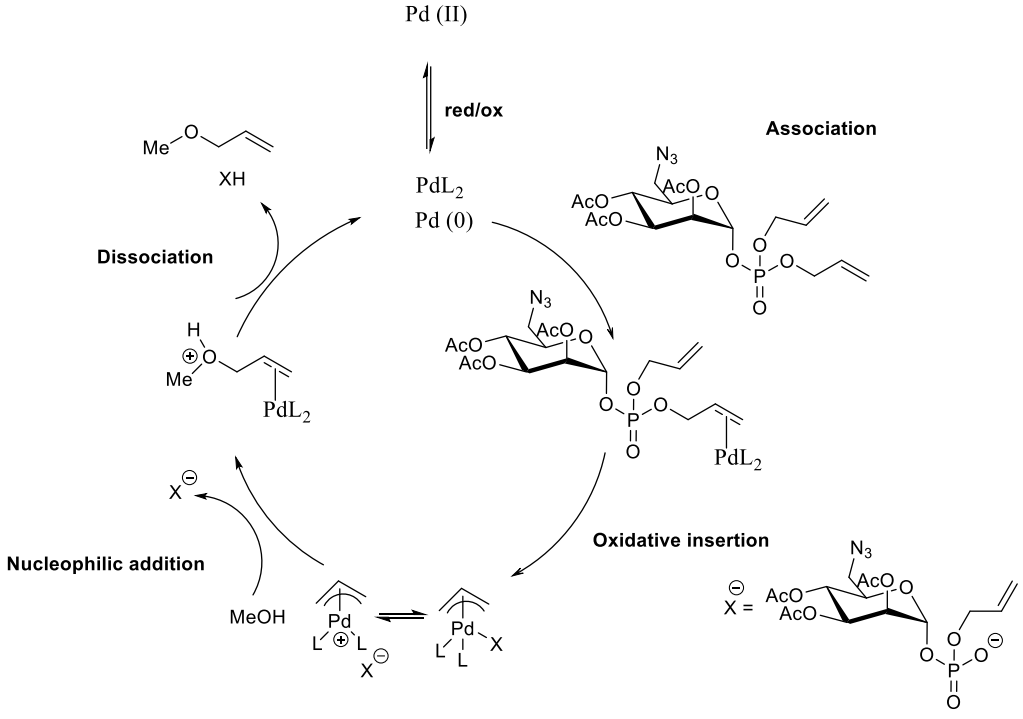

Scheme 16. Pd-catalysed deallylation reaction

Thus, deallylation of phosphate **9** was performed using 50 mol % of $PdCl_2$ in a mixture DCM/MeOH, to obtain the deprotected phosphate **10** which was recovered directly as a bis triethylammonium salt due to the use of triethylamine in the elution solvent of the column chromatography. However, the moderate 43% yield obtained for this reaction, encouraged us to attempt another Pd-catalyzed deallylation. Inspired by other published works,[26,40] reaction using catalytic amount of tetrakis triphenylphosphine Pd and sodium p-toluenesulfinate as an allyl scavenger was launched and led to the bis triethylammonium salt form of phosphate **10** in 60% yield after silica gel chromatography.

The deprotected phosphate **10** is a key precursor for this synthesis, because it constitutes the sugar building block of the target sugar nucleotide **1a**. Despite the benefits of enhancing further the yield of such important intermediate, the priority was to pursue the rest of the sequence and test the feasibility of the chemical formation of the pyrophosphate bond in molecule **1a**.

At this stage of the sequence, another possible pathway is to totally deprotect the α phosphate **9** by removing also the acetyl groups **11** in order to try a protecting-group free chemical coupling, whose success affords directly the desired molecule **1a**. To do so, Zemplén deacetylation using sodium methoxide (NaOMe) in dry MeOH, known for its fast kinetic, seemed attractive. Thus, it was tested on the phosphate analogue **9.** Unfortunately, no reaction occurred after 24h of stirring. Alternatively, the deallylated precursor **10** was suspended in a mixture of 5:2:1 MeOH/H_2O/TEA and stirred during 22h, which resulted quantitatively in the fully deprotected precursor **11**.

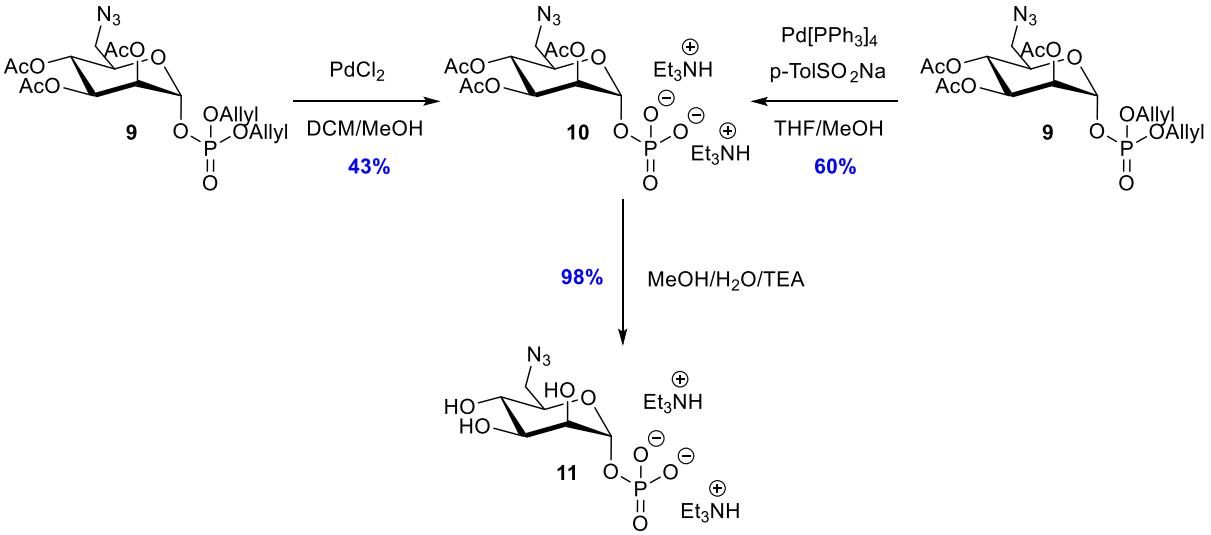

Scheme 17. the pathways tested for the deprotection of phosphate 9

Both mannosyl-1-phosphate analogues **10** and **11** were then engaged in the chemical coupling, whose results are detailed in the following section.

III.1.3. Synthesis of guanosine phosphorimidazolide (GMP-Im)

Mannosyl-1-phosphate analogues previously described could now be coupled with another key building block: the activated guanosine-5'-monophosphate (GMP) to induce the chemical formation of the pyrophosphate linkage, and hence, afford GDP-6-azido-mannose **1a** (scheme 18). Noteworthy, another possibility to synthesise NDP-sugars in general, while bypassing the challenging P-O-P connection, is through the anomeric linkage between an electrophilic glycoside and a nucleoside-5'-diphosphate.[41] Nevertheless, the latter procedure remains less attractive because it requires to find the suitable electrophile and has the inconvenient of lacking anomeric diasteroselectivity.[42] It is mainly for this second reason that we have decided to achieve the synthesis of GDP-6-azido-mannose by going through pyrophosphate bond construction. Indeed, such mechanism has the advantage of keeping unmodified the α-anomeric configuration of mannosyl-1-phosphate analogues while building the final molecule, and thus, allows to afford a crucial anomeric pure GDP-6-azido-α-mannose **1a**.

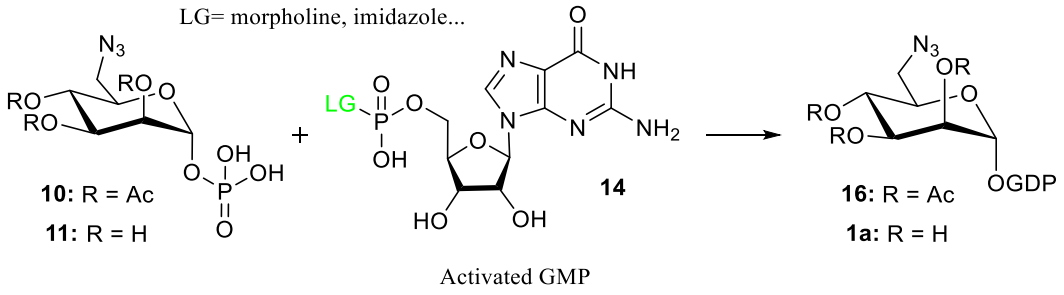

Scheme 18. the selected strategy for pyrophosphate bond formation.

The challenge in the selected approach, arises from slow kinetics and possible side reactions which highly complicate the purification step, usually performed by HPLC and/or size exclusion chromatography. However, many advances have been published, so as to increase both the kinetic and the yield of the reaction.[43] They have mainly focused on improving the activation of the nucleoside precursor through the selection of different attached leaving groups (LG). In this case, various activated nucleosides can be employed: starting from the classical nucleoside phosphomorpholidate (Khorana's strategy), to newer activated intermediates such as nucleoside phosphoramidites,[35] cyclosal nucleotide,[44] and also nucleoside phosphorimidazolide.[45] The latter intermediate has been chosen herein, since it was already successfully adopted for the synthesis of ADP-heptose in our laboratory.[27]

Inspired by Jemielity et al,[45] the first attempt to afford this second important building block **14** consisted in exploiting two coupling reagents: 2-2'-dithiopyridine and triphenylphosphine - as in the Mukaiyama Hashimoto procedure[46] - to induce the condensation of imidazole with the guanosine monophosphate (GMP) triethylammonium salt **13**. Hence, preparation of **14** was launched in DMF using triethylamine as a base. Unfortunately, the product recovered after precipitation still contained non activated GMP **13** as monitored by ^{31}P NMR. In fact, GMP conversion to GMP-Im **14** was only 57%. In contrast, performing in parallel, an AMP activation under the same conditions resulted in a total conversion.

This outcome might be related to the limited solubility of GMP (even its triethylammonium salt form) into DMF. Besides the solubility issue in organic solvents, strict anhydrous conditions have to be employed in order to avoid the easy hydrolysis of the desired GMP-Im intermediate **14** into the starting GMP **13**.

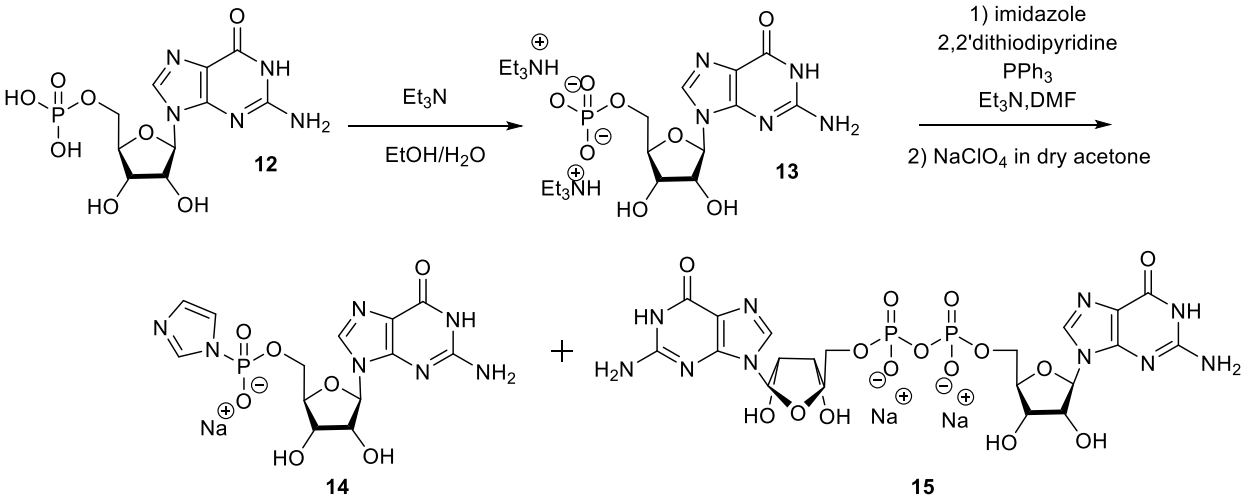

*Scheme 19. formation of GMP-Im **14** and the by-product GPPG **15**.*

Improvements for this step were most needed also because the GMP which remains non activated **13** inevitably self-couples with the highly reactive GMP-Im **14**, and hence interferes with the necessary cross coupling of GMP-Im and mannosyl-1-phosphate analogue. Other than decreasing the yield, this self-coupling side reaction affords the GPPG dimer **15**: a by-product difficult to separate by HPLC from the target GDP-6-azido-mannose **1a**, because both share close polarity. These transformations can be easily followed by ^{31}P NMR as each molecule gives a characteristic singlet: **13** (4.36 ppm); **14** (-7.30 ppm); **15** (-10.72 ppm) in D_2O.

In order to circumvent the issues related to GMP solubility and thus conversion, we decided to tune some factors such as: increasing solvent volume and/or reaction time, but also, transforming GMP into a tributylammonium salt rather than the triethylammonium one, affording a slightly more lipophilic counterion. Unfortunately, none of these changes leads to considerable improvements.

In another attempt and inspired by the synthesis of GDP-fucose analogues, published by Baisch *et al*,[47] we chose to use carbonyl diimidazole (CDI) to generate the desired GMP-Im intermediate. Reaction between GMP tributylammonium salt and 3 equivalents of CDI was launched in DMF. After stirring overnight, the conversion into GMP-Im was only 32% according to the ^{31}P NMR evaluation of the product which was recovered by precipitation. Gratifyingly, increasing the amount of CDI to 6 equivalents afforded 90% of GMP-Im **14**.

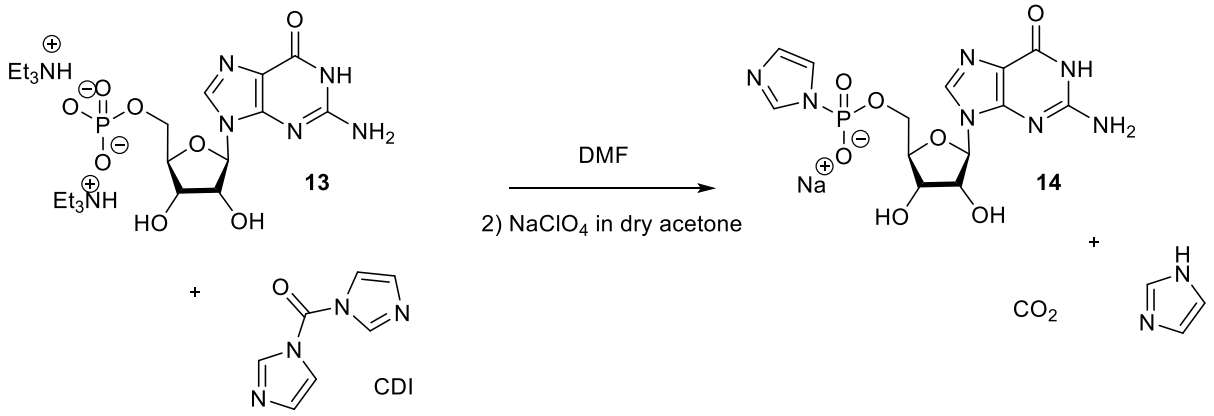

Scheme 20. GMP-Im synthesis using CDI

Due to the high reactivity of GMP-Im intermediate **14**, it would be interesting to generate it *in situ*, and start the coupling reaction right after, in a one-pot procedure.

III.1.4. Chemical coupling: pyrophosphate bond formation

At this stage of the sequence, both building blocks of the GDP-6-azido-mannose (sugar and nucleotide moieties) are synthesised and the chemical coupling reaction between them can be performed. Several aspects might be considered in order to find optimal reaction conditions which lead to an effective pyrophosphate bond construction. Indeed, solvent, counterions, activators, to only name a few, have to be well chosen for this reaction step. Another strategic choice previously evoked is whether it is necessary or not to perform the chemical coupling on a protected mannosyl-1-phosphate analogue.

Generally, the presence of acetyl protecting groups slightly decrease the polarity of glycosyl-1-phosphate analogue which facilitate both its solubility in organic solvents, and the purification of the resulting sugar-nucleotide. For instance, acetylated heptose phosphates led to better yields for the coupling reaction with AMP and to more efficient purification than the deprotected ones, according to Zamyatina *et al.*[48] In contrast, a protecting-group free coupling reaction remains attractive because it permits to avoid a deacetylation step once the sensitive pyrophosphate bond formed. In addition, the solubility of a deprotected glycosyl-1-phosphate could always be improved through its trialkylammonium salt form and also by the presence of metal ions.

In our case, we have decided to test the coupling with GMP-Im **14** on both the protected **10** and the deprotected **11** mannosyl-1-phosphate, following Jemielity's procedure which exploits $MgCl_2$.[45] The latter is presumably playing multiple roles in the coupling reaction. In fact, magnesium chloride is used in order to increase the solubility of the reactants. Moreover, by acting as a Lewis acid catalyst, it would increase the nucleofugacity of imidazole and would also facilitate the pyrophosphate bond formation by coordinating the sugar and the nucleotide moieties.[45]

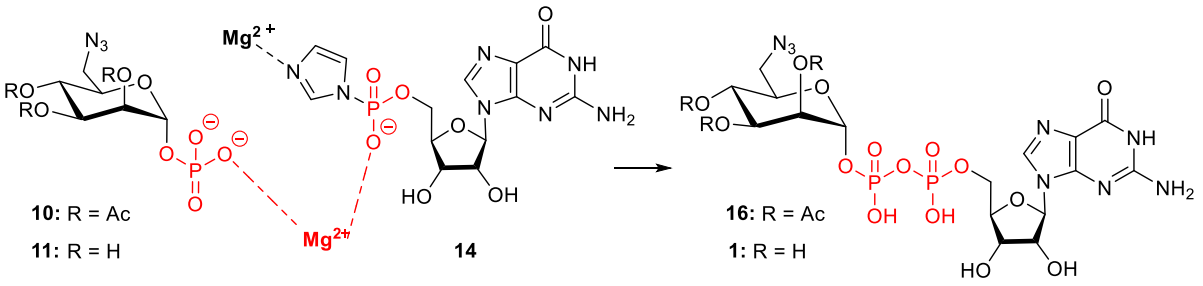

Scheme 21. $MgCl_2$ catalysis for pyrophosphate bond chemical formation.

First, the triacetylated mannosyl-1-phosphate **10** was reacted with GMP-Im **14** in DMF, in presence of $MgCl_2$. After 24h of reaction, TLC (C18 plate) showed a total conversion of the glycoside which was supported by the ^1H NMR spectra of the reaction mixture. A purification by reverse phase HPLC (50mM triethylammonium acetate, 1-5% acetonitrile gradient) was then realised. However, the desired product **16** still presented impurities that could not be successfully separated. Thus, we decided to pursue the final deacetylation step, and reconduct a purification on the deprotected sugar nucleotide.

Due to the lability of both glycosidic and pyrophosphate bonds, it was important to achieve the deacetylation of the sugar nucleotide in very mild conditions. Hence, starting from the protected analogue **16**, acetyl groups were removed by reaction with NH_4HCO_3 in aqueous solution in the presence of Et_3N. Finally, a purification by reverse phase HPLC was successfully achieved following the same conditions previously cited. GDP-6-azido-α-D-mannose **1a** was obtained with a good purity. However, the yield was only 5% over two steps. Such low value, which could possibly arise from a hydrolytic cleavage during the deacetylation step, encouraged us to test further the protecting-group free chemical coupling.

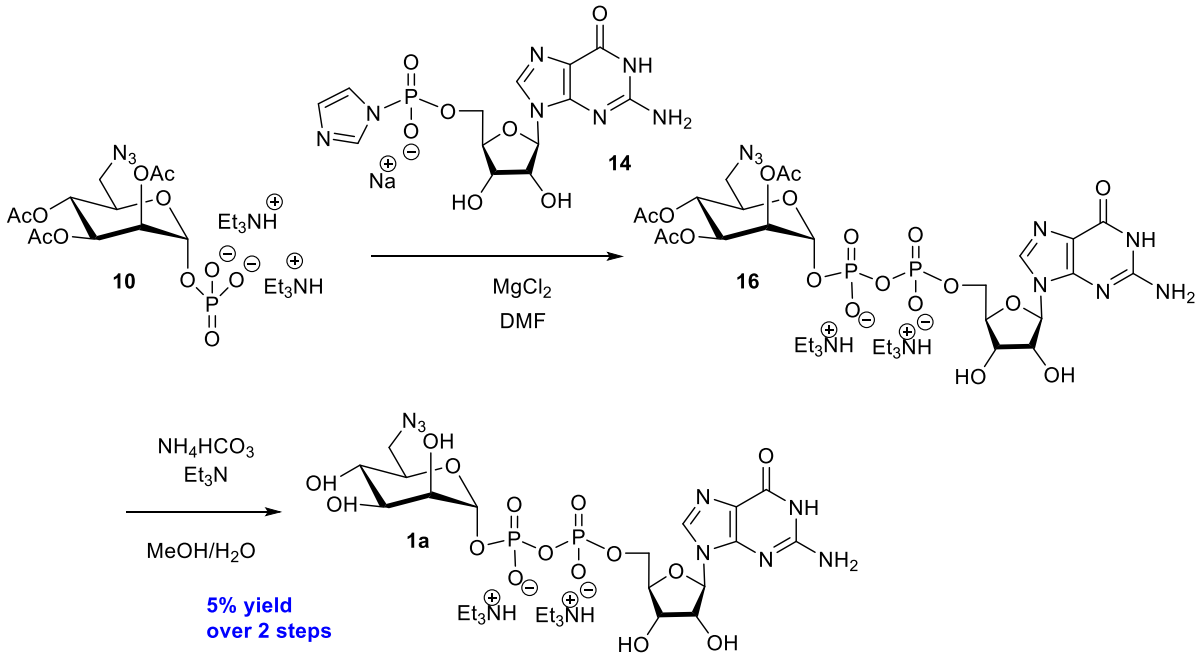

*Scheme 22. GDP-6-azido-mannose synthesis starting from the protected mannosyl-1-phosphate **10**.*

Therefore, and following the same Jemielity's procedure, the fully deprotected mannosyl-1-phosphate analogue **11**, was reacted with GMP-Im **14** in DMF, in presence of $MgCl_2$. After 20h, the reaction was quenched and the mixture was lyophilised. The ^{31}P NMR spectrum of the reaction mixture clearly showed the pyrophosphate bond formation by displaying two characteristic doublets at -10 and -13 ppm. The following purification was performed by RP-HPLC (50mM triethylammonium acetate, 1-5% acetonitrile gradient), to obtain a pure GDP-6-azido-α-D-mannose **1**.

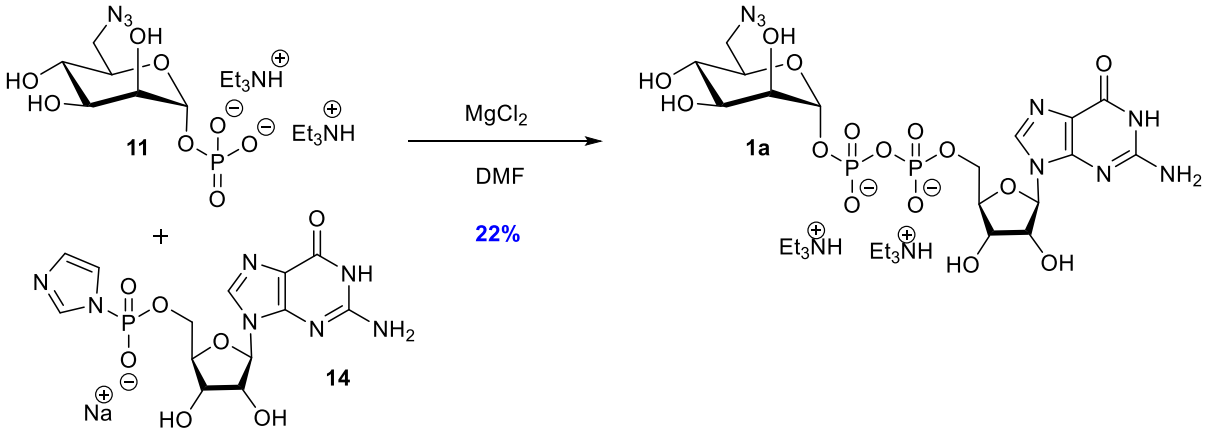

Scheme 23. a protecting-group free chemical coupling for the synthesis of GDP-6-azido-mannose

Compared to the first coupling reaction, this protecting-group free chemical coupling, not only proved to be effective for leading to the target molecule **1a**, but afforded it with a higher yield of 22%. The latter could certainly be improved by adjusting the purification conditions. In fact, the selected gradient elution resulted in a lengthy purification step, which could be shortened, especially because no GPPG by-product **15** was noticed according to the ^{31}P NMR spectrum of the reaction mixture.

III.2 GDP-α-D-manno-hept-6-ynopyranoside

The last part of this section will focus on the advances made in the chemical synthesis of the second clickable GDP-mannose analogue: the GDP-α-D-manno-hept-6-ynopyranoside **1b**. Herein, the clickable function consists of a terminal alkyne born at position 5 of the mannose analogue. Key steps of the chosen synthetic approach are highlighted in the retrosynthetic analysis depicted in scheme 24.

While the strategy previously adopted for the chemical coupling with GMP and the alpha-phosphorylation could be extrapolated and tested for the synthesis of molecule **1b**, a viable synthetic route has to be found concerning the C-homologation necessary to afford the C6 alkyne **18**.

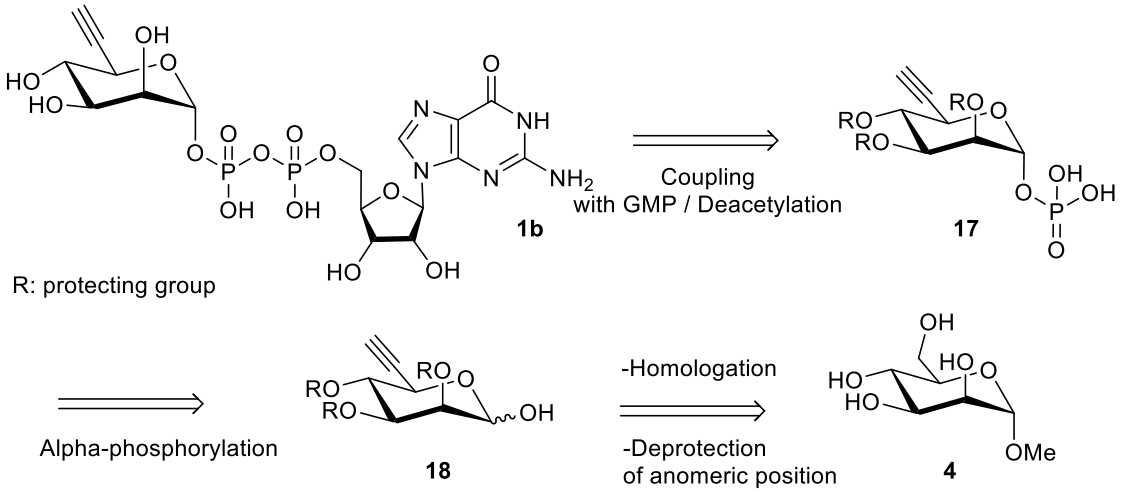

*Scheme 24. retrosynthetic pathway of the GDP-α-D-manno-hept-6-ynopyranoside **1b***

Hence, the first attempt to obtain intermediate **18** started by the selective protection of the primary alcohol carried on the commercially available precursor: α-methyl-D-mannopyrannoside **4** (scheme 25). For this purpose, a bulky silyl chloride (TBDMSCl) was used which afforded compound **19** after reaction in DMF and in presence of imidazole. The latter was engaged in the next step without further purification. After that, the orthogonal protection of all secondary alcohols was performed using benzyl bromide (BnBr) in presence of sodium hydride (NaH). However, after 20 hrs the reaction was not complete and the purification by silica gel column chromatography failed in separating the tribenzylated intermediate **20** from BnOH impurity.

Despite the improvements needed for this step, the objective (considering the time left) was to reach the main step of this reaction sequence: the homologation. Hence, we decided to resume the sequence directly from the intermediate **21**, previously synthesised in large scale in our laboratory. The primary alcohol of analogue **21** had to be oxidized in order to afford a key aldehyde necessary for the following reaction. To do so, both Dess-Martin and Swern oxidations were tested and, both led to the desired aldehyde according to the ^{1}H NMR. Nevertheless, Swern oxidation resulted in less minor impurities: which is an advantage especially because it is crucial to use the obtained aldehyde **22** without further purification, considering its high reactivity.

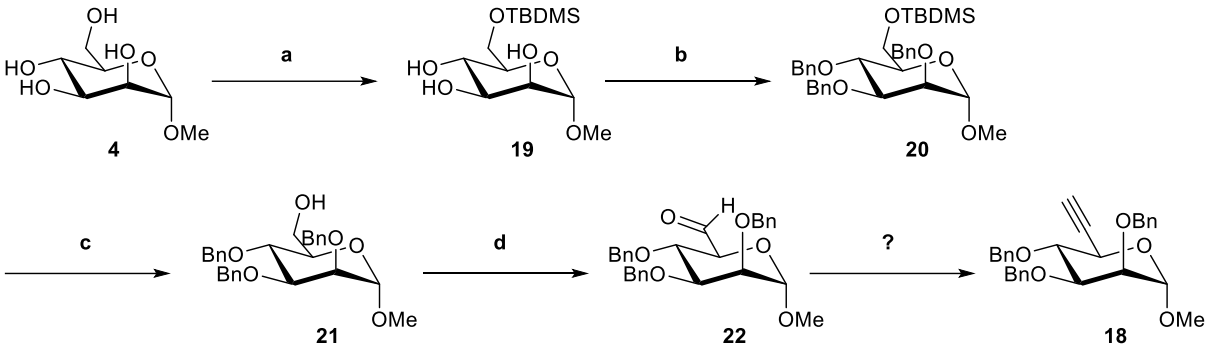

*Scheme 25. Proposed sequence for the synthesis of alkyne **18**.*
a) TBDMSCl, Im, DMF; **b)** BnBr, NaH, DMF, 0°C to r.t; **c)** H_2SO_4, MeOH, r.t (work in progress); **d)** DMP, $NaHCO_3$, DCM, 0°C to r.t (Dess Martin oxidation) or DMSO, oxalyl chlorid, NEt_3, DCM -78°C to r.t (Swern oxidation).

Once the aldehyde function installed, several methods could be tested for the formation of the terminal alkyne **18**. Indeed, since the historical Corey-Fuchs method,[49] which consists in the formation of a dibromoolefin followed by the elimination of a hydrogen halide; other alternatives have emerged, especially reactions which exploit diazo derivatives.

Herein the first attempt to obtain the alkyne **18** was by reacting at -78°C, aldehyde **22** with a diazosilyl derivative: the trimethylsilyldiazomethane which was priorly deprotonated in presence of LDA. Such reaction was successfully applied for the transformation of benzophenone into diphenylacetylene.[50] It was extended later for the conversion of aryl alkyl ketones and aldehydes into their homologous alkynes, by subsequent heating under reflux.[51] The mechanism is based on Colvin rearrangement, which involves first nucleophilic attack at the carbonyl carbon by $TMSC(Li)N_2$ to give the α-diazoalkoxide **23** (scheme 26). Then, subsequent elimination of TMSOLi and N_2 gives the alkylidene carbene **24**. The latter undergoes a rearrangement to lead to the target alkyne.

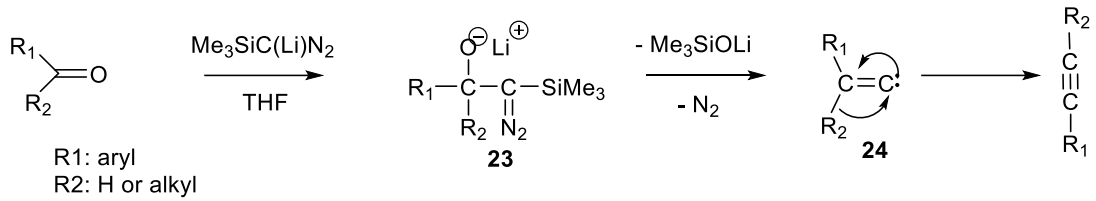

Scheme 26. alkyne formation using trimethylsilyldiazomethane.

Unfortunately, when we tested this reaction on aldehyde **22**, a complex mixture was obtained apparently without any alkyne, according to the ^{1}H NMR analyses.

In another attempt, rather than using a diazo silyl compound, we have decided to exploit a diazo phosphonate one.[52] This approach has already been used in the CBO laboratory for a similar homologation on a galactose analogue.[53] It consists first on preparing *in situ* the dimethyldiazomethylphosphonate (DAMP) **26** through diazotransfer between p-toluenesulfonylazide and dimethyl-2-oxopropylphosphonate **25**, then, a subsquent reaction with an aldehyde in a one pot procedure generates an alkyne following a similar mechanism than the one evoked below.

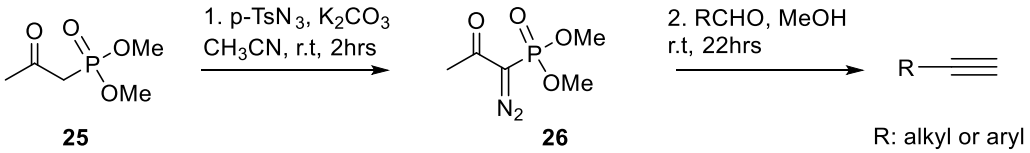

Scheme 27. alkyne formation using DAMP prepared in situ.

Here again, the result of this reaction with aldehyde **22** was not satisfactory. Further investigations have to be done in order to understand the issues, and propose a viable synthetic route.

IV. Conclusion

The objective of this Master thesis was to chemically synthesise clickable GDP-mannose analogues as potential ManT substrates, to be exploited in a glycan-mediated conjugation in order to functionalise site-selectively antibodies. Compared to the natural GDP-mannose, such analogues are distinguished by the integration of either an azide or an alkyne functions.

The first analogue that captured our attention was GDP-6-Azido-α-D-mannose **1a**. While a chemoenzymatic synthesis of this molecule has already been achieved, using pyrophosphorylase to construct the key P-O-P linkage, a viable chemical synthetic route had to be found, especially to accomplish the enzyme-independent pyrophosphate bond formation (scheme 28).

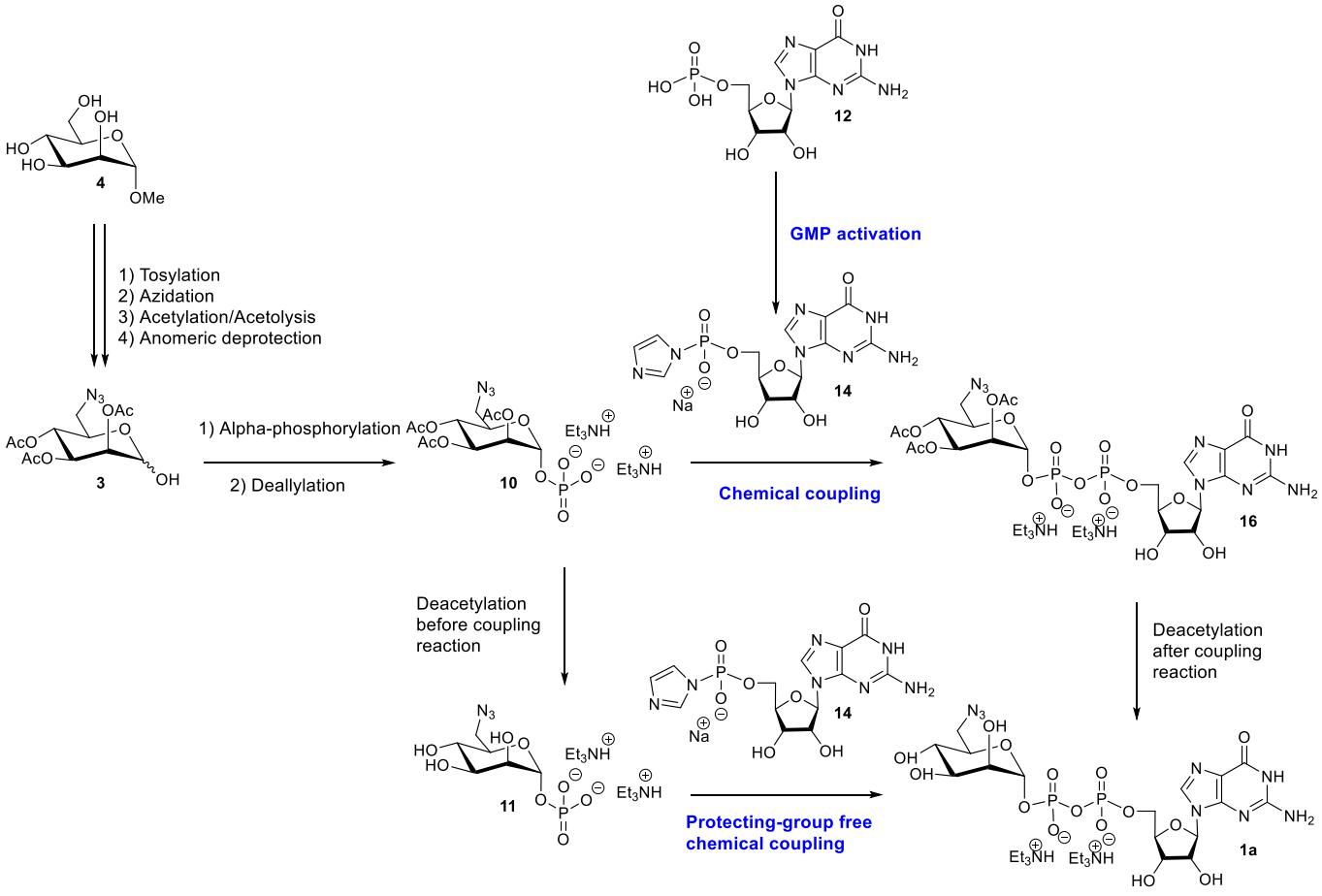

*Scheme 28. overview of the chemical synthesis of GDP-6-azido-mannose **1a**.*

The first target intermediate that was synthesised was lactol **3**, which was obtained in 4 steps without major issues.

Lactol **3** was then engaged in a phosphorylation reaction, where we exploited the previous screening of phosphorylating agents realised in the CBO laboratory, to select the suitable conditions that led to the necessary α-phosphate. After that, Pd-catalysed deallylation reaction was performed to obtain the first key building block: a protected mannosyl-1-phosphate **10**.

The synthesis of the second building block; GMP-Im **14,** was somehow challenging, due to the lack of solubility of GMP in organic solvents and the high reactivity of the target GMP-Im which could be easily hydrolysed and self-couple with GMP, leading to a non-desirable GPPG dimer. Several conditions were tested and it turned out that the use of a large excess of CDI in DMF afforded the activated GMP **14** with good purity.

Then, the chemical coupling between the two building blocks was pursued. Two pathways were possible depending on the necessity or not to maintain the acetyl protecting groups of **10** during the coupling reaction. After testing both pathways, it appeared that a protecting-group free chemical coupling was more indicated for the synthesis of GDP-6-azido-α-D-mannose **1a**. It led to a better yield while avoiding a tricky deacetylation step once the key pyrophosphate bond chemically formed.

Considering the time left, the synthesis of the second analogue: GDP-α-manno-hept-6-ynopyranoside (scheme 29), could not be totally achieved. Nevertheless, some conditions have been screened, which might be useful especially for the obtention of the key homologous alkyne.

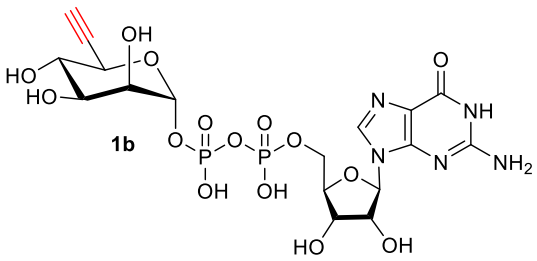

*Scheme 29. structure of GDP-α-manno-hept-6-ynopyranoside **1b.***

Despite the work that remains to be done concerning the synthesis of **1b**, the objective of the master can be considered fulfilled. Indeed, the clickable GDP-6-azido-α-D-mannose **1a** will permit to pursue the rest of the project by testing the tolerance of ManTs toward the 6-N_3 modification of its donor substrate. Besides improving the fundamental insights about ManT activity, these enzymatic tests, could hopefully initiate the use of a mannosylation machinery in the glycoengineering of glycoproteins in general and in a glycan-mediated Ab functionnalisation in particular.

V. Perspectives

Even if the GDP-6-azido-α-D-mannose has been successfully synthesised, by employing a P^V-P^V approach to construct chemically the pyrophosphate bond, the overall yield of the multistep sequence remains low, and has to be improved for a more reliable synthesis.

An interesting outlook would be to optimise further the yield of the deallylation reaction. The reason is that such reaction affords a key building block, which constitute the limiting reactant in the follow up coupling reaction. Hence, enhancing the yield of this step, would positively influence the scale in which the pyrophosphate bond is formed. A gram scale of all the sequence could then be attempted.

Moreover, it is crucial to tune the elution conditions of the final HPLC purification, in order to have a shorter elution time. The latter may be one reason of decreasing the yield in the performed protecting-group free coupling reaction. Noteworthy, the same conditions were successfully applied for the purification of other sugar nucleotides in our laboratory and prevented also from performing a dual size exclusion and HPLC purifications, frequently encountered in sugar nucleotide synthesis.

Other than these adjustments, the major remaining work will particularly focus on the synthesis of the second clickable GDP-mannose analogue, where a viable synthetic route has to be found. Attempts using diazo derivatives were launched in order to afford the key homologous alkyne, without any good results. As a perspective, it would be interesting to retry the alkynylation with dimethyldiazomethylphosphonate (DAMP) **26**, following a non *in situ* protocol through the original Bestmann-Ohira method (scheme 30).

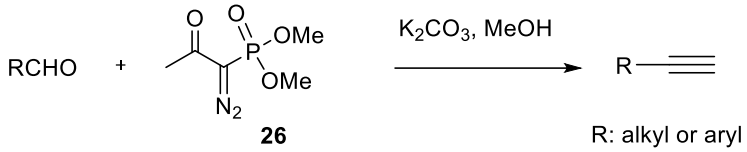

Scheme 30. conversion of an aldehyde into an alkyne following Bestmann-Ohira method.

Alternatively to the use of diazo derivatives, the Corey Fuchs reaction could be tested as well (Scheme 31).

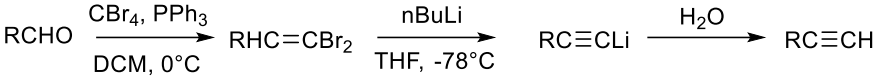

Scheme 31. conversion of an aldehyde into an alkyne following the Corey-Fuchs reaction.

Ultimately, the total sequence previously used to afford the alkyne function could be re-thought. In fact, it might be useful to tune the protection strategy, by using other groups than the benzyl ethers. For instance, a sequence, which exploits silyl ether protection, was successfully applied for the C6 alkynylation of D-glucopyranose,[54] and could be hence followed as another attempt to afford the desired homologous alkyne, starting from D-mannopyranose **27** in our case (scheme 32).

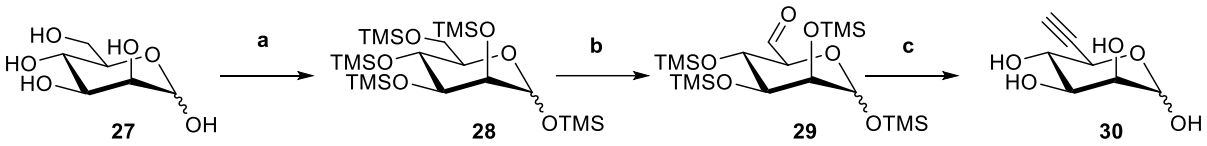

Scheme 32. another eventual sequence for the C6 alkynylation of D-mannopyranose.
a) TMSCl, pyridine, 0°C to r.t**; b)** DMSO, oxalyl chloride, DCM, then TEA, -78°C to 0°C to r.t; **c)** K_2CO_3, Bestmann-Ohira reagent, MeOH 0°C to r.t.

VI. Experimental part

VI.1 Generalities

The molecular weight of the different molecules were calculated with the software ChemDraw 20.1.1.

The NMR spectra used for the characterization of the synthesized molecules were recorded either on a JEOL JNM EX-400 (at 400 MHz for ^{1}H, 100 MHz for ^{13}C) or on a JEOL KNM EX-500 (at 500 MHz for ^{1}H, 126 MHz for ^{13}C and 202 MHz for ^{31}P). All the spectra were realised in CD_3OD, $CDCl_3$, D_2O or DMSO-6D. The chemical shifts (δ) are quoted in part per million (ppm) and are calibrated with solvent residual peak (CD_3OD: ^{1}H 3.31 ppm, ^{13}C 49.0 ppm, $CDCl_3$: ^{1}H 7.26 ppm, ^{13}C 77.0 ppm, D_2O: ^{1}H 4.79 ppm, DMSO-6D: ^{1}H 2.50 ppm ^{13}C 39.52 ppm). The chemical shifts of ^{31}P spectra are uncorrected.

Each ^{1}H NMR spectrum is described in the following manner: chemical shift (ppm), integration, multiplicity, coupling constants (Hz).

The multiplicity is reported in the following manner: s= singlet, d= doublet, t= triplet, m= multiplet, dd = doublet of doublets, dt = doublet of triplet, ddd = doublet of doublets of doublets.

All 1-D spectra are analysed thanks to MestReNova 14.2 and all the 2-D spectra (COSY (1H, 1H), HMQC (13C, 1H)) are analysed thanks to MestReNova 14.2 and/or Delta 6.1.0.

The carbon (and the related hydrogen) numbering follows the classical numbering of carbohydrates with the position 1 being the anomeric carbon. Quaternary carbons are indicated as Cq.

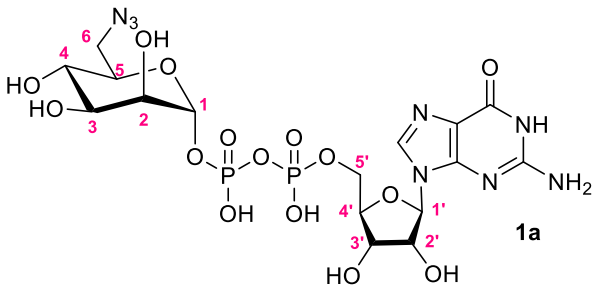

1a

The TLCs were performed aluminium-baked 0.2 mm thick Merck Silica gel 60F 254 plates. The compounds were detected by one of the following methods:

- Dipping into a 5 % phosphomolybdic acid solution in ethanol and heating.
- Dipping into a solution of ceric (IV) ammonium nitrate (10 g/L), ammonium molybdate tetrahydrate (50 g/L) in 50 mL of concentrated sulfuric acid and 450 mL of water. Heating is also applied.

The chromatographies were performed on silica Davisil (particle size 40-63 µm, 60 A). The solvents were at least of technical grade and distilled prior to use. The indicated mixture ratios are given as volumic ratios.

The reagents and chemicals were obtained from Merck, Fischer, ABCR, Carbosynth and were used without purification if not stated. The reactions were performed using purified and dried solvents if necessary. Dichloromethane and Tetrahydrofuran were dried…Pyridine was distilled from CaH_2 and stored over 4 Å molecular sieves. DMF and MeOH were bought anhydrous and stored over 4 Å molecular sieves.

All reactions were carried out under an argon atmosphere in a round bottom flask closed by a septum and a rubber balloon filled up with argon, and stirred with a Teflon stirring rod

Nucleotide-sugars were purified by semi-preparative HPLC on Waters 600 systems :

- Column = Agilent Zorbax SB-C18 21.2x250mm 7µM;
- Flow = 15 mL/min;
- Detection: UV 254 & 262nm (Waters 2486 Dual λ Absorbance detector).
- Volume injection = 1 – 5 mL.

The infrared spectra were acquired on a Perkin-elmer Spectrum Two FT-IR system UATR two on neat compounds mounted with a diamond crystal. The selected absorption bands are reported by wavenumber (cm^{-1}). The Spectra were measured between wavenumbers of 4000-500 cm^{-1}.

VI.2 Synthesis and protocols

VI.2.1. Synthesis of 6-*O*-toluenesulfonyl-α-methyl-D-mannopyranoside (5)

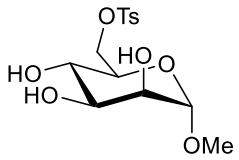

Based on Marchesan *et al*,[26] a solution of α-methyl-D-mannopyranoside **4** (2.06 g, 10.6 mmol, 1eq) in dry pyridine (12.0 mL) was cooled to 0 ºC and stirred under argon atmosphere. A solution of p-toluenesulfonyl chloride (2.29 g, 11.66 mmol, 1.1 eq) and 4-dimethylamino pyridine (DMAP, 0.13 g, 1.06 mmol, 0.1 eq) in dry pyridine (28.0 mL) was then added dropwise. After 15min the ice bath was removed and the stirring was continued at r.t overnight until the reaction appeared complete by TLC. The solvent was then removed *in vacuo* to afford a crude product, which was purified by column chromatography over silica gel (1%-10% MeOH in DCM) to afford 6-*O*-toluenesulphonyl-α-methyl-D-mannopyranoside (2.21 g, 60%).

- Formula: $C_{14}H_{20}O_8$
- Molecular weight: 348.37 g/mol
- Rf: 0.44 (DCM/MeOH 9:1)
- Aspect: white solid
- **^{1}H NMR (500 MHz, CD_3OD)** δ(ppm)= 7.81 (2H, d, *J* = 8.4 Hz, 2x ArH), 7.44 (2H, d, *J* = 8.0 Hz, 2x ArH), 4.54 (1H, d, *J* = 1.6 Hz, H1), 4.34 (1H, dd, *J* = 10.6, 1.8 Hz, H4), 4.15 (1H, dd, *J* = 10.6, 6.9 Hz, H5), 3.74 (1H, dd, *J* = 3.4, 1.7 Hz, H2), 3.64-3.57 (2H, H3, $H6_a$), 3.51 – 3.47 (1H, m, $H6_b$), 3.29 (3H, s, OCH_3), 2.46 (3H, s, CH_3).
- **^{13}C NMR (126 MHz, CD_3OD)** δ (ppm) = 146.47 (1C, d, *J*= 12.8 Hz, Cq Ar), 134,35 (1C, d, *J*=14.6, Cq Ar), 130.95 (2C, d, *J*=13.5 Hz, 2x CH Ar), 129.07 (2C, d, *J*=13.6 Hz, 2x CH Ar), 102.66 (1C, d, *J*=12.9 Hz, C1), 72.36 (1C, d, *J*=13.2 Hz, C3), 71.94 (1C, d, *J*=13.6 Hz, C2), 71.76 (1C, d, *J*=13.6 Hz, C5), 71.27 (1C, d, *J*=13.5 Hz, C4), 68.11 (1C, d, *J*=13.5 Hz, C6), 55.21 (1C, d, *J*=13.5 Hz, OCH_3), 21.50 (1C, d, *J*=13.7 Hz, CH_3).

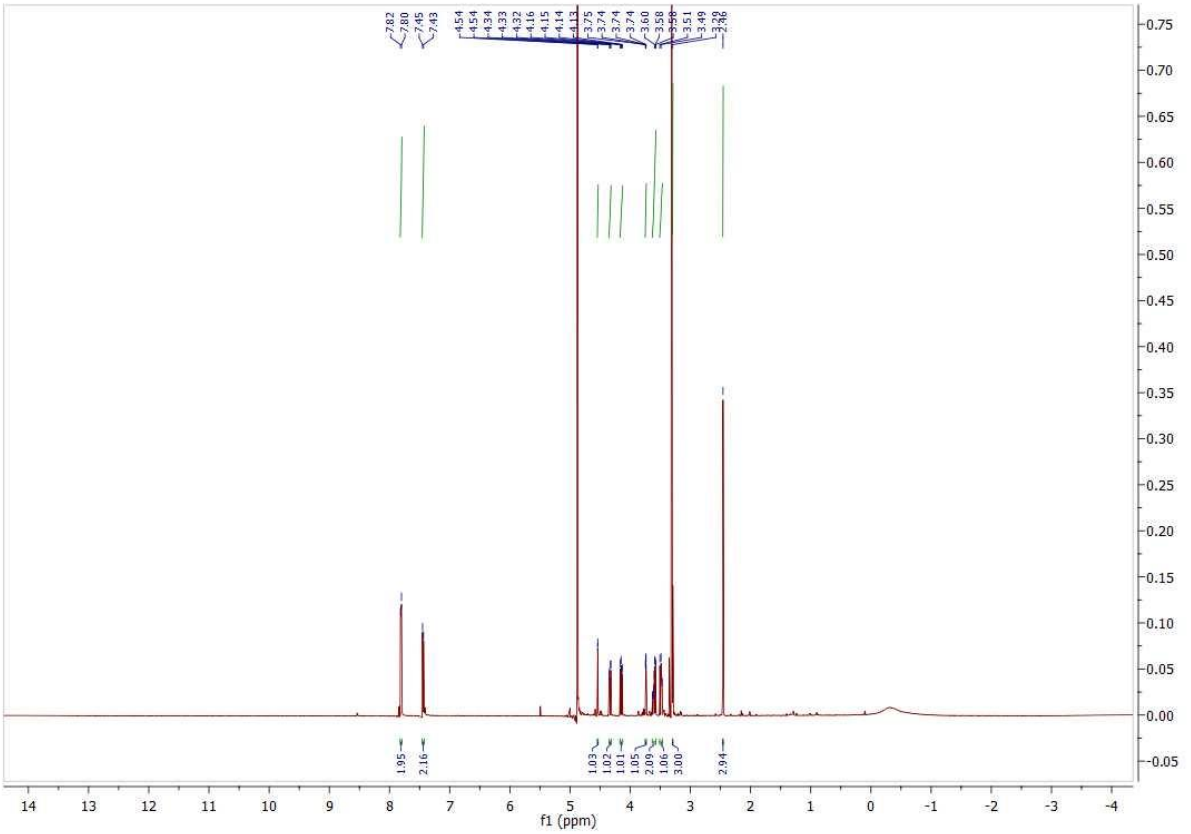
7.82
7.80
7.45
7.43
4.54
4.54
4.34
4.33
4.32
4.16
4.15
4.14
4.13
3.75
3.74
3.74
3.74
3.60
3.58
3.56
3.51
3.49
3.48
3.40
2.48
1.95
2.16
1.03
1.02
1.01
1.05
2.09
1.06
3.00
2.94
f1 (ppm)

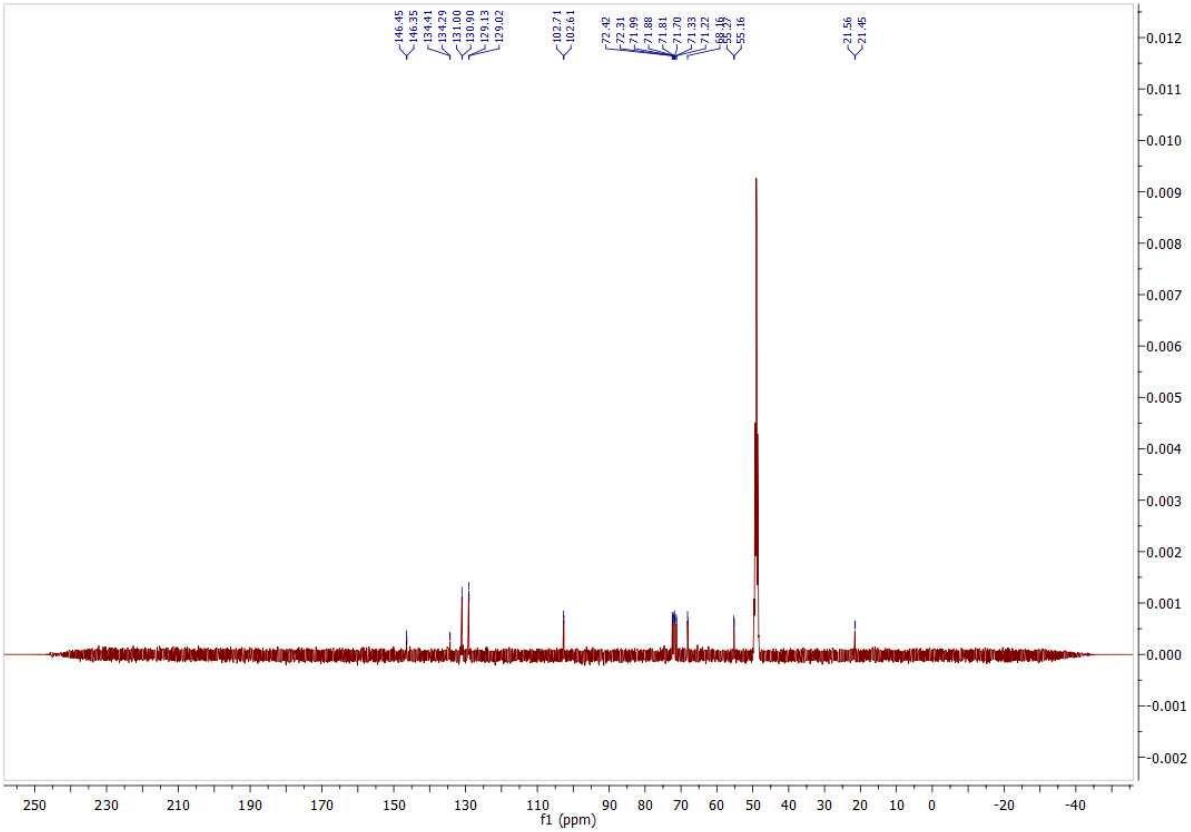
146.45
146.35
134.41
134.29
131.00
130.90
129.13
129.02
102.71
102.61
72.42
72.31
71.99
71.88
71.81
71.70
71.33
71.22
55.16
21.56
21.45
f1 (ppm)

VI.2.2. Synthesis of 6-azido-6-deoxy- α-methyl-D-mannopyranoside (6)

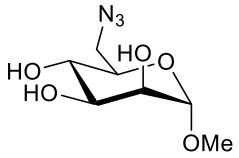

Based on Marchesan *et al*,[26] a solution of 6-*O*-toluenesulfonyl-α-methyl-D-mannopyranoside **5** (4.5 g, 12.8 mmol, 1 eq) in dry DMF (63.0 mL) was prepared in a two neck round bottom flask, under argon atmosphere. NaN_3 (5.8 g, 89.8 mmol, 7 eq) was then added carefully. The mixture was stirred and heated to 80°C overnight. After having checked the conversion by TLC, the crude was filtered on celite and the solvent was removed *in vacuo*. The product was then purified by column chromatography over silica gel (1%-10% MeOH in DCM) to afford 6-azido-6-deoxy-α-methyl-D-mannopyranoside (2.29 g, 81%).

- Formula: $C_7H_{13}N_3O_5$
- Molecular weight: 219.2 g/mol
- Rf: 0.24 (DCM/MeOH 9:1)
- Aspect: colourless oil
- **^{1}H NMR (500 MHz, CD_3OD)** δ (ppm)= 4.64 (1H, d, *J* = 1.6 Hz, H1), 3.79 (1H, dd, *J* = 3.2, 1.7 Hz, H2), 3.62 (2H, td, *J* = 9.3, 2.8 Hz, H3, H4), 3.59 – 3.54 (1H, m, H5), 3.48 (1H, dd, *J* = 13.0, 2.3 Hz,$H6_a$), 3.45 – 3.42 (1H,m, $H6_b$), 3.41 (3H, s, OCH_3).
- **^{13}C NMR (126 MHz, CD_3OD)** δ = 102.83 (1C, s, C1), 73.69 (s), 72.36 (s), 71.94 (s), 69.44 (s) (4C, C2-C5), 55.33 (1C, s, OCH_3), 52.90 (1C, s, C6).
- **FTIR:** 2097.34 cm^{-1} (N_3 antisymmetric stretching).

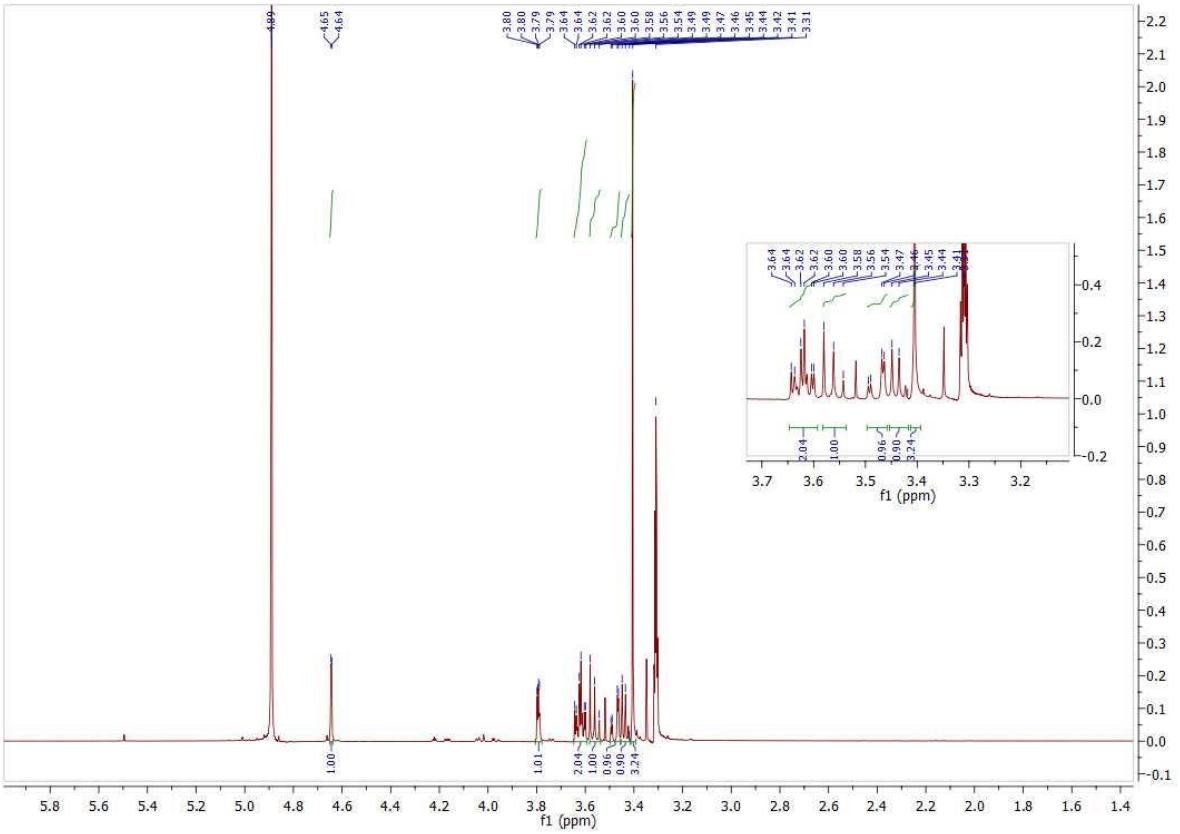
4.89
4.65
4.64
3.80
3.80
3.79
3.79
3.64
3.64
3.62
3.62
3.60
3.60
3.58
3.56
3.54
3.49
3.47
3.46
3.45
3.44
3.42
3.41
3.31
1.00
1.01
2.04
1.00
0.96
0.90
3.24
f1 (ppm)

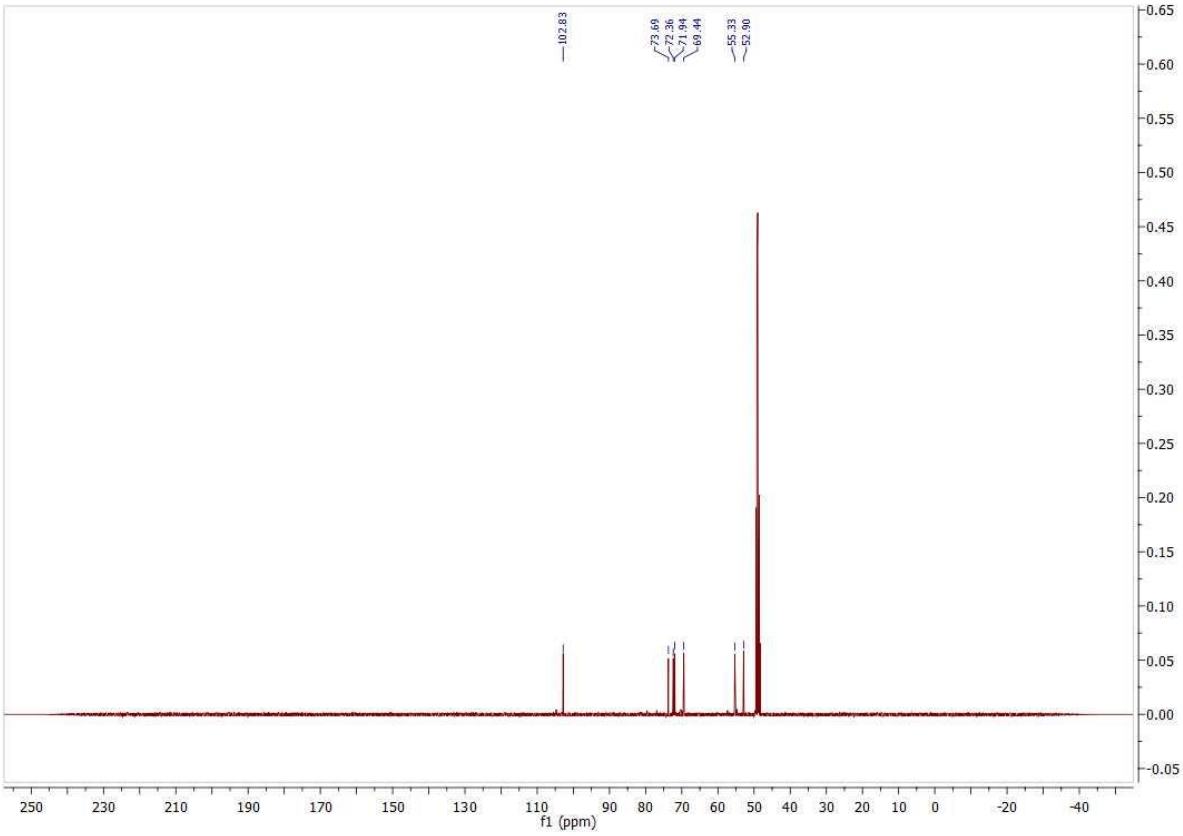
102.83
73.69
72.36
71.94
69.44
55.33
52.90
f1 (ppm)

VI.2.3. Synthesis of 1,2,3,4-tetra-*O*-acetyl-6-azido-6-deoxy- α-D-mannopyranose (7).

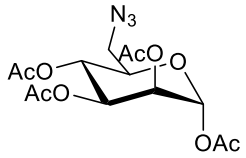

Based on Marchesan *et al*,[26] the 6-azido-6-deoxy-α-methyl-D-mannopyranoside **6** (1.15 g, 5.2 mmol, 1 eq) was dissolved in 1:1 (v/v) Ac_2O/AcOH (7.2 mL) and cooled to 0 ºC. Concentrated H_2SO_4 (1.1 mL) was added dropwise with stirring. The reaction was then allowed to come to room temperature and stirring was continued overnight. After having checked the conversion by TLC, ice water (10 mL) was added. The aqueous phase was then extracted with DCM (3x15 mL) and the combined organic phase extracts were washed with water (15 mL), sat.aq. $NaHCO_3$ (15 mL) and dried with $MgSO_4$.The solvent was removed *in vacuo* to obtain 1,2,3,4-tetra-*O*-acetyl-6-azido-6-deoxy-α-D-mannopyranoside **7** (1.02 g, 52%) which was used without further purification in the next step.

- Formula: $C_{14}H_{19}N_3O_9$
- Molecular weight: 373.32 g/mol
- Rf: 0.55 (Cy/EtOAc 1:1)
- Aspect: colourless oil
- **^{1}H NMR (400 MHz, CD_3Cl)** δ (ppm) = 6.10 (1H, d, *J* = 1.6 Hz, H1), 5.36 – 5.33 (2H, m, H3, H4), 5.27 – 5.25 (1H, m, H2), 4.04 – 3.96 (1H, m, H5), 3.39 (1H, dd, *J* = 13.5, 2.9 Hz, $H6_a$), 3.31 (1H, dd, *J* = 13.5, 5.7 Hz, $H6_b$), 2.18 (3H, s, CH_3 Ac), 2.18(3H, s, CH_3 Ac), 2.06 (3H, s, CH_3 Ac), 2.01 (3H, s, CH_3 Ac).
- **^{13}C NMR (126 MHz, CD_3Cl)** δ(ppm) = 170.11 (s), 169.87 (s), 169.68 (s), 168.14 (s) (4 Cq, CO Ac), 90.40 (1C, s, C1), 71.92 (1C, s, C5), 68.62 (1C, s, C4), 68.34 (1C, s, C2), 66.52 (1C, s, C3), 50.77 (1C, s, C6), 20.94 (s), 20.85 (s), 20.78 (s), 20.74 (s) (4C, CH_3 Ac).
- **FTIR:** 2102.62 cm^{-1} (N_3 antisymmetric stretching).

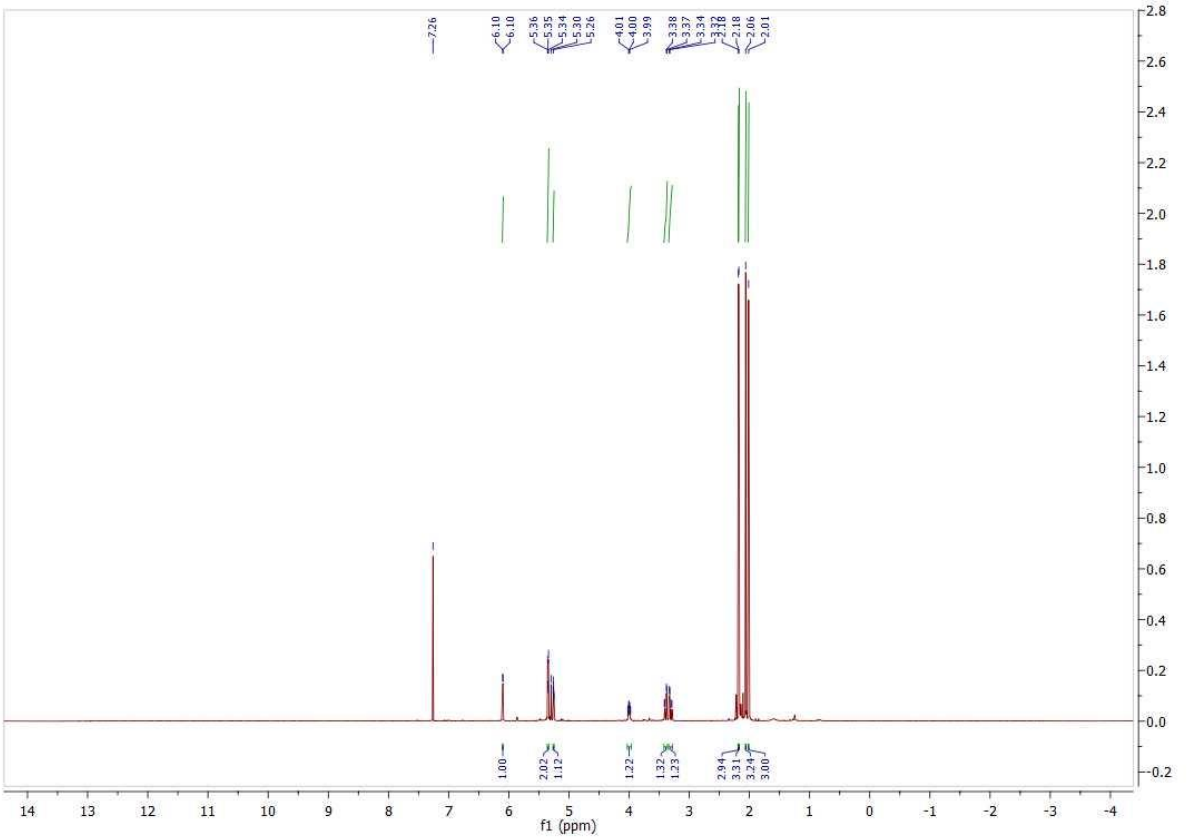
7.26
6.10
6.10
5.36
5.35
5.34
5.30
5.26
4.01
4.00
3.99
3.38
3.37
3.34
2.18
2.06
2.01
1.00
2.02
1.12
1.22
1.32
1.23
2.94
3.31
3.24
3.00
f1 (ppm)

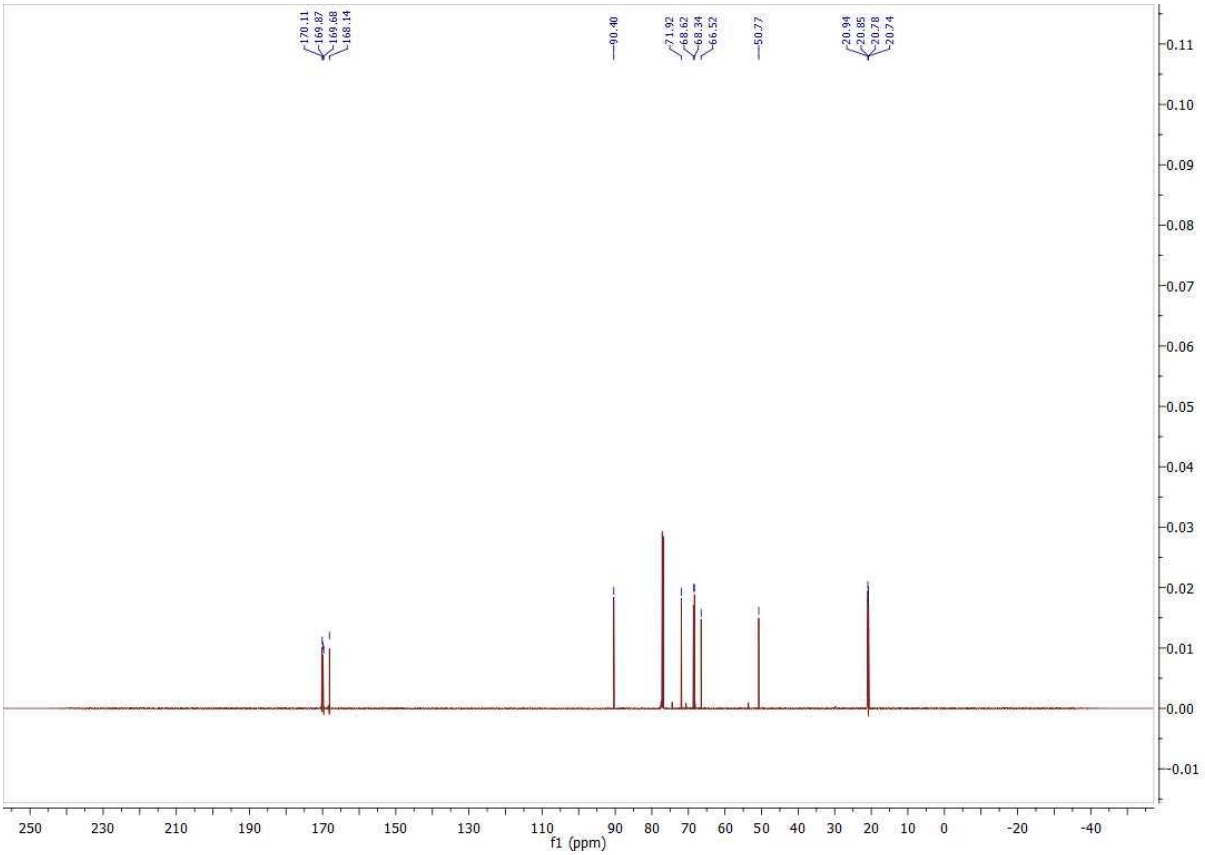
170.11
169.87
169.68
168.14
90.40
71.92
68.62
68.34
66.52
50.77
20.94
20.85
20.78
20.74
f1 (ppm)

VI.2.4. Synthesis of 2,3,4-tri-*O*-acetyl-6-azido-6-deoxy- α-D-mannopyranose (3)

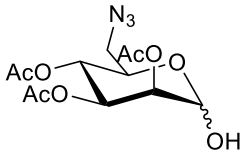

To a solution of peracetylated 6-azido-6-deoxy-α-D-mannose **7** (0.55 g, 1.47 mmol, 1 eq) in dry DMF (38.0 mL) was added hydrazine acetate (0.19 g, 2.06 mmol, 1.4 eq) under argon atmosphere, at room temperature and the solution was stirred for 4h at the same temperature. After having checked the conversion by TLC, water (50 mL) was added. The aqueous phase was extracted with EtOAc (50 mL), then, the combined organic extracts were washed with water and brine and dried with $MgSO_4$. The product was purified by column chromatography over silica gel (Cy/EtOAc 7:3 to 1:1). The solvent was then removed *in vacuo* to afford **3** (0.325 g, 67%). Known molecule. [26]

- Formula: $C_{12}H_{17}N_3O_8$
- Molecular weight: 331.28 g/mol
- Rf: 0.50 (Cy/EtOAc 1:1)
- Aspect: colourless oil
- **^{1}H NMR (500 MHz, CD_3Cl)** δ (ppm) = 5.42 (1H, dd, *J*=10.1, 3.2 Hz, H1), 5.30 – 5.23 (3H, m, H2, H3, H4), 4.22 – 4.15 (1H, m, H5), 3.35 (2H, d, *J*=4.8 Hz, $H6_a$, $H6_b$), 2.17 (3H, s, CH_3 Ac), 2.06 (3H, s, CH_3 Ac), 2.01 (3H, s, CH_3 Ac).
- **^{13}C NMR (126 MHz, CD_3Cl)** δ = 170.38 (s), 170.19 (s), 170.07 (s) (3Cq, 3x CO Ac), 69.93 (1C, s, C1), 92.18 (s), 70.02 (s), 68.64 (s), 67.31 (s) (4C, C2-C5), 51.26 (1C,s, C6), 21.04 (s), 20.89 (s), 20.85 (s) (3C, 3x CH_3 Ac).
- **FTIR:** 2102.36 cm^{-1} (N_3 antisymmetric stretching).

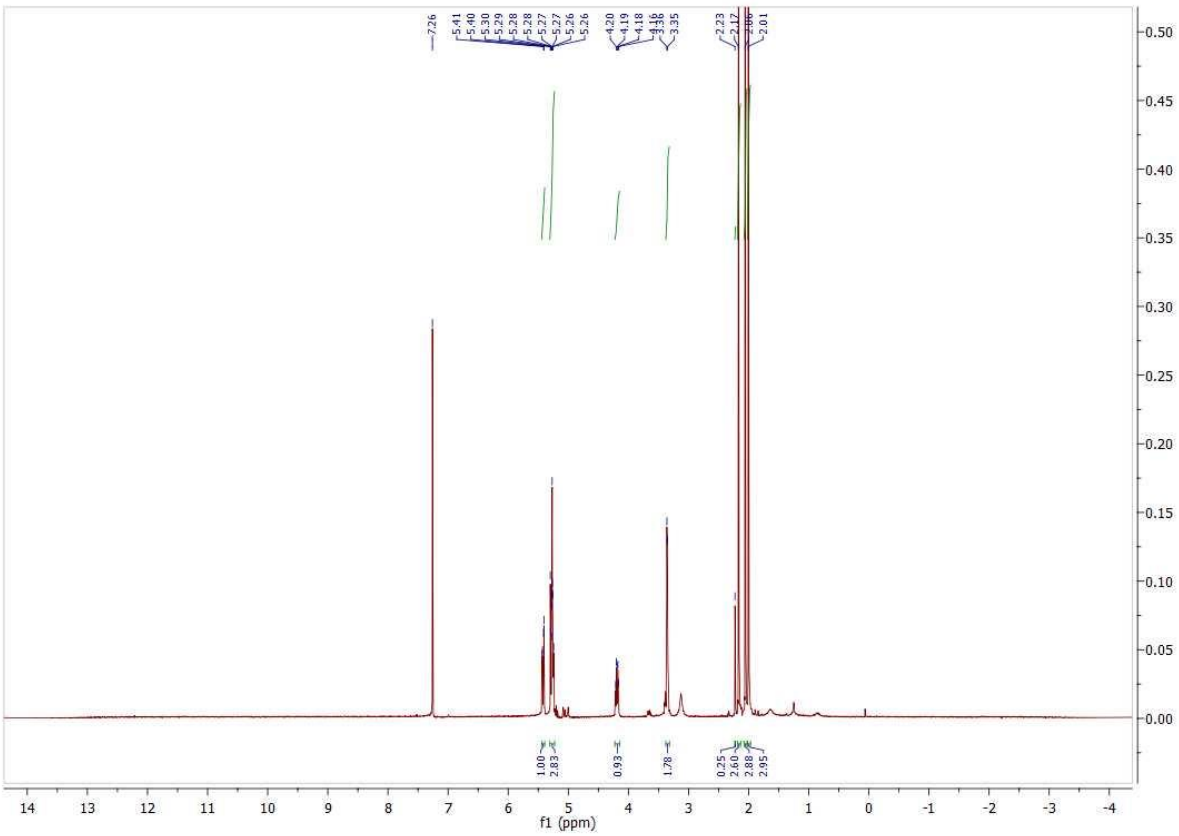
7.26
5.41
5.40
5.30
5.29
5.28
5.28
5.27
5.27
5.26
5.26
4.20
4.19
4.18
3.35
2.23
2.12
2.01
1.00
2.83
0.93
1.78
0.25
2.60
2.88
2.95
f1 (ppm)

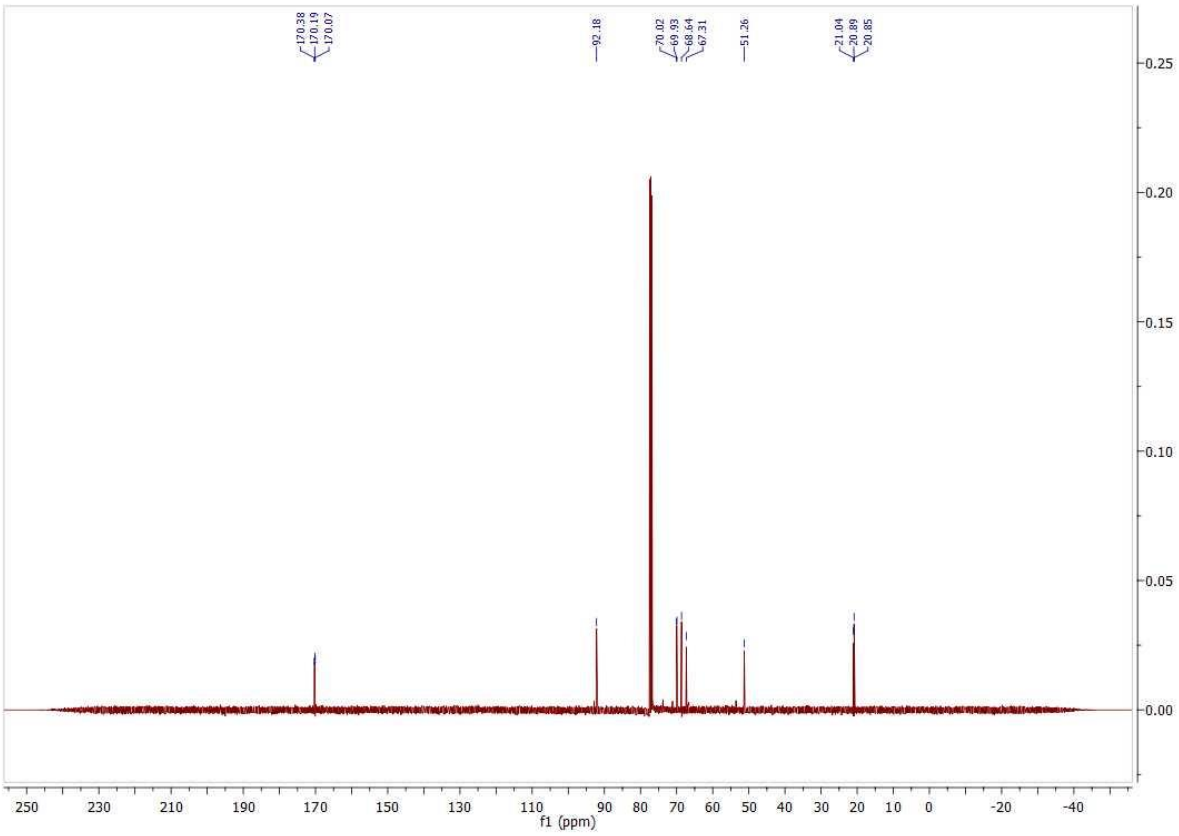
170.38
170.19
170.07
92.18
70.02
69.93
68.64
67.31
51.26
21.04
20.89
20.85
f1 (ppm)

VI.2.5. Synthesis of 1-*O*-(diallyl phosphoryl)-2,3,4-tri-*O*-acetyl-6-azido-6-deoxy-α-D-mannopyranose (9)

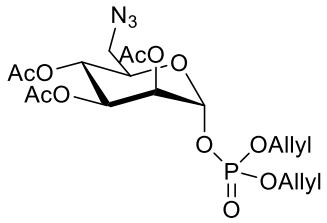

To a solution of the 2,3,4-tri-*O*-acetyl-6-azido-6-deoxy-α-D-mannopyranose **3** (339 mg, 1.02 mmol, 1eq) in dry DCM (28.5 mL) was added 1-H-tetrazole (11.4 mL, 5.12 mmol, 5 eq) under argon atmosphere and the solution was stirred at room temperature for 10 minutes. Diallyl-*N*,*N*-diisopropyl-phosphoramidite (657 µL, 2.45 mmol, 2.4 eq) was then added dropwise and stirring was continued overnight. After having checked the conversion by TLC, the reaction mixture was cooled at -40 °C and m-chloroperbenzoic acid (mCPBA, 1.15 g, 5.12 mmol, 5 eq) was added. The reaction mixture was allowed to come slowly to room temperature over approximately 1 h, then it was diluted with DCM (15.0 mL) and washed with 10 % $NaHSO_3$ (2 x 15.0 mL), sat. aq. $NaHCO_3$ (2 x 15.0 mL), and water (2 x 15.0 mL). The organic phase was separated, dried with $MgSO_4$, and evaporated under vacuum. The resulting mixture was purified by column chromatography over silica gel (7:3 to 1:1 Hex/EtOAc) to afford **9** (0.308 g, 61%, α/β = 8:1).

- Formula: $C_{18}H_{26}N_3O_{11}P$
- Molecular weight: 491.39 g/mol
- Rf: 0.38 (Cy/EtOAc 1:1)
- Aspect: colourless oil
- **^{1}H NMR (500 MHz, CD_3Cl)** δ(ppm) = 5.97 (2H, ddd, *J*=22.4, 10.7, 5.7 Hz, 2x CH allyl), 5.66 (1H, dd, *J*=6.6, 1.8 Hz, H1), 5.44 – 5.38 (2H, m, 2x C**H**H allyl), 5.38 – 5.28 (5H, m, H2,H3,H4, 2x CH**H** allyl), 4.64 – 4.60 (4H, m, 2x CH_2 vinyl), 4.16 (1H, ddd, *J*=10.7, 5.3, 2.4 Hz, H5), 3.40 (1H, dd, *J*=13.5, 2.8 Hz, $H6_a$), 3.33 (1H, dd, *J*=13.5, 5.6 Hz, $H6_b$), 2.17 (3H, s, CH_3 Ac), 2.06 (3H, s, CH_3 Ac), 2.00 (3H, s, CH_3 Ac).
- **^{31}P NMR (202 MHz, CD_3Cl)** δ (ppm) = -2.58 (s).
- **^{13}C NMR (126 MHz, CD_3Cl)** δ (ppm) = 169.96 (s), 169.79 (s), 169.75 (s) (3Cq, 3x CO Ac), 132.11 (2C, dd, *J*=8.6, 6.7 Hz, 2CH allyl), 119.18 (2C, d, *J*=22.8 Hz, CH_2 allyl), 94.96 (1C, d, *J*=5.4 Hz, C1), 71.77 (1C, s, C5), 66.43 (s), 68.22 (s), 69.06 (d, *J*=5.3 Hz) (3x C, C2-C4), 68.95 – 68.79 (2C, m, CH_2 vinyl), 50.93 (1C, s, C6), 20.86 (s), 20.82 (s), 20.75 (s) (3C, 3x CH_3 Ac).

- **FTIR:** 2102.19 cm^{-1} (N_3 antisymmetric stretching).
- **HRMS (ESI+)**: calc. for $C_{18}H_{26}N_3O_{11}P$ $[M-H]^+$: 492.13; found: 492.13.

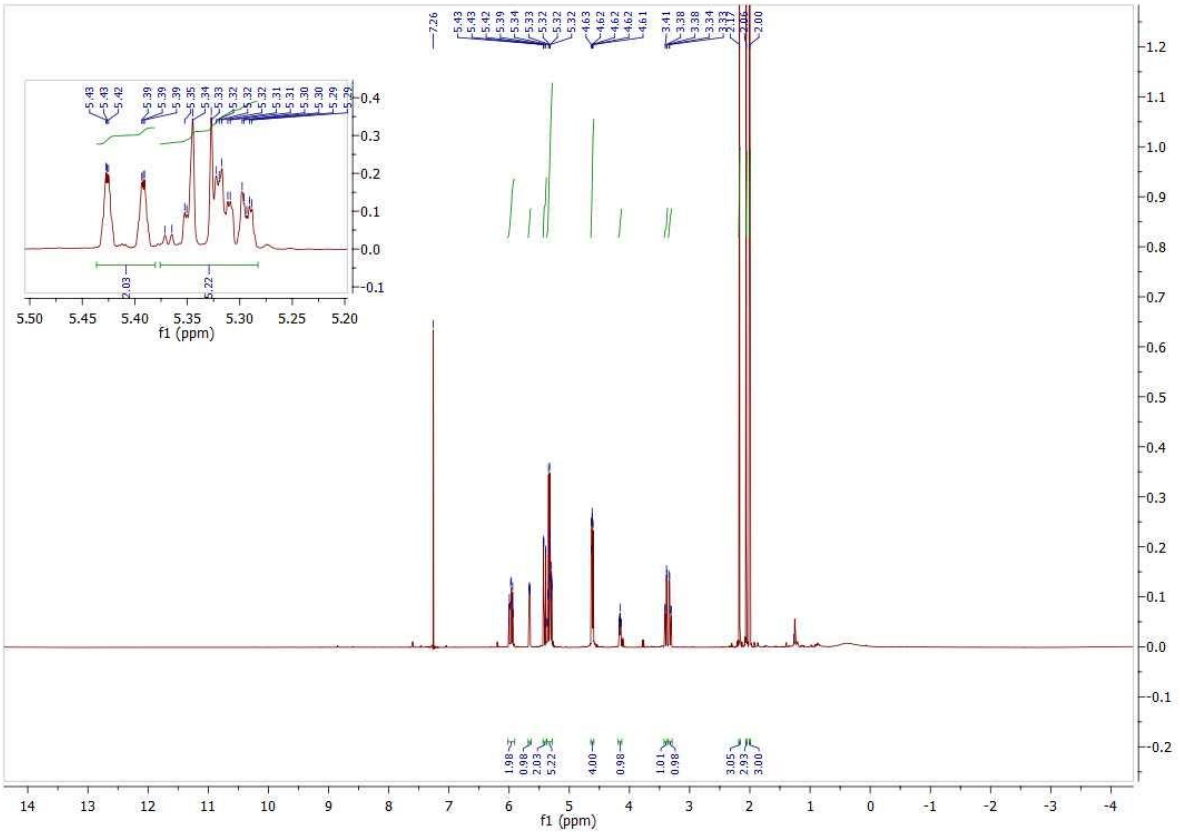

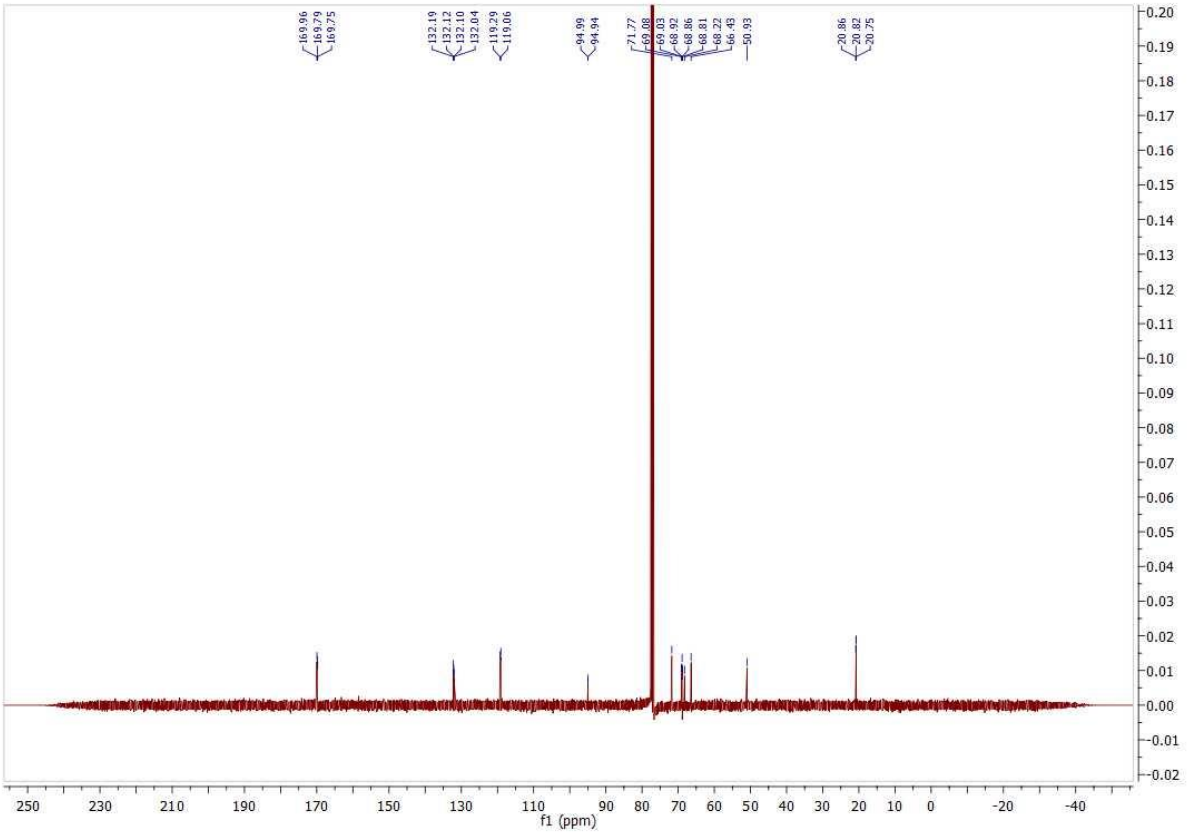

^{31}P NMR of **9** ($CDCl_3$)

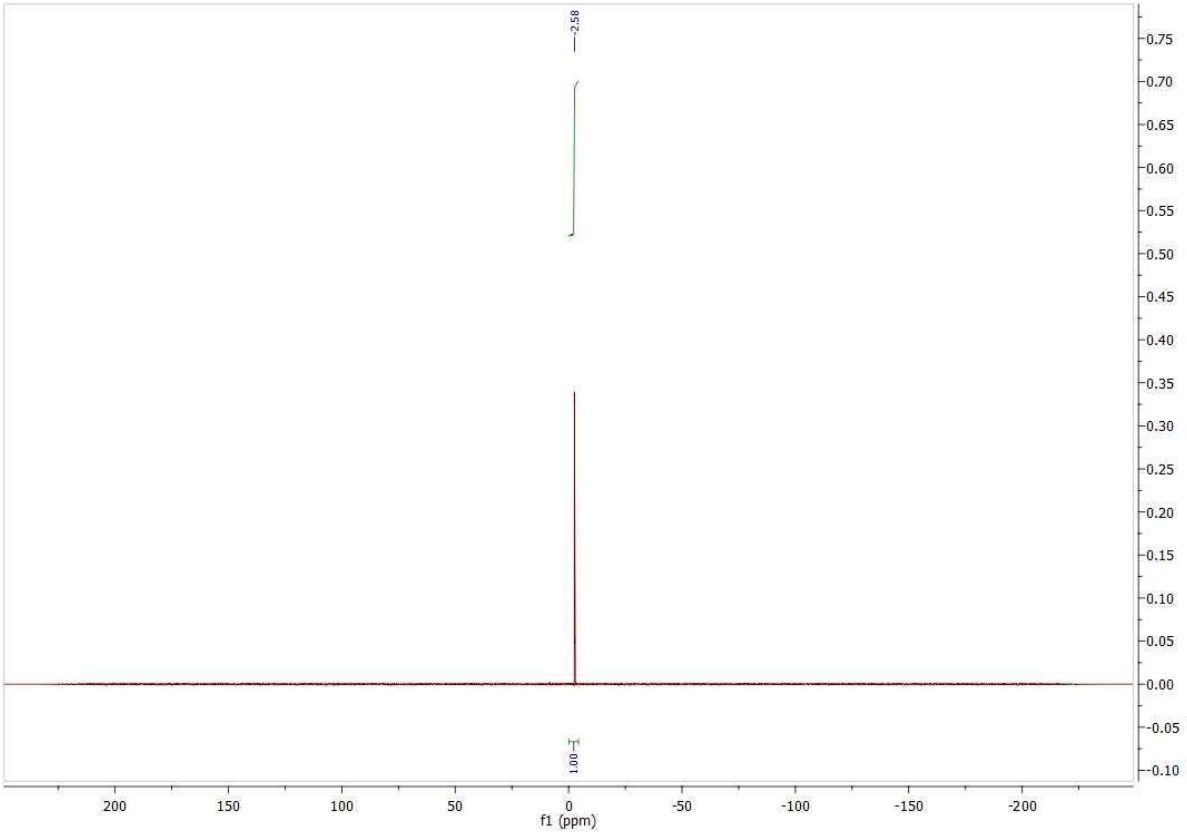

VI.2.6. Synthesis of 1-*O*-(phosphoryl)-2,3,4-tri-*O*-acetyl-6-azido-6-deoxy-α-D-mannopyranose (10)

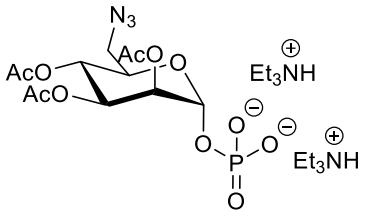

Procedure A

To a solution of 1-*O*-(diallyl phosphoryl)-2,3,4-tri-*O*-acetyl-6-azido-6-deoxy-α-D-manno-pyranoside **9** (94 mg, 0.19 mmol) in 3:2 (v/v) anhydrous DCM/MeOH (2.2ml) was added $PdCl_2$ (17 mg, 0.1 mmol, 0.5 eq) under argon atmosphere. The reaction was stirred overnight at room temperature. The solvents were removed under vacuum and the residue was purified by silica gel column chromatography (chloroform/methanol 7:3 to 1:1, all eluents contained 2% v/v of triethylamine) to afford **10** (50 mg, 43%) as a bis-triethylammonium salt.

Procedure B

Diallylmonophosphate **9** (126 mg, 0.26 mmol, 1 eq), was dissolved in 1:1 (v/v) anhydrous THF/MeOH (18 mL), under argon atmosphere. Tetrakis-triphenylphosphine palladium (21 mg, 0.018 mmol, 0.07 eq) and p-toluenesulfinic acid sodium salt (91.4 mg, 0.51 mmol, 2 eq) were added. The reaction mixture was stirred for 17h, then, concentrated *in vacuo*. The crude was purified by silica gel column chromatography (chloroform/methanol 7:3 to 1:1, all eluents contained 2% v/v of triethylamine) to afford the 1-*O*-(phosphoryl)-2,3,4-tri-*O*-acetyl-6-azido-6-deoxy-α-D-mannopyranose **10** (98 mg, 60%) as a bis-triethylammonium salt.

- Formula: $C_{12}H_{18}N_3O_{11}P$
- Molecular weight: 411.26 g/mol
- Rf: 0.23 (Chloroform/MeOH 1:1 with 2% Et_3N)
- Aspect: yellow solid.
- **^{1}H NMR (500 MHz, D2O)** δ (ppm) = 5.51 (1H, dd, *J*=7.6, 1.2, H1), 5.43 (1H, dd, *J*=10.1, 3.1, H3), 5.39 – 5.32 (2H, m, H2, H4), 4.31 (1H, dt, *J*=9.8, 3.1, H5), 3.70 (1H, dd, *J*=13.9, 2.5, $H6_a$), 3.52 (1H, dd, *J*=13.9, 3.8, $H6_b$), 3.21 (q, *J*=7.3, $N(\mathbf{CH_2}CH_3)_3$), 2.22 (3H, s, CH_3 Ac), 2.13 (3H, s, CH_3 Ac), 2.05 (3H, s, CH_3 Ac), 1.28 (t, *J*=7.3, $N(CH_2\mathbf{CH_3})_3$).
- **^{31}P NMR (202 MHz, D_2O)** δ (ppm) = -1.24 (s).
- **^{13}C NMR (126 MHz, D_2O)** δ (ppm) = 173.10 (s), 172.93 (s), 172.84 (s) (3Cq, 3x CO Ac), 92.92 (1C, d, *J*=4.8, C1), 69.99 (d, *J*=9.8), 69.56 (s), 69.48 (s), 66.58 (s) (4C, C2, C3, C4, C5) , 50.14 (1C, s, C6), 46.70 (s, N(**CH2**CH3)3), 20.22 (s), 20.17 (s) (3C, 3x CH_3 Ac), 8.29 (s, $N(CH_2\mathbf{CH_3})_3$)
- **FTIR:** 2102.7 cm^{-1} (N_3 antisymmetric stretching).
- **HRMS (ESI-)**: calc. for $C_{12}H_{18}N_3O_{11}P$ $[M-H]^-$: 410.07; found: 410.06.

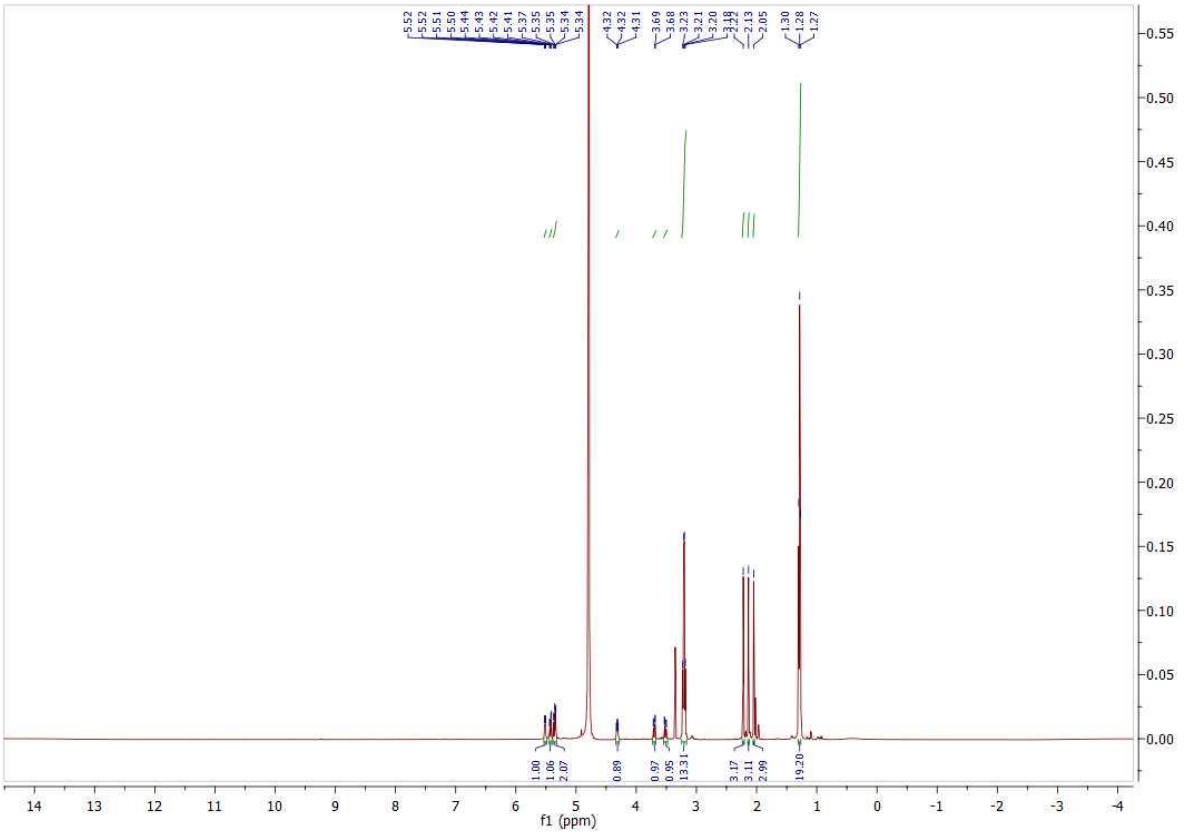
5.52
5.52
5.51
5.50
5.44
5.43
5.42
5.41
5.37
5.35
5.34
5.34
4.32
4.32
4.31
3.69
3.68
3.23
3.21
3.20
2.22
2.18
2.13
2.05
1.30
1.28
1.27
1.00
1.06
2.07
0.89
0.97
0.95
13.31
3.17
3.11
2.99
19.20
f1 (ppm)

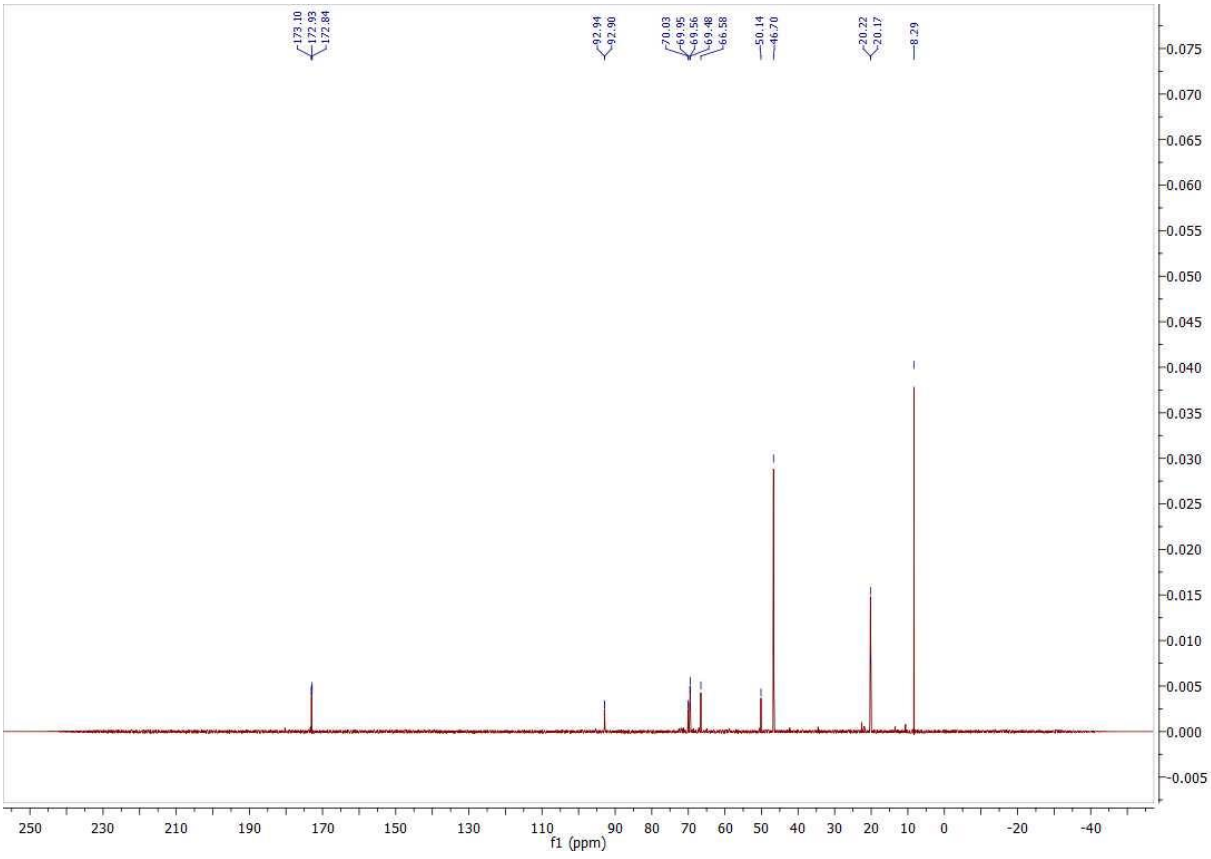
173.10
172.93
172.84
92.94
92.90
70.03
69.95
69.56
69.48
66.58
50.14
46.70
20.22
20.17
8.29
f1 (ppm)

^{31}P NMR of **10** (D_2O)

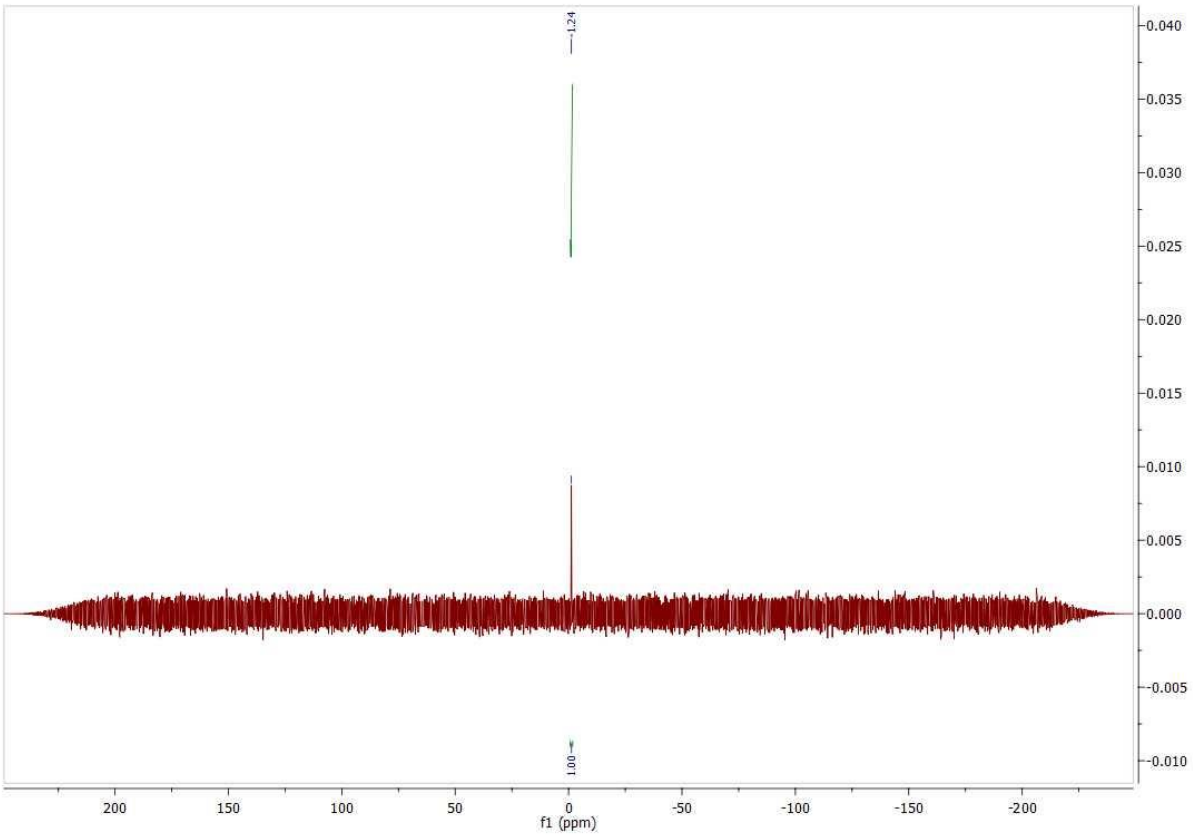

VI.2.7. Synthesis of monophosphate-6-azido-6-deoxy-α-D-mannopyranoside (11)

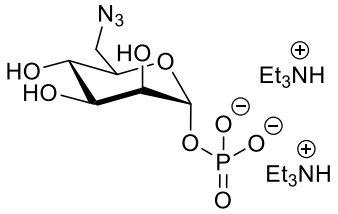

The triethylammonium salt of monophosphate **10** (50 mg, 0.08 mmol) was suspended in a 5:2:1 mixture of MeOH/H_2O/TEA (10 mL), and stirred at room temperature for 24h. The crude was then washed with DCM (3x 10 mL) to remove organic impurities. The aqueous layer was lyophilized to afford the monophosphate-6-azido-6-deoxy-α-D-mannopyranoside **11** (39 mg, 98%) as a bis-triethylammonium salt.

- Formula: $C_6H_{12}N_3O_8P$
- Molecular weight: 285.15 g/mol
- Aspect: pale yellow solid.
- ^{1}H NMR (500 MHz, D_2O) δ (ppm) = 5.34 (1H, dd, *J*=8.1, 1.8 Hz, H1), 3.97 – 3.96 (1H, m, H2), 3.92 (1H, d, *J*=3.5 Hz, H3), 3.90 (1H, d, *J*=3.4 Hz, H4), 3.71 (1H, dd, *J*=9.0, 4.5 Hz, $H6_a$), 3.68 (1H, t, *J*=6.7 Hz, H5), 3.60 (1H, dd, *J*=13.5, 5.0, $H6_b$), 3.19 (q, *J*=7.4 Hz, N((**CH_2**CH_3)$_3$), 1.27 (t, *J*=7.3 Hz, N((CH_2**CH_3**)$_3$).
- ^{13}C NMR (126 MHz, D_2O) δ = 95.89 (1C, d, *J*=5.3Hz, C1), 72.11 (1C, s, C3), 70.56 (1C, d, *J*=8.5 Hz, C2), 69.83 (1C, s, C4), 67.27 (1C, s, C5), 51.06 (1C, s, C6), 46.75 (s, N(**CH2**CH3)3), 8.31 (s, N(CH_2**CH_3**)$_3$).
- ^{31}P NMR (202 MHz, D_2O) δ (ppm) = 0.41 (s).
- **FTIR:** 2106.02 cm^{-1} (N_3 antisymmetric stretching).
- **HRMS (ESI-)**: calc. for $C_6H_{12}N_3O_8P[M-H]^-$: 284.04; found: 284.03.

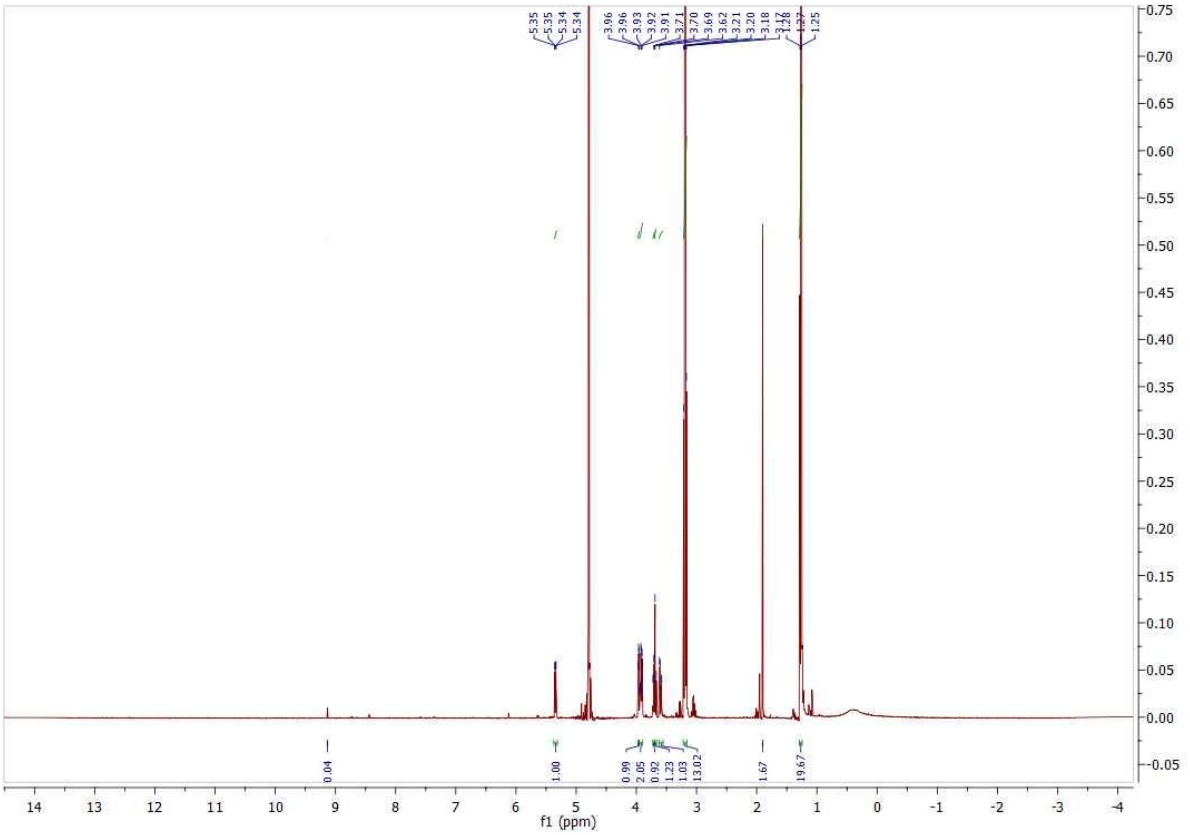
5.35
5.35
5.34
5.34
3.96
3.96
3.93
3.92
3.91
3.71
3.70
3.69
3.62
3.21
3.20
3.18
3.17
1.28
1.27
1.25
0.04
1.00
0.99
2.05
0.92
1.23
1.03
13.02
1.67
19.67
f1 (ppm)

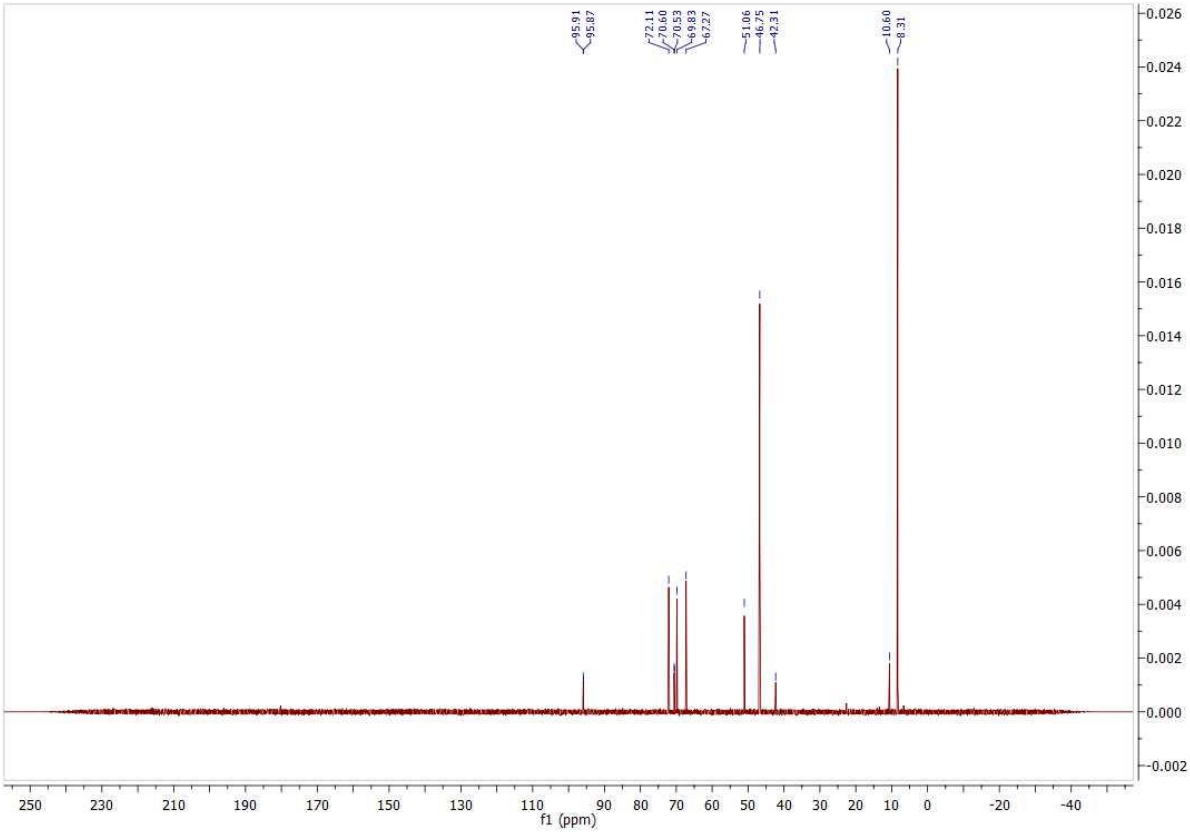
95.91
95.87
72.11
70.60
70.53
69.83
67.27
51.06
46.75
42.31
10.60
8.31
f1 (ppm)

^{31}P NMR of **11** (D_2O)

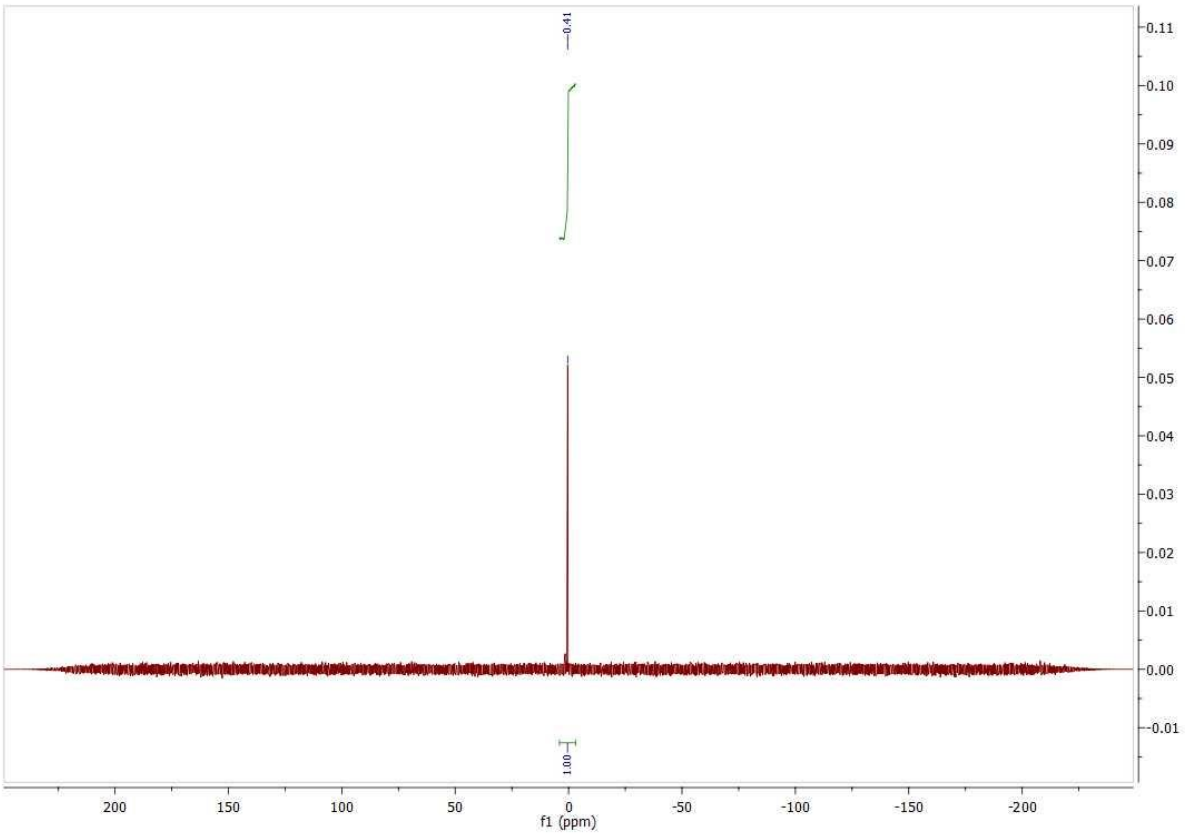

VI.2.8. Synthesis of GMP-imidazolide (14)

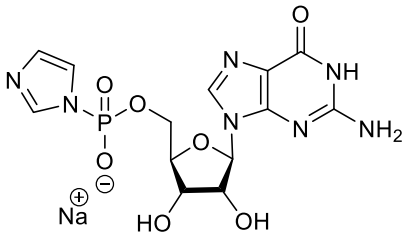

A guanosine mono phosphate (GMP) tributylammonium salt **13** was first obtained by suspending GMP (free acid) **12** in a water/ethanol mixture and neutralizing to pH 7 by a stepwise addition of tributylamine under vigorous stirring. Solvent was then removed and the residue was dried *in vacuo* to obtain the GMP tributyl ammonium salt as a white solid.

A solution of GMP tributylammonium salt **13** (500mg, 0.68 mmol, 1 eq) in dry DMF (6 mL) was prepared under argon atmosphere, sonication and vigorous stirring during 10 minutes. Carbonyl diimidazole (CDI, 660 mg, 4.1 mmol, 6 eq) was then added and the stirring was pursued overnight. After 17h, dry MeOH (0.2mL) was added to quench excess of CDI. The product was then precipitated from the reaction mixture by the addition of an anhydrous solution of $NaClO_4$ (0.1M) in dry acetone (60 mL) priorly cooled at 0 °C. The precipitate was filtered, washed repeatedly with cold, dry acetone, and dried *in vacuo* to afford the desired GMP-imidazolide as sodium salt (192 mg).

- Formula: $C_{13}H_{16}N_7O_7P$
- Molecular weight: 413.28 g/mol
- Aspect: White solid
- **^{1}H NMR (500 MHz, DMSO-D6)** δ (ppm) = 10.80 (1H, s, -NH), 7.81 (1H, s, N-CH-N), 7.63 (1H, s, CH Im), 7.07 (1H, s, CH Im), 6.99 (2H, d, *J*=16.1 Hz, NH_2), 6.84 (1H, s, CH Im), 6.30 (1H, s, H1'), 5.82 (1H, dd, *J*=7.5, 3.4 Hz, H3'), 5.70 (1H, dd, *J*=7.5, 1.3 Hz, H2'), 4.36 (1H, ddd, *J*=8.5, 5.1, 3.6, H4'), 4.26 (1H, dd, *J*=18.5, 9.9 Hz, $H5_a$'), 3.53 (1H, ddd, *J*=10.0, 6.9, 5.4 Hz, $H5_b$').
- **^{13}C NMR (126 MHz, DMSO-D6)** δ (ppm) = 157.30 (1C, s, CO), 154.27 (1C, d, *J* = 62.2 Hz, -C-NH2), 150.55 (1C, s, N-C-N), 139.69 (1C, s, CH Im), 136.93 (1C, s, N-CH-N), 129.11 (1C, s, CH Im), 120.33 (1C, s, CH Im), 117.34 (1C, s, C-CO), 88.63 (1C, s, C1'), 85.79 (1C, d, *J*=7.2 Hz, C4'), 84.24 (1C, s, C2'), 81.47 (1C, s, C3'), 63.94 (1C, d, *J*=5.4 Hz, C5').
- **^{31}P NMR (202 MHz, DMSO-D6)** δ (ppm) = -9.64 (s).
- **HRMS (ESI-)**: calc. for $C_{16}H_{24}N_8O_{15}P_2$ $[M-H]^-$: 412.08; found: 412.07.

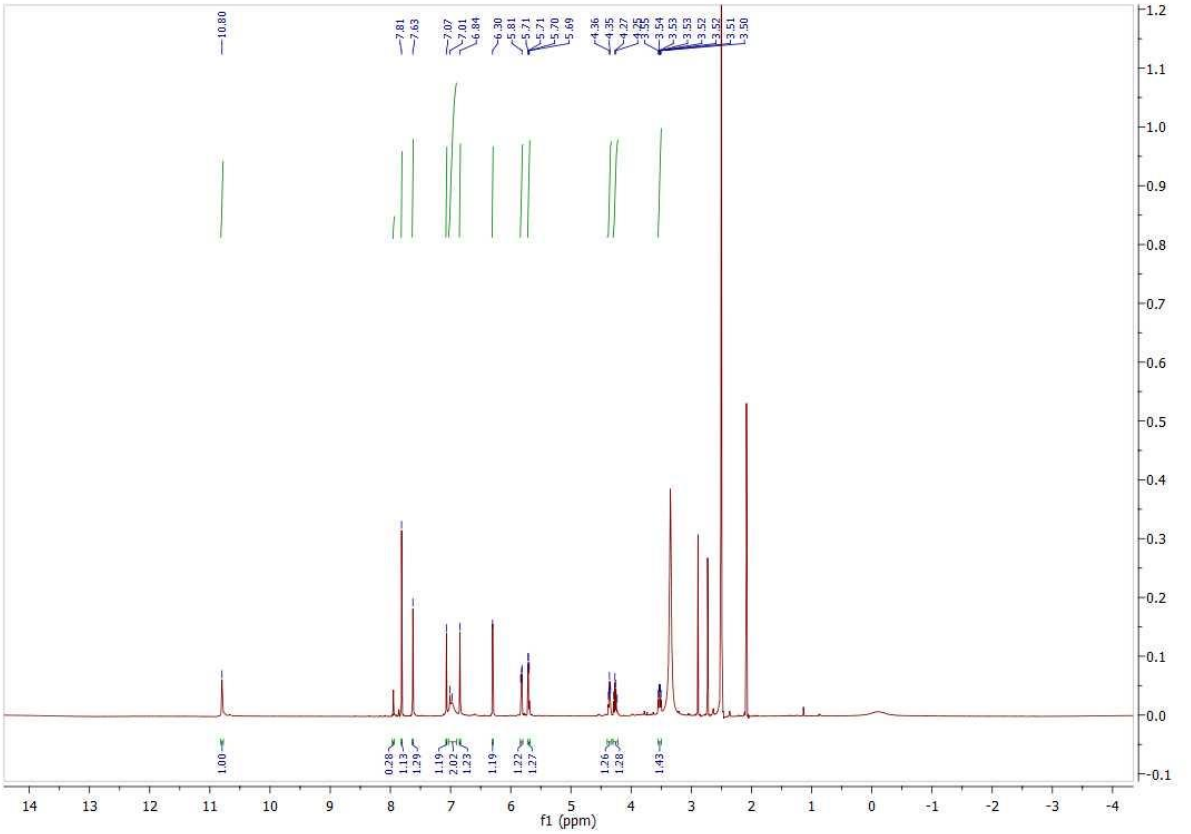
10.80
7.81
7.63
7.07
7.01
6.84
6.30
5.81
5.71
5.71
5.70
5.69
4.36
4.35
4.27
4.25
3.55
3.54
3.53
3.53
3.52
3.52
3.51
3.50
1.00
0.28
1.13
1.29
1.19
2.02
1.23
1.19
1.23
1.27
1.26
1.28
1.43
f1 (ppm)

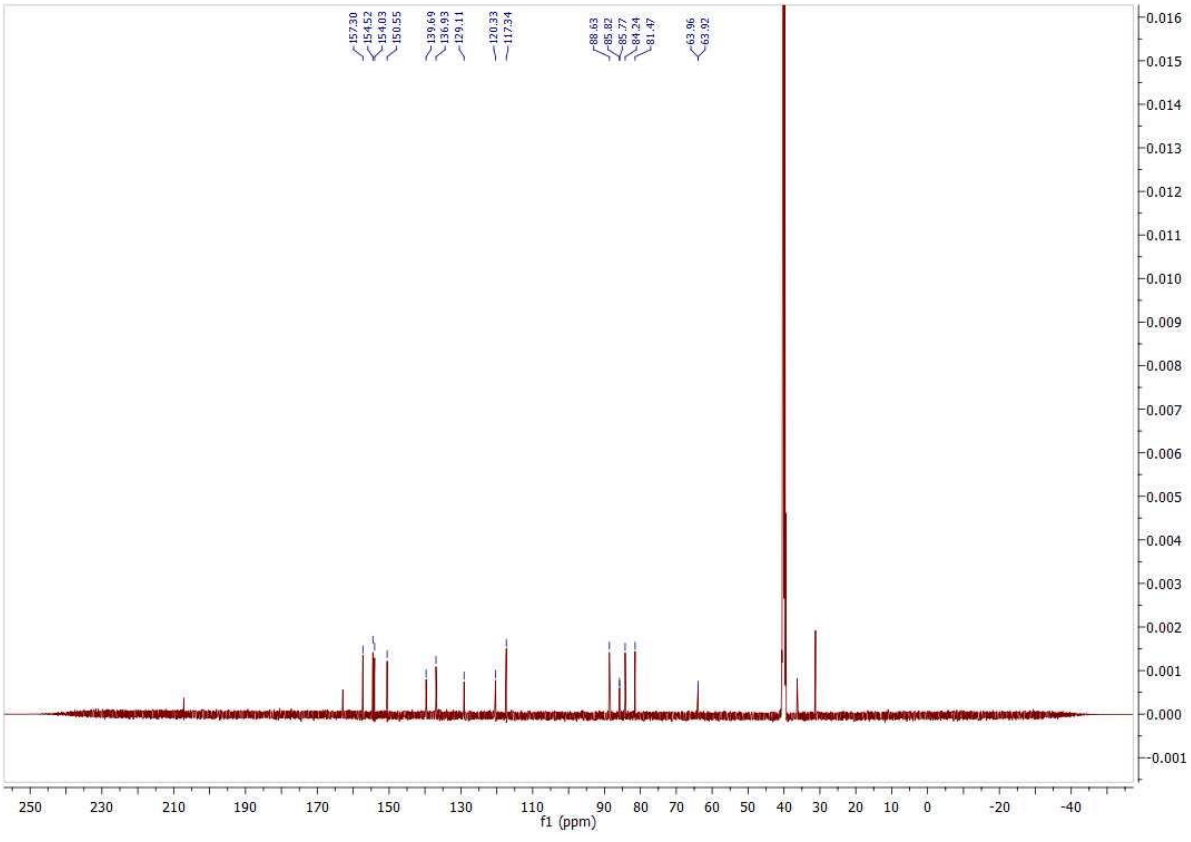
157.30
154.52
154.03
150.55
139.69
136.93
129.11
120.33
117.34
88.63
88.82
85.77
84.24
81.47
63.96
63.92
f1 (ppm)

^{31}P NMR of **14** (DMSO-D6)

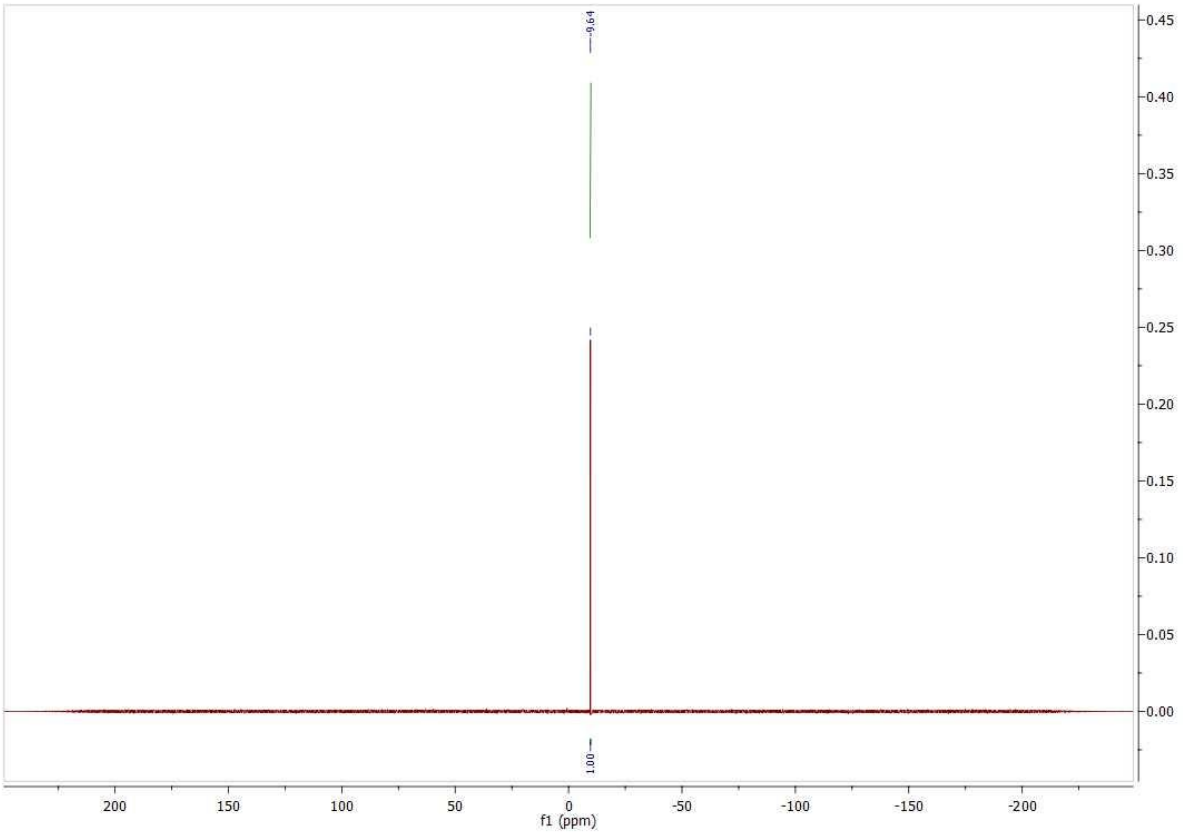

VI.2.9. Synthesis of GDP-6 azido-α-D-mannose (1a)

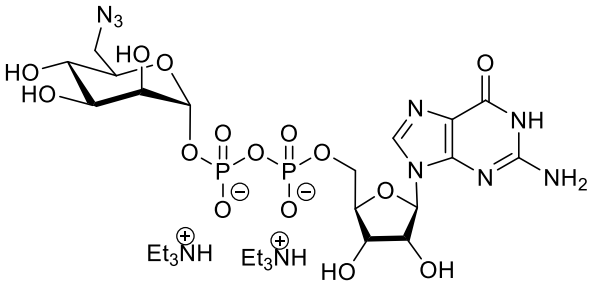

Procedure A:

The monophosphate **10** (40 mg, 0.07 mmol, 1 eq) and $MgCl_2$ (19 mg, 0.14 mmol, 2 eq) were vigorously stirred in anhydrous DMF (1.3 mL) until a clear solution was obtained (approximately 10 min). To this mixture was then added a solution of GMP-imidazolide sodium salt **14** (71 mg, 0.16 mmol, 2.5 eq) in anhydrous DMF (1.3 mL) under argon. This reaction mixture was stirred for 20h at room temperature. The reaction was quenched by the addition of water (2 mL, HPLC grade) and lyophilized to give the crude product. The latter was purified by reverse phase HPLC (50 mM triethylammonium acetate, 1-5% acetonitrile) to afford the triacetylated GDP-6-azido mannose as a bis-triethylammonium salt **16** with some remaining impurities (25mg).

Deprotection of the acetyl groups: the triacetylated GDP-6-azido mannose **16** (1 eq) and NH_4HCO_3 (20 mg, 0.31 mmol, 9.5 eq) were dissolved in 1:1 (v/v) H_2O/MeOH (0.8ml) under argon atmosphere. After cooling to 0°C, Et_3N (0.07 mL, 0.81 mmol, 27 eq) was added and the stirring was pursued for 3 days in a cold room (4°C). The reaction mixture was diluted with cool water (0.4 mL), the pH was then adjusted to 7 by addition of Amberlyst resin under slow stirring. The resin was filtrated off, washed with water and the combined filtrates were lyophilized. The crude was then purified by reverse phase HPLC (50 mM triethylammonium acetate, 1-5% acetonitrile) to afford the GDP-6-azido-α-D-mannose **1a** as a bis-triethylammonium salt (2.7 mg, 5% over two steps).

Procedure B:

The monophosphate-6-azido-6-deoxy-α-D-manno-pyranoside triethylammonium salt **11** (30 mg, 0.06 mmol, 1 eq) and $MgCl_2$ (12 mg, 0.12 mmol, 2 eq) were vigorously stirred in anhydrous DMF (1mL) until a clear solution was obtained (approximately 10 min). The mixture was then added to a solution of GMP-imidazolide sodium salt **14** (40 mg, 0.09 mmol, 1.5 eq) in anhydrous DMF (1mL) under argon atmosphere. This reaction mixture was stirred for 20h at room temperature. The reaction was quenched by the addition of water (2 mL, HPLC grade) and lyophilized to give the crude product. The latter was purified by reverse phase HPLC (50 mM triethylammonium acetate, 1-5% acetonitrile, tr: 102min) to afford the GDP-6 azido-α-D-mannose **1a** as a bis-triethylammonium salt (11 mg, 22%).

- Formula: $C_{16}H_{24}N_8O_{15}P_2$
- Molecular weight: 630.36 g/mol
- Aspect: white solid.
- **^{1}H NMR (500 MHz, D_2O)** δ (ppm) = 7.94 (1H, s, N-CH-N), 6.36 (1H, d, *J*=2.4, H1'), 5.93 (1H, dd, *J*=7.7, 2.4, H2'), 5.77 (1H, dd, *J*=7.7, 3.3, H3'), 5.44 (1H, dd, *J*=7.7, 1.5, H1), 4.76 – 4.72 (1H, m, H4'), 4.30 – 4.25 (1H, m, $H5_a$'), 4.19 – 4.13 (1H, m, $H5_b$'), 4.00 (1H, dd, *J*=3.2, 1.9, H2), 3.92 – 3.85 (2H, m, H3,H5), 3.68 (1H, t, *J*=9.9, H4), 3.60 (1H, dd, *J*=13.6, 2.6, $H6_a$), 3.50 (1H, dd, *J*=13.6, 4.6, $H6_b$).
- **^{31}P NMR (202 MHz, D_2O)** δ (ppm) = -11.07 (d, *J*=19.8), -13.47 (d, *J*=13.6).
- **^{13}C NMR (126 MHz, D_2O)** δ (ppm) = 159.01 (s), 155.66 (s), 153.89 (s) (3x Cq), 138.32 (1C, s, N-CH-N), 96.47 (1C, d, *J*=5.9, C1), 89.13 (1C, s, C1'), 84.86 (1C, d, *J*=9.1, C4'), 83.50 (1C, s, C2'), 81.19 (1C, s, C3'), 72.23 (1C, s, C5), 70.22 (1C, d, *J*=9.1, C2), 69.65 (1C, s, C3), 66.97 (1C, s, C4), 64.76 (1C, d, *J*=5.4, C5'), 50.79 (s, 1C, C6).
- **FTIR**: 2109.55 cm^{-1} (N_3 antisymmetric stretching).
- **HRMS (ESI-)**: calc. for $C_{16}H_{24}N_8O_{15}P_2$ $[M-H]^-$: 629.08; found: 629.067.

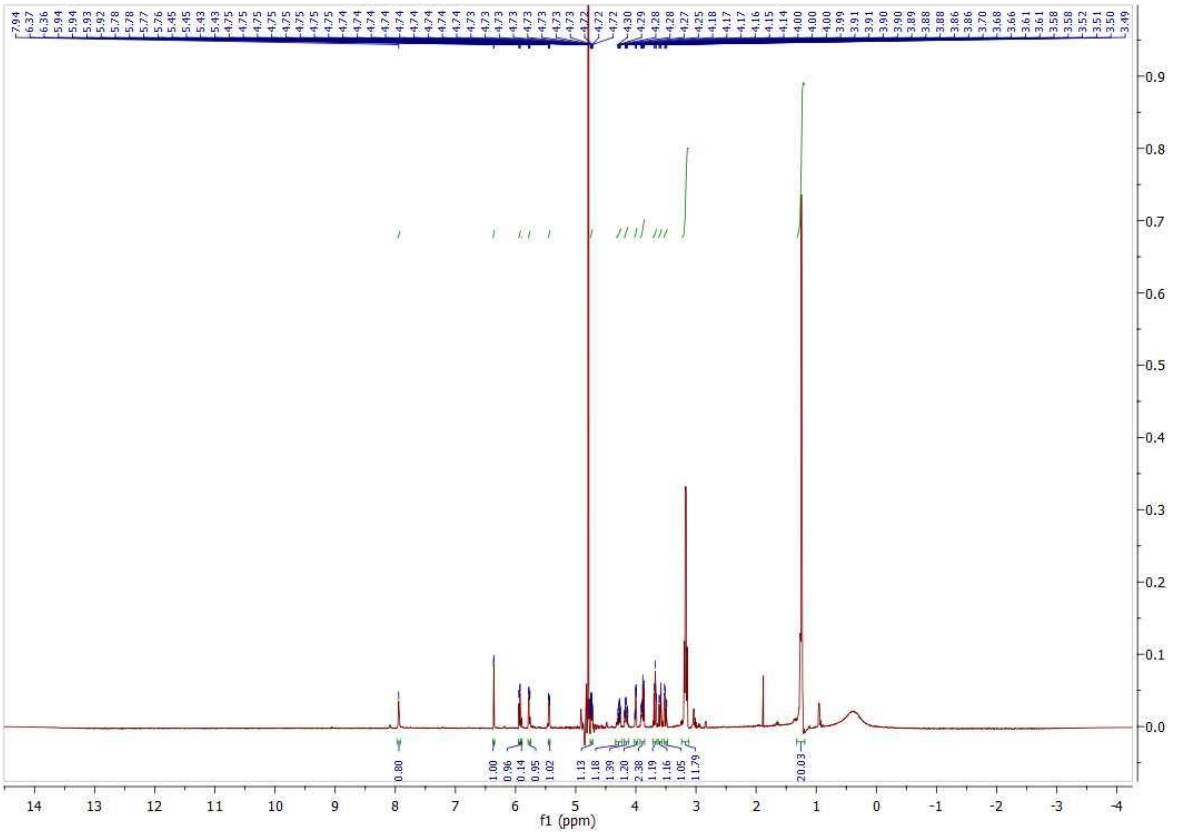
f1 (ppm)

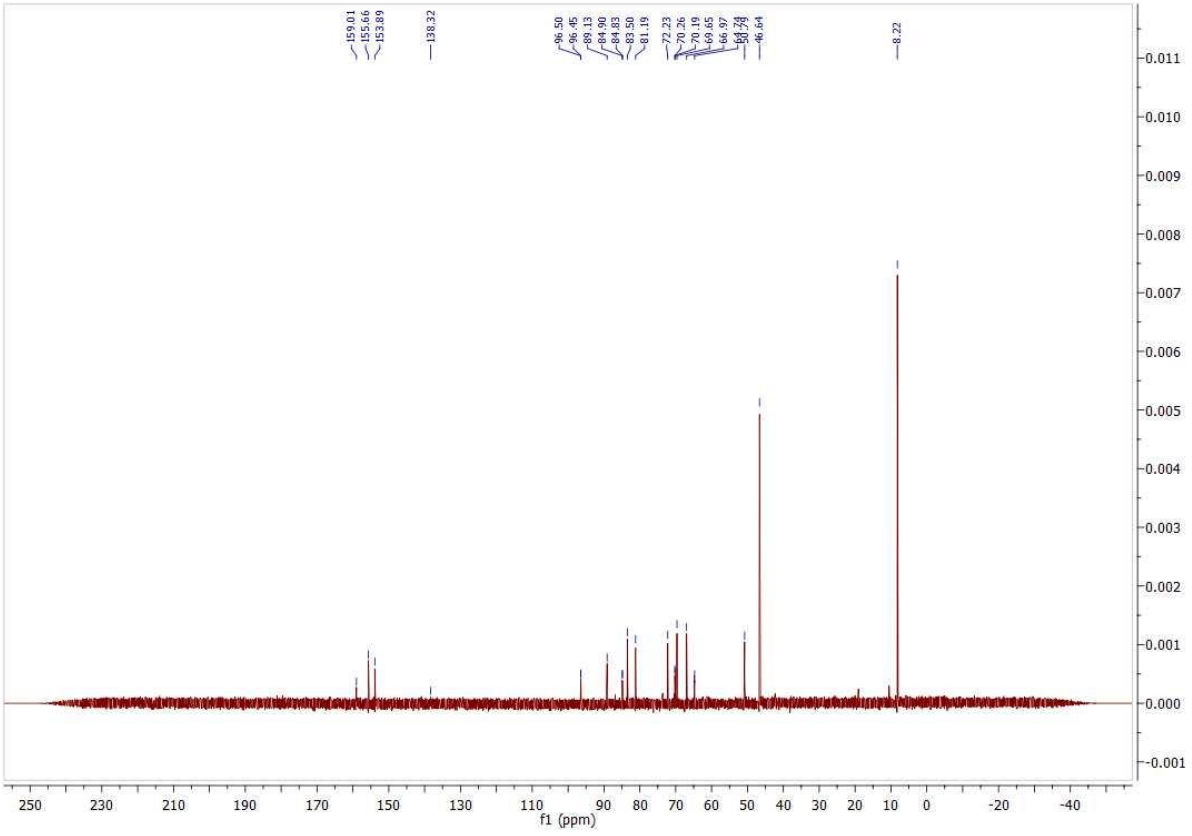
159.01
155.66
153.89
138.32
96.50
96.45
89.13
84.90
84.83
83.50
81.19
72.23
70.26
70.19
69.65
66.97
50.74
46.64
8.22
f1 (ppm)

^{31}P NMR of **1a** (D_2O)

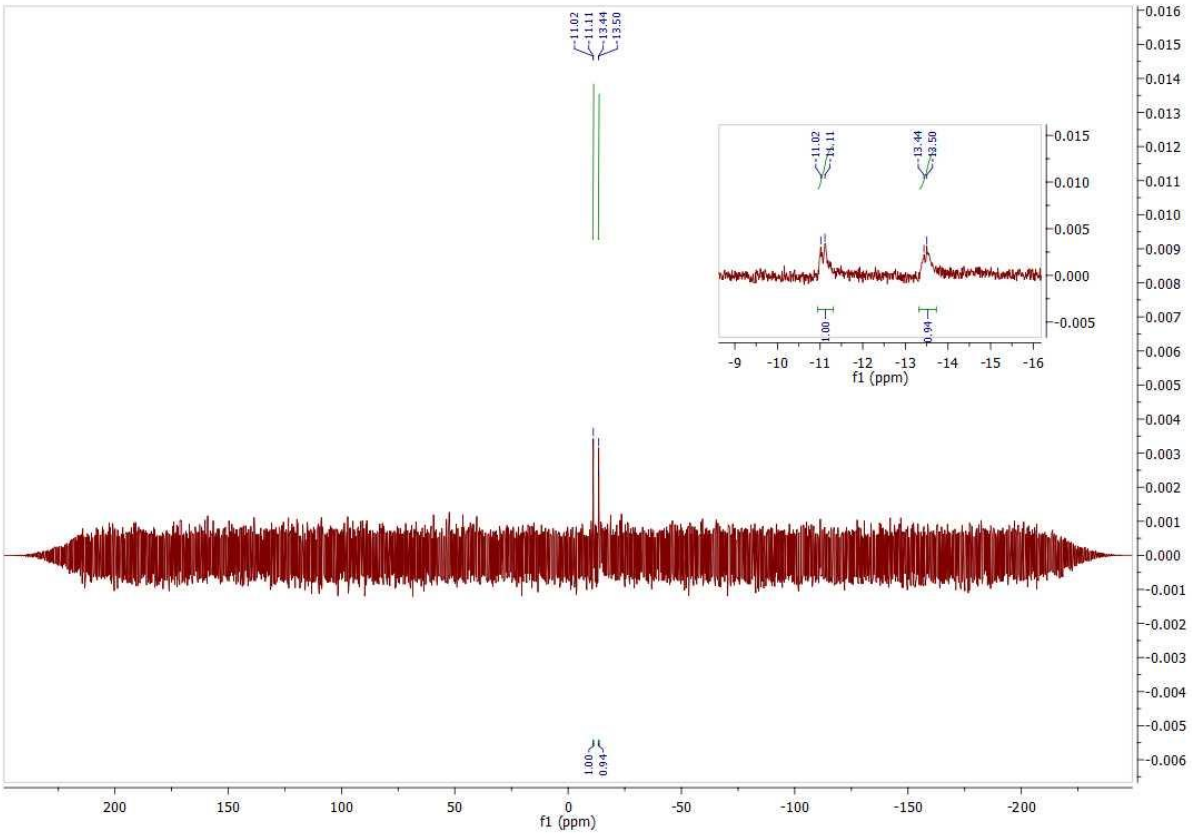

VII. Bibliography

1. Vidarsson, G., Dekkers, G. & Rispens, T. IgG subclasses and allotypes: From structure to effector functions. *Front Immunol,* **2014**, *5*.

2. Goydel, R. S. & Rader, C. Antibody-based cancer therapy. *Oncogene,* **2021**, *40*, 3655–3664.

3. Brezski, R. J. & Georgiou, G. Immunoglobulin isotype knowledge and application to Fc engineering. *Curr. Opin. Immunol,* **2016**, *40*, 62–69.

4. Jennewein, M. F. & Alter, G. The Immunoregulatory Roles of Antibody Glycosylation. *Trends Immunol,* **2017**, *38*, 358–372.

5. Sliwkowski, M. X. & Mellman, I. Antibody Therapeutics in Cancer. *Science*, **2013**, *341*, 1192-1198.

6. Liu, R., Oldham, R. J., Teal, E., Beers, S. A. & Cragg, M. S. Fc-engineering for modulated effector functions—improving antibodies for cancer treatment. *Antibodies,* **2020**, *9*, 1–34.

7. Khongorzul, P., Ling, C. J., Khan, F. U., Ihsan, A. U. & Zhang, J. Antibody–Drug Conjugates: A Comprehensive Review. *Mol. Cancer,* **2020**, *18*, 3–19.

8. Zhou, Q. Site-Specific Antibody Conjugation for ADC and Beyond. *Biomedicines,* **2017**, *5*, 64.

9. Kostova, V., Désos, P., Starck, J. B. & Kotschy, A. The chemistry behind ADCs. *Pharmaceuticals,* **2021**, *14*.

10. Senter, P. D. & Sievers, E. L. The discovery and development of brentuximab vedotin for use in relapsed Hodgkin lymphoma and systemic anaplastic large cell lymphoma. *Nat. Biotechnol*, **2012**, *30*, 631–637.

11. Walsh, S. J. *et al.* Site-selective modification strategies in antibody-drug conjugates. *Chem. Soc. Rev,* **2021**, *50*, 1305–1353.

12. Badescu, G. *et al.* Bridging disulfides for stable and defined antibody drug conjugates. *Bioconjugate Chem.,* **2014**, *25*, 1124–1136.

13. Sadiki, A. *et al.* Site-specific conjugation of native antibody. *Antib. Ther.*,**2020**, *3*, 271–284.

14. Liu, L., Bennett, C. S. & Wong, C.-H. Advances in glycoprotein synthesis. *Chem. Commun.*, **2006**.

15. Leung, D. *et al.* Antibody conjugates-recent advances and future innovations. *Antibodies,* **2020**, *9*.

16. Axup, J. Y. *et al.* Synthesis of site-specific antibody-drug conjugates using unnatural amino acids. *Proc. Natl. Acad. Sci. U. S. A,* **2012**, *109*, 16101–16106.

17. Strop, P. *et al.* Location matters: Site of conjugation modulates stability and pharmacokinetics of antibody drug conjugates. *Chem. Biol.,* **2013**, *20*, 161–167.

18. Sjögren, J., Lood, R. & Nägeli, A. On enzymatic remodeling of IgG glycosylation; Unique tools with broad applications. *Glycobiology*, **2020**, *30*, 254–267.

19. Wang, L. X., Tong, X., Li, C., Giddens, J. P. & Li, T. Glycoengineering of antibodies for modulating functions. *Annu. Rev. Biochem.*, **2019**, *88*, 433–459.

20. Li, T. *et al.* Modulating IgG effector function by Fc glycan engineering. *Proc. Natl. Acad. Sci. U. S. A*, **2017**, *114*, 3485–3490.

21. Zhu, Z. *et al.* Site-specific antibody-drug conjugation through an engineered glycotransferase and a chemically reactive sugar. *MAbs*, **2014**, *6*, 1190–1200.

22. Van Geel, R. *et al.* Chemoenzymatic Conjugation of Toxic Payloads to the Globally Conserved N-Glycan of Native mAbs Provides Homogeneous and Highly Efficacious Antibody-Drug Conjugates. *Bioconjugate Chem.*, **2015**, *26*, 2233–2242.

23. Kolb, H. C., Finn, M. G. & Sharpless, K. B. Click Chemistry: Diverse Chemical Function from a Few Good Reactions. *Angew. Chem. Int. Ed.*, **2001**, *40*, 2004–2021.

24. Sletten, E. M. & Bertozzi, C. R. Bioorthogonal chemistry: Fishing for selectivity in a sea of functionality. *Angew. Chem. In. Ed.*, **2009**, *48*, 6974–6998.

25. Li, X., Fang, T. & Boons, G. J. Preparation of well-defined antibody-drug conjugates through glycan remodeling and strain-promoted azide-alkyne cycloadditions. *Angew. Chem. Int. Ed.*, **2014**, *53*, 7179–7182.

26. Marchesan, S. & Macmillan, D. Chemoenzymatic synthesis of GDP-azidodeoxymannoses: non-radioactive probes for mannosyltransferase activity. *Chem. Commun.*, **2008**, 4321– 4323.

27. Li, T. *et al.* A General Strategy to Synthesize ADP-7-Azido-heptose and ADP-Azido-mannoses and Their Heptosyltransferase Binding Properties. *Org. Lett.*, **2021**, *23*, 1638–1642.

28. El Bkassiny, S., N'Go, I., Sevrain, C. M., Tikad, A. & Vincent, S. P. Synthesis of a novel UDP-carbasugar as UDP-galactopyranose mutase inhibitor. *Org. Lett.*, **2014**, *16*, 2462–2465.

29. Dohi, H. *et al.* Stereoselective glycal fluorophosphorylation: Synthesis of ADP-2-fluoroheptose, an inhibitor of the LPS Biosynthesis. *Chem. Eur. J.*, **2008**, *14*, 9530–9539.

30. Kumar, A., Doddi, V. R. & Vankar, Y. D. Mild and efficient chemoselective deprotection of anomeric *O*-methyl glycosides with trityl tetrafluoroborate. *J. Org. Chem.*, **2008**, *73*, 5993–5995.

31. Ahmadipour, S. & Miller, G. J. Recent advances in the chemical synthesis of sugar-nucleotides. *Carbohydr. Res.* **2017**, *451*, 95–109.

32. Li, T., Tikad, A., Pan, W. & Vincent, S. P. β-Stereoselective Phosphorylations Applied to the Synthesis of ADP- and Polyprenyl-β-Mannopyranosides. *Org. Lett.*, **2014**, *16*, 5628–5631.

33. M. H. Caruthers, *et al*. Chemical Synthesis of Deoxyoligonucleotides by the Phosphoramidite Method . *Science*, **1985***, 230*, 281-313.

34. Mui Mui Sim, Hirosato Hondo, Chi-Huey Wong. Synthesis and use of glycosyl phosphite. *J. Am. Chem. Soc.*, **1993***, 115*, 2260-2267.

35. Gold, H. *et al.* Synthesis of Sugar Nucleotides by Application of Phosphoramidites. *J. Org. Chem.*, **2008***, 73*, 9458–9460.

36. Wittmann, V. & Wong, C.-H. 1H-Tetrazole as Catalyst in Phosphomorpholidate Coupling Reactions: Efficient Synthesis of GDP-Fucose, GDP-Mannose, and UDP-Galactose. *J. org. chem.*, **1997***, 62*, 2144-2147.

37. Luning, J., Debski, N. & Welzel, P. A New Method For The Cleavage Of Allyl Glycosides. Tetrahedron Lett., **1993**, *34*, 5871-5874.

38. Gola, G., Libenson, P., Gandolfi-Donadío, L. & Gallo-Rodriguez, C. Synthesis of 2,3,5,6-tetra-O-benzyl-D-galactofuranose for α-glycosidation. ARKIVOC, **2006**, *2005*, 234-242.

39. J. Tsuji, T. Mandai. Pd catalyzed hydrogenolysis of allylic and propargylic compounds with various hydrides. *Synthesis*, **1996**.

40. Honda, M., Morita, H. & Nagakura, I. Deprotection of Allyl Groups with Sulfinic Acids and Palladium Catalyst. *J. org. chem.*, **1997***, 62*, 8932-8936.

41. Timmons, S. C. & Jakeman, D. L. Stereoselective chemical synthesis of sugar nucleotides via direct displacement of acylated glycosyl bromides. *Org. Lett.*, **2007***, 9*, 1227–1230.

42. Wagner, G. K., Pesnot, T. & Field, R. A. A survey of chemical methods for sugar-nucleotide synthesis. *Nat. Prod. Rep.*, **2009***, 26*, 1172–1194.

43. Xu, Z. A review on the chemical synthesis of pyrophosphate bonds in bioactive nucleoside diphosphate analogs. *Bioorganic Med. Chem. Lett.*, **2015***, 25*, 3777–3783.

44. Wolf, S., Zismann, T., Lunau, N. & Meier, C. Reliable Synthesis of Various Nucleoside Diphosphate Glycopyranoses. *Chem. Eur. J*., **2009**, *15*, 7656–7664.

45. Dabrowski-Tumanski, P., Kowalska, J. & Jemielity, J. Efficient and Rapid Synthesis of Nucleoside Diphosphate Sugars from Nucleoside Phosphorimidazolides. *Eur. J. Org. Chem.* **2013**, *2013*, 2147–2154.

46. Mukaiyama, T. & Hashimoto, M. Synthesis of Oligothymidylates and Nucleoside Cyclic Phosphates by Oxidation-Reduction Condensation. *J. Am. Chem. Soc.*, **1972**, *94*, 8528-8532.

47. Baisch, G. & Ohrlein, R. Convenient Chemoenzymatic Synthesis of P-Purine-diphosphate Sugars (GDP-fucose-analogues). *Bioorg. Med. Chem.*, **1997***, 5*, 383-391.

48. Zamyatina, A. *et al.* Efficient Chemical Synthesis of The Two Anomers of ADP L-glycero and D-glycero-D-manno-heptopyranoses Allows The Determination of The Substrate Specificities of Bacterial Heptosyltransferases . *Angew. Chem. Int. Ed.*, **2000***, 39*, 4150-4153.

49. Corey, E. J. & Fuchs, P. L. *A* Synthetic Method For Formyl Ethynyl Conversion. *Tetrahedron Lett.*, **1972**, *13*, 3769 - 3772.

50. Ernest Colvin, B. W. & Hamill, B. J. One-step Conversion of Carbonyl Compounds into Acetylenes. *J. Chem. Soc. Chem. Comm.*, **1973**, 151-152.

51. Kazuhiro Miwa, Toyohico Aoyama, Takayuki Shioiri. Extention of Colvin Rearrangement using trimethylsilyldiazométhane. *Synlett*, **1994**, *1994*, 107-108.

52. Roth, G. J., Liepold, B., Müller, S. G. & Bestmann, H. J. Further Improvements of the Synthesis of Alkynes from Aldehydes. *Synthesis*, **2003**, *2004*, 59–62.

53. Ansiaux, C., N'Go, I. & Vincent, S. P. Reversible and efficient inhibition of UDP-galactopyranose mutase by electrophilic, constrained and unsaturated UDP-galactitol analogues. *Chem. Eur. J.*, **2012**, *18*, 14860–14866.

54. Pijnenborg, J. F. A. Development of substrate based inhibitors targeting human glycosylation, **2022**. https://hdl.handle.net/2066/252747. (thesis)